University of Stavanger

Faculty of Science and Technology

MASTER'S THESIS

Study program/ Specialization: Environmental Engineering Waster Science and Technology	Spring semester, 2010 Open / ~~Restricted access~~
Writer: Jovan Popov	…… (Writer's signature)
Faculty supervisor: Roald Kommedal External supervisor(s):	
Titel of thesis: Model Based Optimization of Biogas Production at SNJ Plant	
Credits (ECTS): 30	
Key words: Anaerobic digestion Anaerobic digestion model Codigestion Simulation	Pages: 73 + enclosure: …… Stavanger, 02/07/2010 Date/year

Model based optimization of biogas production at SNJ plant

Jovan Popov

Abstract

The main purpose of this thesis is the acquisition of knowledge and familiarization with the SNJ biogas plant and effects of codigestion. Plant operation and performance was monitored in order to understand and evaluate the factors affecting the efficiency of the sludge treatment process. The thesis also presents an overview of anaerobic digestion process, modelling of anaerobic codigestion process, and a general presentation of the Regional Wastewater Treatment Plant of Nord-Jæren (SNJ). More precisely, the study provides experimental data of several parameters at SNJ plant. Methane production and Chemical Oxygen Demand (COD) removals were quantified under steady state conditions for a wide range of operating parameters. Mathematical model (ADM1) was successfully adapted to reactor system. Non-steady state analysis was performed to assess the effect of food waste loading on biogas production by codigestion.

Calculations reveal that 0.6142 m^3 of methane is produced per kg COD removal, based on theoretically estimated biogas production by using the measured data. There is big discrepancy of 29.7% in comparison between the theoretical estimated methane production and the actual methane production measured at SNJ plant. The Volatile Suspended Solids (VSS) reduction during the digestion of raw sludge along with septic sludge and food waste was 58.69%. Likewise, Total Suspended Solids (TSS) reduction was calculated as 47.57%. Results gained by simulation showed differences between the steady state and measured data. The simulated biogas production showed lower values then the measured at SNJ.

The result of non-steady state analysis shows that the biogas production had increased by 62 % in reactor 1 in comparison with reactor 2. The biogas production obtained here, by the addition of food waste, could be attributed to the higher biodegradability of food waste. On the other hand, the high contents of polysaccharides and assembly the carbohydrates in the food waste have been recognized as a main reason for the increased biogas production. Therefore, food waste codigestion with raw sludge is a sustainable and environmentally attractive method to treat and simultaneously convert such a waste mixture to a useful energy source.

Acknowledgements

This thesis is prepared for the partial fulfilment of the requirements for the degree of Master of Science in Environmental Technology, in the department of Mathematics and Natural Science, Faculty of Science and Technology at University of Stavanger.

I heartily thankful to my Supervisor Roald Kommedal (Professor of Environmental Biotechnology, University of Stavanger) whose encouragements, guidance, patience, dedicated attitude, and continuous support from the initial to the final level enabled me to develop an understanding of the subject.

I would like to thank Leif Ydstebø (Professor of Bioprocess Analyses, University of Stavanger), who never hesitated to provide me guidance and consultancy in the data processing and help me with the research material.

I also would like to make a special reference to Andrea Bagi (PhD student at University of Stavanger) for proofreading of the manuscripts and for getting my English smoother. It is her credit that this thesis does not only consist of long twisted sentences.

I would like to thank IVAR-SNJ for giving me opportunity to work with this project. I would like to thank Kjetil Pedelsen (plant operator) who provided me detailed data from SNJ plant. I would like to thank Synnøve Talgø with whom I shared and worked in the same laboratory at SNJ plant. Many thanks to my all brilliant class fellows we have been encouraging each other throughout the studies and dreaming for better future.

I would like to show my gratitude to my mother Zora Popova and my brother Vlado Popov as they are supporting me throughout my life. They always encourage me even though they missed me a lot during my study. The greatest honour is for my father (late) Dimitar Popov who put me on the right track to achieve the destiny. I would like to thank my aunt Petrija Trandafilovska and my first cousins Ivana Trandafilovska, Vera Trandafilovski, Pero Traev and Vasko Traev.

I would also like to sincerely thank all my friends in Macedonia and also Stavanger for all your love, continuous support and prayers.

Model based optimization of biogas production at SNJ plant

Contents

		Page Number
	Abstract	
	Acknowledgement	
	List of Figures	I
	List of Tables	III
	List of Graphs	V
Chapter One	**Introduction**	**1**
1.1	Theoretical Background	1
1.2	Scope of the Study	2
1.3	Overview of anaerobic digestion process	2
1.3.1	Disintegration	3
1.3.2	Hydrolysis	4
1.3.3	Acidogenesis	4
1.3.4	Acetogenesis	6
1.3.5	Methanogenesis	8
1.4	General aspects of codigestion	10
1.5	Modelling of Anaerobic Digestion	11
1.6	Case Study	12
1.6.1	Rogaland Country	12
1.6.2	SNJ Plant	12
Chapter Two	**Materials and Methods**	**19**
2.1	Model Formulation AQUASIM	19
2.2	Nomenclature, state variables and expressions	20
2.2.1	Units	20
2.2.2	Nomenclature and description of parameters and variables	20
2.2.3	Dynamic State Variables	21
2.3	Biochemical Processes	22
2.3.1	Structure of Biochemical Reactions in the ADM1	22
2.4	Model presentation in matrix format	24
2.5	Laboratory Experiments	25

Chapter Three	**Results**	**27**
3.1	Monitoring of operational parameters at SNJ plant	27
3.2	Calculating mass balance based on the measured data	38
3.3	Determination of Volatile Solids Reduction	39
3.4	Estimation of SRT, volumetric loading and percentage stabilization at SNJ plant	41
3.5	Steady State Simulation	43
3.6	Non Steady State Analysis	50
Chapter Four	**Discussion**	**61**
Chapter Five	**Conclusion**	**69**
	Appendix A	70
	References	72

List of Figures

	Page Number
Figure 1.1 COD flux for a particulate composite	3
Figure 1.2 Syntrophy: Inter species H2 transfer	7
Figure 1.3 Free energy changes as a function of the H2 partial pressure	8
Figure 1.4 Principle of codigestion at SNJ plant	10
Figure 1.5 The balance of codigestion	11
Figure 1.6 The network of wastewater treatment facility in Rogaland region	13
Figure 1.7 Sedimentation basin	14
Figure 1.8 Cross section of SNJ plant	15
Figure 1.9 Flow diagram of SNJ plant	16
Figure 1.10 Biopellets	17
Figure 1.11 Flow diagram of facilities where sludge is received at SNJ plant	18
Figure 2.1 Main elements of model structure	19
Figure 2.2 The anaerobic model as implemented including biochemical processes	23
Figure 3.1 Hydraulic loading during steady state conditions as measured	45
Figure 3.2 COD concentrations during simulated steady state	45
Figure 3.3 Simulated and measured biogas flow rates	46
Figure 3.4 Methane biogas volumetric ratio	46
Figure 3.5 Reactor pH during the test period	47
Figure 3.6 Buffer tank pH as measured and simulated	47
Figure 3.7 Simulated VFA (fermentation products) in the digester 1	48
Figure 3.8 Simulated VFA and monomers in the buffer tank	48
Figure 3.9 Simulated inhibitions (relative) in anaerobic digesters	49

Figure 1.10 Simulated relative inhibition (kinetic) in the buffer tank 49

List of Tables

Page Number

Table 1.1 Acidogenic reactions with sucrose as the substrate and the corresponding free energy change (ΔG0') at 25°C 5

Table 1.2 Averaged kinetic properties of acidifiers and methanogens 5

Table 1.3 Stoichiometry and change of free energy (ΔG°') for some acetogenic reactions at neutral pH and STP 6

Table 1.4 Most important methanogenic reactions, the corresponding free energy change (ΔG°') and some kinetic properties 9

Table 2.1 Units 20

Table 2.2 Stoichiometric coefficients 20

Table 2.3 Equilibrium coefficients and constants 21

Table 2.4 Kinetic parameters and rates 21

Table 2.5 Dynamic state and algebraic variables (and derived variables) 21

Table 2.6 Dynamic state variable characteristic (DAE) system 22

Table 3.1 Characteristics of sludge in reactor 1 27

Table 3.2 Characteristics of sludge in the reactor 2 29

Table 3.3 Characteristics of slurry in buffer tank 32

Table 3.4 Characterization of raw sludge 34

Table 3.5 Characterization of external sludge 36

Table 3.6 Characterization of food waste 37

Table 3.7 Extended mass balance over one week 38

Table 3.8 Parameters analysed at SNJ plant during one week 42

Table 3.9 Represents several operational parameters measured at SNJ plant 43

Table 3.10 Represents COD loading rates from different wastes 43

Table 3.11 COD fractions in three different waste types 44

Table 3.12 Characteristics of food waste obtained during non steady state analyses 58

Table 4.1 Estimated volatile solids destruction in high-rate complete-mix mesophilic anaerobic digestion 65

Table A.1 Biochemical rate coefficient and kinetic rate equations for soluble components 64

Table A.2 Biochemical rate coefficient and kinetic rate equations for particulate components 65

List of Graphs

	Page Number
Graph 3.1 Behaviour of pH in the reactor 1	28
Graph 3.2 COD data obtained in reactor 1	28
Graph 3.3 Solids content in the reactor 1	29
Graph 3.4 Concentration of acetic acid in reactor 1	29
Graph 3.5 Behaviour of pH in reactor 2	30
Graph 3.6 COD data obtained in reactor 2	30
Graph 3.7 Solids content in reactor 2	31
Graph 3.8 Concentration of acetic acid in reactor 2	31
Graph 3.9 Behaviour of pH in buffer tank	32
Graph 3.10 COD data obtained in buffer tank	33
Graph 3.11 Solids content in buffer tank	33
Graph 3.12 Concentrations of volatile fatty acids in buffer tank	34
Graph 3.13 Monitoring of pH in raw sludge over time	35
Graph 3.14 COD data obtained in raw sludge	35
Graph 3.15 Solids content in raw sludge	36
Graph 3.16 Concentration of VFA's in raw sludge	36
Graph 3.17 Monitoring the pH in external sludge over time	37
Graph 3.18 Solids content in external sludge	37
Graph 3.19 Plotted biogas measured at SNJ plant over COD removed	39
Graph 3.20 Flow characteristics during the survey period	50
Graph 3.21 Monitoring the pH behaviour in reactor 1	51

Graph 3.22 COD changes in the reactor 1 51

Graph 3.23 Solids analyses conducted in reactor 1 52

Graph 3.24 Concentrations of volatile fatty acids in reactor 1 52

Graph 3.25 Monitoring the pH behaviour in reactor 2 53

Graph 3.26 COD concentration in reactor 2 53

Graph 3.27 Solids analyses conducted in reactor 2 54

Graph 3.28 Concentration of volatile fatty acids in reactor 2 54

Graph 3.29 Measured pH values in buffer tank over time 55

Graph 3.30 COD concentration in buffer tank 55

Graph 3.31 Solids content in buffer tank 56

Graph 3.32 Concentrations volatile fatty acids in buffer tank 56

Graph 3.33 Monitoring the pH behaviour in raw sludge 57

Graph 3.34 COD concentration in raw sludge 57

Graph 3.35 Solids content in raw sludge 58

Graph 3.36 Concentration of volatile fatty acids in raw sludge 58

Graph 3.37 Concentration of volatile fatty acids in food waste 59

Graph 3.38 Biogas productions from reactor 1 and reactor 59

Graph 3.39 Methane concentrations in biogas vary over time 60

Graph 4.1 Interdependency between COD loading rates and COD removal rates 63

Graph 4.2 Theoretically biogas produced over COD removed 64

1. INTRODUCTION

1.1 Theoretical Background

The process by which organic waste materials are converted into biogas and carbon dioxide is referred to as anaerobic digestion (AD). It involves the breakdown of organic matter by the concerted actions of a wide range of microorganisms in the absence of oxygen. The process consists of a complex series of reactions. The sum of these being a fermentation which converts a wide array of substrate materials, having carbon atoms at various oxidation/reduction states, to molecules containing one carbon in its most oxidized (CO_2) and the most reduced (CH_4) state. Minor quantities of nitrogen, hydrogen, ammonia and hydrogen sulphide (usually less than 1% of the total gas volume) are also generated (Angelidaki et al.).

Anaerobic conversions are among the oldest biological technologies utilised by mankind, initially for food and beverage production. They have been applied and developed over centuries, although the most dramatic advances have been achieved in the last few decades with the introduction of various form of high-rate treatment processes, particularly for industrial wastewater. Biogas production is a natural process which takes place in a variety of anaerobic environments such as the intestinal tract of animals, marine and fresh water sediment, sewage sludge, paddy fields, water logged soils and in the regions of volcanic hot springs and deep sea hydrothermal vents (Angelidaki et al.).

There are many ways to treat municipal solid waste (MSW), industrial wastewater, sewage sludge or waste materials from food production industry including biological operations. High organic loading rates and low sludge production are among the many advantages anaerobic processes exhibit over other biological unit operations. The main characteristic of anaerobic process is biogas produced which can replace fossil fuel sources and therefore has a direct positive effect on greenhouse gas reduction. In the foreseeable future building of anaerobic treatment plant for these reasons will probably sustain and increase.

One of Norway's largest wastewater treatment plants is the Regional Wastewater Treatment Plant of Nord-Jæren (SNJ; Snetralrenseanlegg Nord-Jæren). SNJ is located in Mekjarvik, municipality of Randaberg near the city of Stavanger. The plant was put into operation March 1992, and was primarily built for waste treatment, including anaerobic sludge digestion. However, SNJ is now starting to import/receive different types of organic wastes such as fish offal, chicken pulp, food waste and septic sludge from six municipalities in the vicinity of Stavanger. The objective of this study is to investigate possibilities of codigestion of different types of organic wastes and municipal wastewater sludge in order to increase the biogas output. This requires optimal operation with frequent controls of the sludge loading and detailed knowledge of qualitative content of different types of sludge.

Simulations by an adequate mathematical model is a novel tool for this purpose, and implementation of the Anaerobic Digestion Model no. 1 (ADM1), originally proposed by the IWA Task Group for Mathematical Modelling of anaerobic digestion process (Batstone et al., 2002), to the SNJ process will be investigated here.

ADM1 was used to assess the present operations of the digestors at SNJ plant, and also to test possible scenarios of combining different types of waste. Also, the model was validated by comparing the simulations with the measured values at SNJ plant survey. A combination of operational measurements and additional off line analysis, such as chemical oxygen demand analysis (COD), solids analysis (TS, VS, and FS), pH measurement, and volatile fatty acids (VFA), was performed.

The biogas plant at SNJ was modelled and simulated by the system analysis tool AQUASIM (Reichert, 1998).

1.2 Scope of the Study

To achieve the objective of this study, the following tasks were included for this master thesis project:

- Investigation and description of the operational conditions of the anaerobic digestion process at SNJ
- Implementation of ADM1 to the reactor system at SNJ using AQUASIM, and evaluation of steady state simulation (comparative study to measured data).
- Comparison between calculated biogas productions based on measured data with actual biogas situation obtained from the monitoring centre at SNJ plant.
- Determination of volatile solids reduction during the digestion process in reactors.
- Estimation of solids retention time (SRT), volumetric loading and percentage of stabilized sludge.
- Non-steady state analysis. To investigate how food waste behaves in the codigestion process

1.3 Overview of Anaerobic Digestion Process

The anaerobic degradation pathway of organic matter is a multi step process. This process is based on parallel and cross linked reactions and proceeds through five successive stages: (i) disintegration, (ii) hydrolysis, (iii) acidogenesis, (iv) acetogenesis, and (v) methanogenesis. The anaerobic ecosystem is the result of complex interactions among microorganisms of several different species. The major functional groups of bacteria according to their

metabolic reactions are: (i) fermentative bacteria, (ii) hydrogen-producing acetogenic bacteria, (iii) hydrogen-consuming acetogenic bacteria, (iv) carbon dioxide-reducing methanogens, and (v) aceticlastic methanogens (Henze, 2008). A schematic of the reaction steps is given below in Figure 1.1.

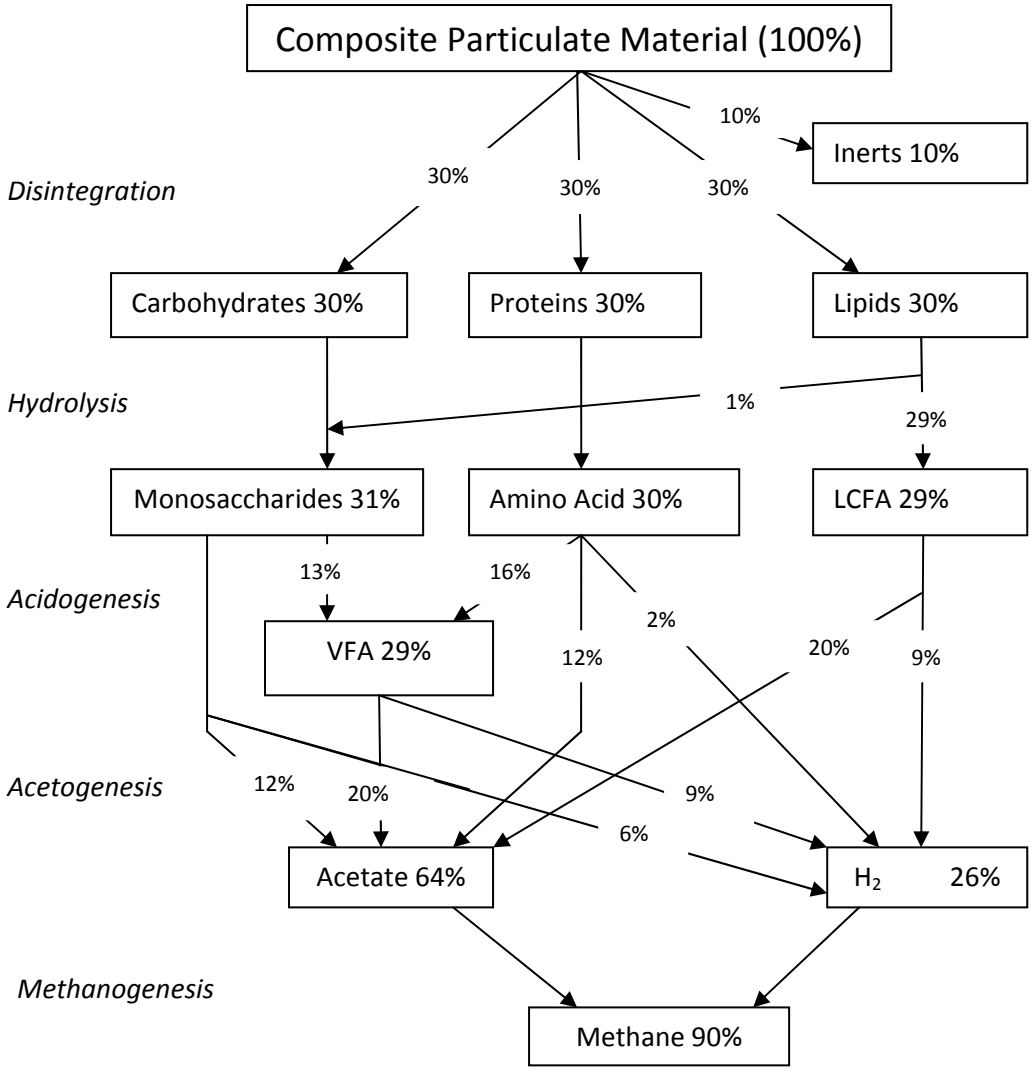

Figure 1.1: COD flux for a particulate composite comprised of 10% inerts, and 30% each of carbohydrates, proteins and lipids (in terms of COD). VFA are represented as propionic acid (10%), butyric acid (12%) and valeric acid (7%) (Batstone et al., 2002).

1.3.1 Disintegration

Disintegration of composites (such as dead biomass and particulate organic carbon) to polymeric constituents and subsequent enzymatic hydrolysis to soluble monomers are extracellular processes. Extracellular depolymerisation enzymes act on the pool of available organic material, dividing them into smaller molecular weight products. Disintegration is also a non-biological process mediating the breakdown and solubilisation of complex

organic material to soluble substrates. The products are complex composite particulates and polymeric carbohydrates, proteins and lipids, which than serve as substrate for the following process of hydrolysis. Other products of disintegration are inert particulate and inert soluble material (Batstone et al., 2002).

The IWA Task Group included disintegration as the first process to allow diversity of applications, and to allow for lysis of biological sludge and complex organic material. The disintegration step was also included to represent the pool of composite organic material. This is especially important for waste-activated and primary sludge digestion, where the disintegration step represent lysis of whole cells and separation of composites (Batstone et al., 2002).

1.3.2 Hydrolysis

In anaerobic digestion (AD) the term hydrolysis is used to describe degradation of a defined particulate or macromolecular substrate to its soluble monomers. For particulates, hydrolysis is merely a surface phenomenon, while the process is molecular for smaller macromolecules (biopolymers). During hydrolysis, proteins are hydrolysed to amino acids, polysaccharide to simple sugars and lipids to long chain fatty acids (LCFA) (Henze, 2008). This is performed by heterotrophic microorganisms that attached to particles, produce enzymes in the vicinity of the particle and benefit from soluble products released by the enzymatic reaction. Therefore, the microorganisms growing on the particle surface, rather than the enzyme produced, should be regarded as the effective catalyst (Batstone et al., 2002). Products from hydrolysis are readily accessible for acidogenic bacteria.

Moreover the hydrolysis process is very sensitive to temperature and temperature fluctuations. Hydrolysis is generally considered to be the rate-limiting step during AD of complex substrates. (Henze, 2008) investigations by Chandler et al., (1980) and Zeeman et al., (1996) showed that this is not because of lack of enzyme activity but more due to the availability of free accessible surface area of the particles and the overall structure of the solid substrate.

1.3.3 Acidogenesis

Acidogenesis (fermentation) is generally defined as an anaerobic acid-producing microbial process without an additional electron acceptor (Batstone et al., 2002). During acidogenesis, amino acids and simple sugars (products of hydrolysis), which are relatively small soluble compounds, are taken up by heterotrophic bacterial cells through the cell membrane and subsequently fermented or an aerobically oxidized (Henze, 2008). The degradation of LCFA is an oxidation reaction with an internal electron acceptor (H^+) (Batstone et al., 2002). During fermentation, energy (ATP) is produced directly from an energy-rich intermediate by substrate-level phosphorilation (Madigan et al., 2006). Electron balancing is achieved either by substrate internal electron translocation (one part of the molecule fermented is oxidized

while another part is reduced), or electrons are transferred to cytoplasmic electron acceptors (most often H^+ or pyruvate).

Characteristically, neutral compounds such as sugars and proteins are converted to acidic compounds like carboxylic acids (also known as Volatile Fatty Acids, VFA's). Hence, fermentative organisms are usually designated as acidifying or acidogenic microorganisms, and the process is called acidogenesis (Henze, 2008). Table 1.1 lists several acidogenic reactions starting from sucrose and generating different amounts of VFA's, HCO_3, H_2, and H^+.

From Table 1.1 it follows that the $\Delta G^{0'}$ of the less energetic acidogenic reactions with sucrose as the substrate strongly depends on the prevailing H_2 concentrations. If H_2 is effectively removed by H_2 scavenging organisms such as methanogens, acetate will be the main end product (Henze, 2008).

Table 1.1 Acidogenic reactions with sucrose as the substrate and the corresponding free energy change ($\Delta G^{0'}$) at 25°C (Henze, 2008)

Reaction	$\Delta G^{0'}$ (kJ/mol)	Eq.
$C_{12}H_{22}O_{11} + 9H_2O \rightarrow 4CH_3COO^- + 4HCO^-_3 + 8H^+ + 8H_2$	-457.5	1.1
$C_{12}H_{22}O_{11} + 5H_2O \rightarrow 2CH_3CH_2CH_2COO^- + 4HCO^-_2 + 6H^+ + 4H_2$	-554.1	1.2
$C_{12}H_{22}O_{11} + 3H_2O \rightarrow 2CH_3COO^- + 2CH_3CH_2COO^- + 2HCO_3^- + 6H^+ + 2H_2$	-610.5	1.3

Acidogenesis is the most rapid conversion step in the anaerobic food chain. The $\Delta G^{0'}$ of acidifying reactions is highest of all anaerobic conversions, resulting in ten to twentyfold higher bacterial growth rates, and fivefold higher bacterial yields and conversion rates compared to methanogenesis (Table 1.2) (Henze, 2008). This can be seen from the Table 1.2 by comparing the parameters between acidogenesis and methanogenesis. Souring of the sludge solution occurs because the products of acidogenesis lower pH and they are produced faster than consumed (kinetic effect).

Table 1.2 Averaged kinetic properties of acidifiers and methanogens (Henze, 2008)

Process	Conversion rate gCOD/gVSS.d	Y gVSS/gCOD	K_S mgCOD/l	μ_m 1/d
Acidogenesis	13	0.15	200	2.00
Methanogenesis	3	0.03	30	0.12
Overall	2	0.03 - 0.18	-	0.12

The acidogenic conversion of amino acids generally follows the Stickland reaction, in which an amino acid is de-ammonified by anaerobic oxidation yielding also VFA and H_2, in conjunction with the reductive de-ammonification of other amino acids consuming the produced H_2. From both reactions NH_3 is released and subsequently acts as a proton

acceptor, thus this can balance the pH drop that would occur when acidic compounds are produced (Henze, 2008).

1.3.4 Acetogenesis

Acetogenic bacterial conversion of products derived from the fermentation process, other than acetate, are further converted to acetate, hydrogen gas and carbon dioxide. The most important acetogenic substrates are propionate and butyrate. But also lactate, ethanol, methanol and even H_2 and CO_2 are (homo)acetogenically converted to acetate as shown in Table 1.3 (Henze, 2008).

LCFAs are converted by specific acetogenic bacteria following the so-called β-oxidation in which acetate moieties are split from the aliphatic chain (Table 1.3) (Henze, 2008).

Table 1.3 Stoichiometry and change of free energy (ΔG°') for some acetogenic reactions at neutral pH and STP (Henze, 2008)

Compound	Reaction	ΔG°(kJ/mole)	Eq.
Lactate	$CH_3CHOHCOO^- + 2H_2O \rightarrow CH_3COO^- + HCO_3^- + H^+ + 2H_2$	-4.2	1.4
Ethanol	$CH_3CH_2OH + H_2O \rightarrow CH_3COO^- + H^+ + 2H_2$	+9.6	1.5
Butyrate	$CH_3CH_2CH_2COO^- + 2H_2O \rightarrow 2CH_3COO^- + H^+ + 2H_2$	+48.1	1.6
Propionate	$CH_3CH_2COO^- + 3H_2O \rightarrow CH_3COO^- + HCO_3 + H^+ + 3H_2$	+76.1	1.7
Methanol	$4CH_3OH + 2CO_2 \rightarrow 3CH_3COOH + 2H_2O$	-2.9	1.8
Hydrogen-CO_2	$2HCO_3^- + 4H_2 + H^+ \rightarrow CH_3COO^- + 4H_2O$	-70.3	1.9
Palmitate	$CH_3\text{-}(CH_2)_{14}\text{-}COO^- + 14H_2O \rightarrow 8CH_3COO^- + 7H^+ + 14H_2$	+345.6	2.0

The acetogenic bacteria are obligate hydrogen producers (H^+ serve as internal electron acceptor during regeneration of intracellular electron carriers, like NADH) and their metabolism is thermodynamically inhibited by hydrogen, which immediately follows from the stoichiometric conversion reaction, such as propionate (Henze, 2008):

$$\Delta G' = \Delta G^{\circ\prime} + RT\ln\frac{[\text{Acetate}] * [CO_2] * [H_2]^3}{[\text{Propionate}]} \qquad (1.1)$$

Acetogenic conversions have elucidated the required narrow associations between the H_2-producing acetogenic bacteria and the H_2-consuming methanogenic bacteria, thereby resulting the H_2 level in their environment (Henze, 2008). Syntrophy is a situation where two different organisms degrade the substance – and conserve energy doing it – that neither can degrade individually. Syntrophic reaction in AD is a secondary fermentation, in which acetogenic bacteria ferment the fermentation products of other anaerobes. The heart

of syntrophic reaction is H_2 production by one partner linked to H_2 consumption by another. Syntrophy is also known as inter species H_2 transfer (Madigan et al., 2006). Schematic diagram of syntrophic reaction is displayed in Figure 1.2.

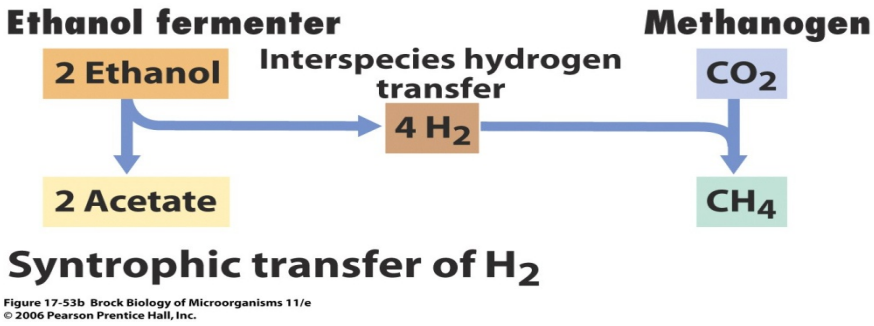

Figure 1.2 Syntrophy: Inter species H_2 transfer (Madigan et al., 2006)

The thermodynamics of syntrophic acetogenesis and hydrogen – utilising methanogenic reactions are only possible in a narrow range of hydrogen or formate concentrations (and are also influenced to a lesser degree by other product and substrate concentrations). This is important for modelling, as the thermodynamic limitations largely determine the parameter for hydrogen inhibition, as well as half saturation coefficients and yields. The limitations are illustrated in Figure 1.3, which shows the thermodynamic yield ($\Delta G'$) for methanogenesis and three anaerobic oxidation reactions. The shaded region indicates where methanogenesis and propionate oxidation are simultaneously possible(Batstone et al., 2002). Thus, there is an upper limit, set by the acetogens, and a lower limit set by the methanogens of syntrophic thermodynamically transfer of VFA's to methane. The local hydrogen concentration must be kept within this so called "hydrogen window", which is in between the partial pressures of 10^{-4} to 10^{-6} bars, otherwise autotrophic methanogens or acetogens will be inhibited (Kommedal, 2008).

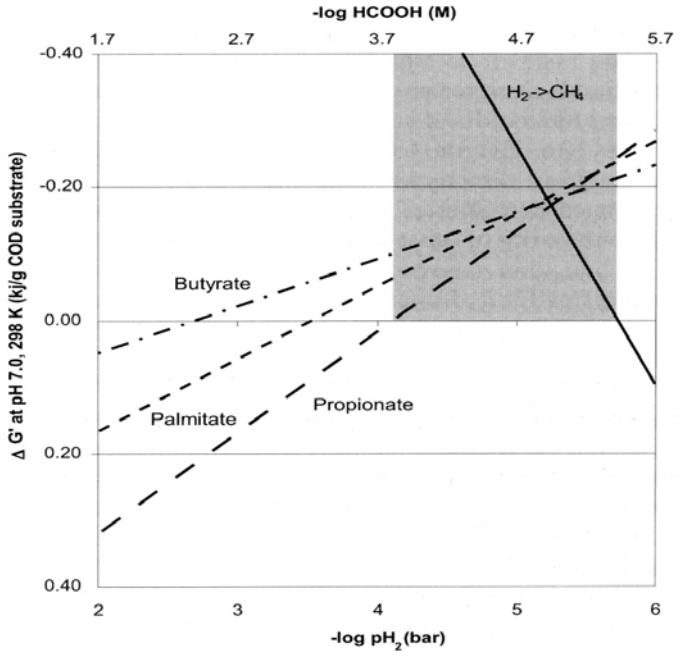

Figure 1.3 Free energy changes as a function of the H_2 partial pressure (Batstone et al., 2002)

1.3.5 Methanogenesis

Methanogenic bacteria accomplish the final stage in the overall anaerobic conversion of organic matter to methane and carbon dioxide. During this fifth and last stage of AD of organic matter, a group of methanogenic archea both reduce carbon dioxide using hydrogen as electron donor (autotrophic methanogens) and decarboxylate acetate to form CH_4 and CO_2 (heterotrophic methanogens). It is only in this stage, when the influent COD is converted to a gaseous form that COD leaves the liquid phase of the reactor system (Henze, 2008). The most important precursor is acetate (70%), while the remaining 30% is formed from H_2/CO_2 or formate (Angelidaki et al.). Methanogens are classified into two major groups: the acetate converting or aceticlastic methanogens and the hydrogen utilising or hydrogenotrophic methanogens (Table1.4).

Table 1.4 Most important methanogenic reactions, the corresponding free energy change (ΔG°′) and some kinetic properties (Henze, 2008)

Functional step	Reaction	ΔG°′ kJ/mole	μ_{max} 1/d	T_d d	K_S mgCOD/l	Eq.
Acetotrophic Methanogenesis*	$CH_3COO^- + H_2O \rightarrow CH_4 + HCO_3^-$	-31	0.12[a] 0.71[b]	5.8[a] 1.0[b]	30[a] 300[b]	2.2
Hydrogenotrophic Methanogenesis	$CO_2 + 4H_2 \rightarrow CH_4 + 2H_2O$	-131	2.85	0.2	0.06	2.3

*Two different methanogenesis belonging to [a]Methanosarcina spec. and [b]Methanosaeta spec.

Table 1.4 lists two types of aceticlastic methanogens with very different kinetic parameters.

1.4 General Aspects of Codigestion

Codigestion of organic wastes is a technology that is increasingly being applied for simultaneous treatment of several solid and liquid organic wastes. The main advantages of this technology are improved methane yield because of the supply of additional nutrients from the codigestates and more efficient use of the equipment and cost-sharing by the processing multiple waste stream in a single facility. Codigestion of organic wastes with municipal wastewater sludge can increase digester gas production and provide savings in the overall energy costs of plant operations (Alatriste-Mondragon et al., 2006).

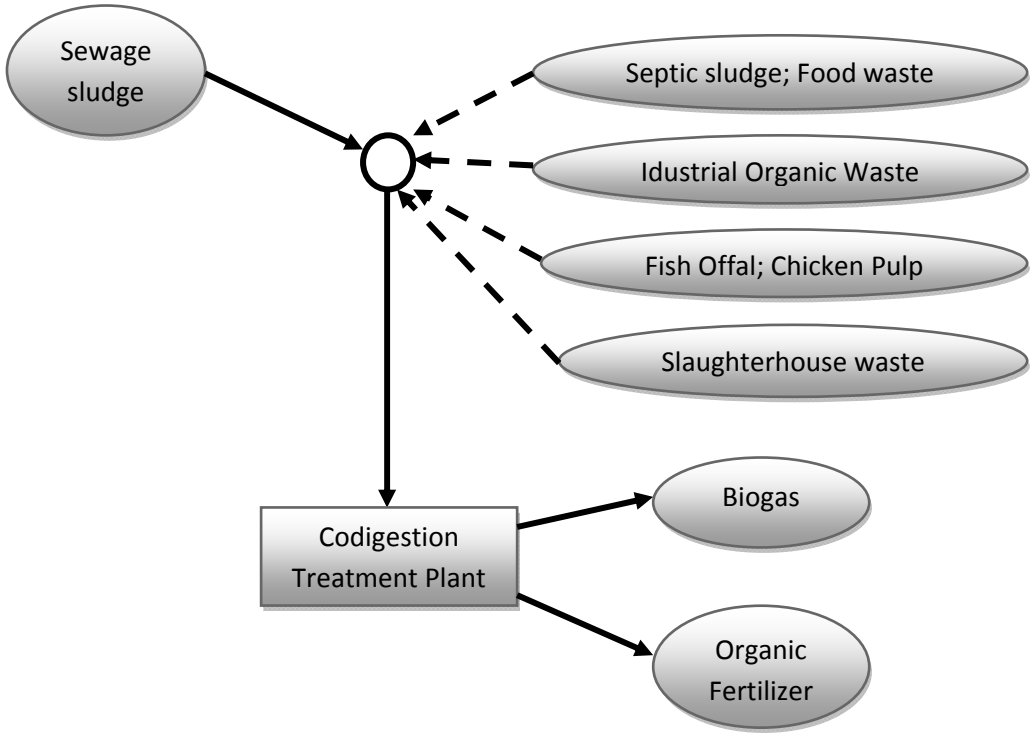

Figure 1.4 Principle of codigestion at SNJ plant; Based on (Hartmann et al., 2002)

(Hartmann et al., 2002) evaluated the profit of codigestion in the anaerobic degradation process that is mainly within the following areas:

- Increasing the methane yield.
- Improving the process stability.
- Achieving better handling of the waste.

Waste treatment by codigestion is economically more favourable due to:

- Combination of different waste streams in one common treatment facility.

- Treatment of larger waste amounts in the centralized large-scale facility.

Generally, the key for codigestion lies in balancing several parameters in the co-substrate mixture (Figure 1.5). Some qualities of each co-substrate can be advantageous for use in the biogas process while other qualities can hinder the degradation solely of this waste type (Hartmann et al., 2002).

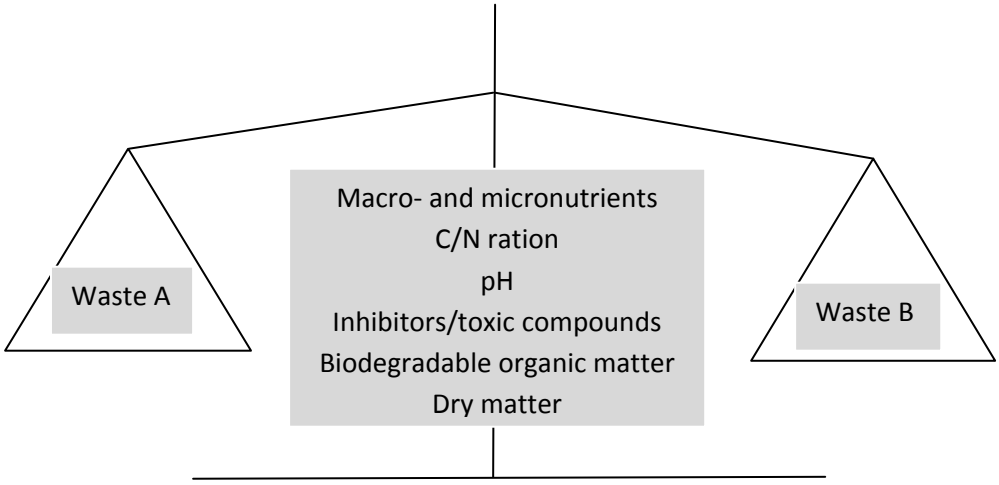

Figure 1.5 The balance of codigestion (Hartmann et al., 2002)

1.5 Modelling of Anaerobic Digestion

(Henze, 2008) evaluated the most prominent advantages of the use of model in anaerobic digestion. These are the following:

- getting inside into plant performance
- evaluating possible scenarios for upgrading
- evaluating new plant design
- supporting management decisions
- developing new control schemes
- providing operator training

The second main reason for using model is the possibility of saving time and money in the process of technology/process selection. Comparison of the system performance in a quantitative instead of a qualitative way allows in many cases for easier decision-making and rapid comparison of options (Henze, 2008).

Another strong reason for using model is the possibility of minimizing risks. By using model, 'what if' scenarios can be examined in a quantitative way in respect of what the effects of

potential risks are. Furthermore, application of models improves knowledge transfer and decision-making (Henze, 2008).

1.6 Case Study

1.6.1 Rogaland Country

Total surface area of Rogaland (including mainland and islands) is 9,325 square kilometres, which represents approximately 2.9% of the country's total area. The region has very versatile and dynamic industry which is dominated by oil and gas related business (30.000 employees compared to the total population of Rogaland which is 408.450). Besides that, the county is also a great producer of electricity and agricultural products. Jæren is the country's major producer of meat, dairy products and vegetables. Approximately 25% of meat production in Norway originates from Rogaland. In addition, large parts of the Norwegian fishing industry takes place in Rogaland. Egersund is one of the largest fish landing ports; large farming companies are located in Stavanger and the Stavanger region is one of the world's largest producers of fish feed (Fylkeskommune, June 2010).

The Regional Wastewater Treatment Plant of Nord-Jæren (SNJ) receives and treats wastewater from residential and industrial sources in the municipalities of Randaberg, Stavanger, Sola, Sandnes and Gjesdal. The design capacity corresponds to a total number of inhabitants and population equivalents (PE) of approximately 240 000. The plant is located at Mekjarvik, where the wastewater facilities of SNJ are located inside a hill (rock) while the sludge treatment and administration building and workshop facilities were built outside the rock. SNJ plant was put in operation 18 years ago in March 1992 (www.ivar.no). On this basis, effective monitoring, process control (operation) and if required expansion of SNJ is of continuous concern. During this master thesis project operation of this plant was studied and a program for process analysis (by measurements) was performed in order to evaluate and better understand the factors affecting sludge treatment process efficiency.

1.6.2 SNJ Plant

The regional network of IVAR facilities in Rogaland County is shown in figure including the SNJ at Mekjarvik. The plant comprises an 8 km tunnel from Bjergsted in Stavanger, as well as a 4 km outlet tunnel to Håsteinfjorden with discharge at a water depth of 80 meters, 1.2 km offshore. The plant is constructed as a primary precipitation plant where the wastewater is mechanically pre-treated in screens and aeration grit chambers, and then chemicals are introduced to initiate precipitation. Flocculated solid particles are separated from liquid phase in sedimentation tanks. Two separate trains of mechanical and chemical treatment processes ensure a high level of operational flexibility according to the actual wastewater load arriving to the plant (www.ivar.no).

Following Figure 1.6 represents IVAR facilities including SNJ plant which was case study in this project.

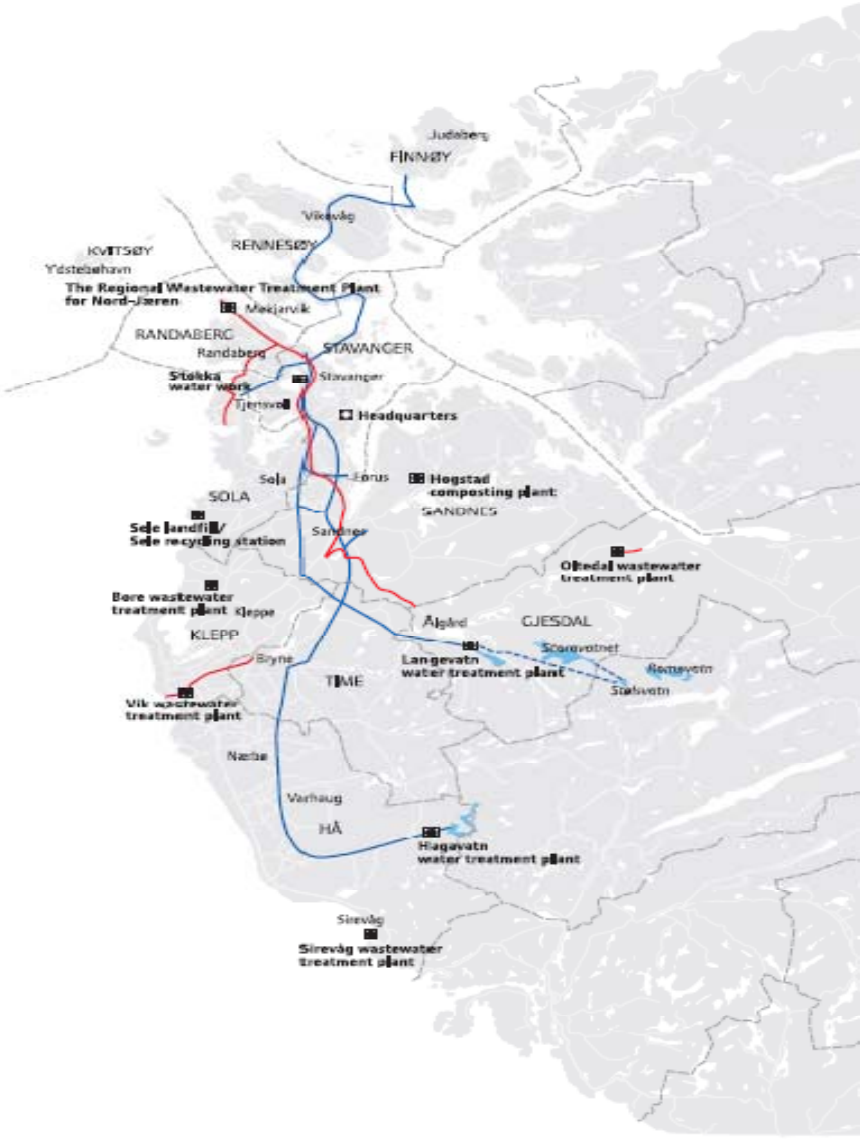

Figure 1.6 The network of wastewater treatment facility in Rogaland region (www.ivar.no)

At SNJ there are six sedimentation basins, which serve to separate solids from suspension in the liquid. When the basins are filled up with wastewater, approximately 50% of suspended solids matter will settle down. Precipitated solid material (raw sludge) is removed by a skimmer from the bottom of basin into a sludge thickening well inside the sedimentation basin. Thickened (raw) sludge is pumped to a 500 m^3 buffer tank. According to design, raw sludge should be fresh before anaerobic processes become active, however, it will become putrescent in a short time if left for prolonged time during storage (http://en.wikipedia.org/wiki/Sludge, June 2010). Figure 1.7 shows the sedimentation basins at SNJ plant.

The SNJ plant receives wastewater sludge from six municipalities in the IVAR region. The solid content of wastewater is relatively low, the raw sludge consists of 95% water, which means that the dried solids content amounts to just 5%. At SNJ, the municipal wastewater sludge is the main waste most often used in the codigestion process which balances the solids contents in the reactors (slurry mode). Wastes that are codigested with these main wastes are industrial food waste, industrial organic waste, septic sludge, chicken pulp, fish offal (fish ensilage) and organic waste from slaughterhouses. Food waste comes from food processing industry. It has high sugar and carbohydrate content and normally comes with a high temperature around 75 °C. Up to the certain level this will contribute to the disintegration and hydrolysis processes.

Figure 1.7 Sedimentation basin (www.ivar.no)

The cross section of the plant at SNJ (see Figure 1.8) shows the facilities, (located inside the rock) where the mechanical pre-treatment and chemical treatment takes place. Good stabilisation of waste can only be possible if the separation system guarantees a good quality collected waste, in terms of low contamination from plastics and inert materials.

Figure 1.8 Cross section of SNJ plant (www.ivar.no)

The schematic flow diagram below (Figure 1.9) shows that the SNJ plant is composed of two reactors (anaerobic digesters), two heat exchangers and two buffer tanks. The output from sedimentation basins first arrives to the buffer tank. Buffer tank 1 (500 m^3) serves as storage for feeding the reactors. It receives raw sludge as described above, in addition to external wastewater sludge (including septic sludge), industrial food waste, slaughterhouse waste and industrial organic waste. Decomposition and digestion of wastes takes place in the reactors. The sizes of reactors are 3500 m^3 and a headspace volume available for short term gas storage inside each reactor of 226 m^3.

When SNJ plant receives fish offal and chicken pulp wastes, these raw materials can be pumped directly into the reactors or to the buffer tank. The function of the buffer tank is important in maintaining a uniform organic and hydraulic load to the reactors. To facilitate constant conditions in the reactors the sludge is pumped to the digesters in a 1 hour cycle at 20 m^3/h (thus, the hydraulic loading per reactor is approximately 240 m^3/d).

The sludge input to reactors approximately equals the amount of sludge leaving the system. Digested sludge is stored in buffer tank 2 and subsequently dewatered in decanter centrifuges. In order to enhance pathogen kill, it is important to withdraw digested sludge from the digesters before adding fresh feed.

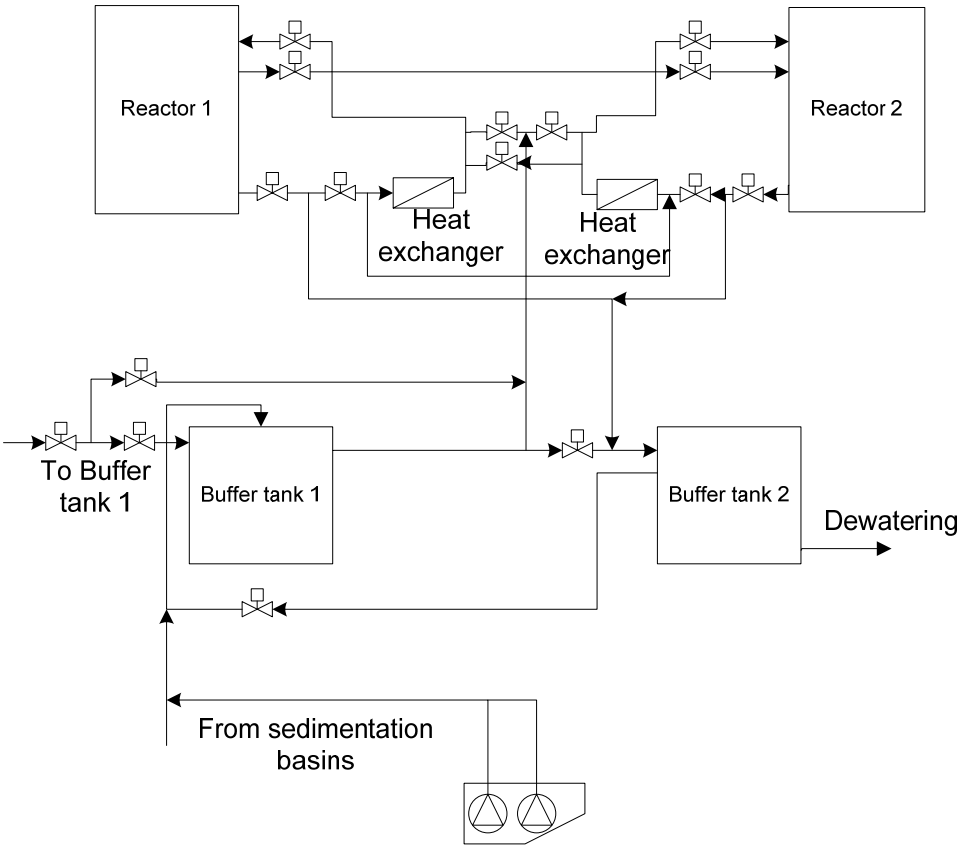

Figure 1.9 Flow diagram of SNJ plant

Inlet heat exchangers ensure that the reactors operate at constant mesophilic conditions maintained at 37°C. High-rate digesters are heated in order to increase disintegration, hydrolysis and methanogenesis rates, as well as to hold digester temperature steady despite fluctuations in the temperature of the incoming sludge (Rittmann and McCarthy, 2001).

Both digesters at SNJ plant are mixed by injecting compressed biogas into the liquid through diffuser pipes (lances). High-rate digesters are mixed in order to improve mass transfer between microorganisms and their substrates and to prevent formation of scum at the water level and sediments at the bottom (Rittmann and McCarthy, 2001). The goal of mixing is to maintain a high enough liquid velocity so that all the solids remain in suspension.

Following centrifugal dewatering, the resulting sludge is dried using heat from the biogas burners. The solids content of the product after centrifugal dewatering and thermal drying is about 85%. It is extruded into small pellets (biopellets shown in Figure 1.10) which are simple to store (biologically stable), handle and transport. One of the objectives of anaerobic wastewater treatment plant is to ensure that most of the nutrient content in the sludge can be returned to productive soils. The final product should be pathogen, stable (not putrefying) and free of priority pollutants in order to meet governmental standards for recycling of pellets as fertilizer for agricultural use.

Figure 1.10 Biopellets (www.ivar.no)

The waste collection facilities at SNJ plant are displayed in the Figure 1.11. When the plant receives fish offal or chicken pulp waste, they are stored in two tanks known at SNJ plat as green tanks from where they can be directly transferred to reactors. Raw sludge coming from the sedimentation basins and industrial organic waste are pumped in the buffer tank 1 before entering the reactors. SNJ plant receives septic sludge and industrial food waste transported from different locations around the region. These wastes first go through coarse grid and then transferred to the buffer tank 1. The green valves and pump in the Figure 1.11 indicates the waste flow pattern.

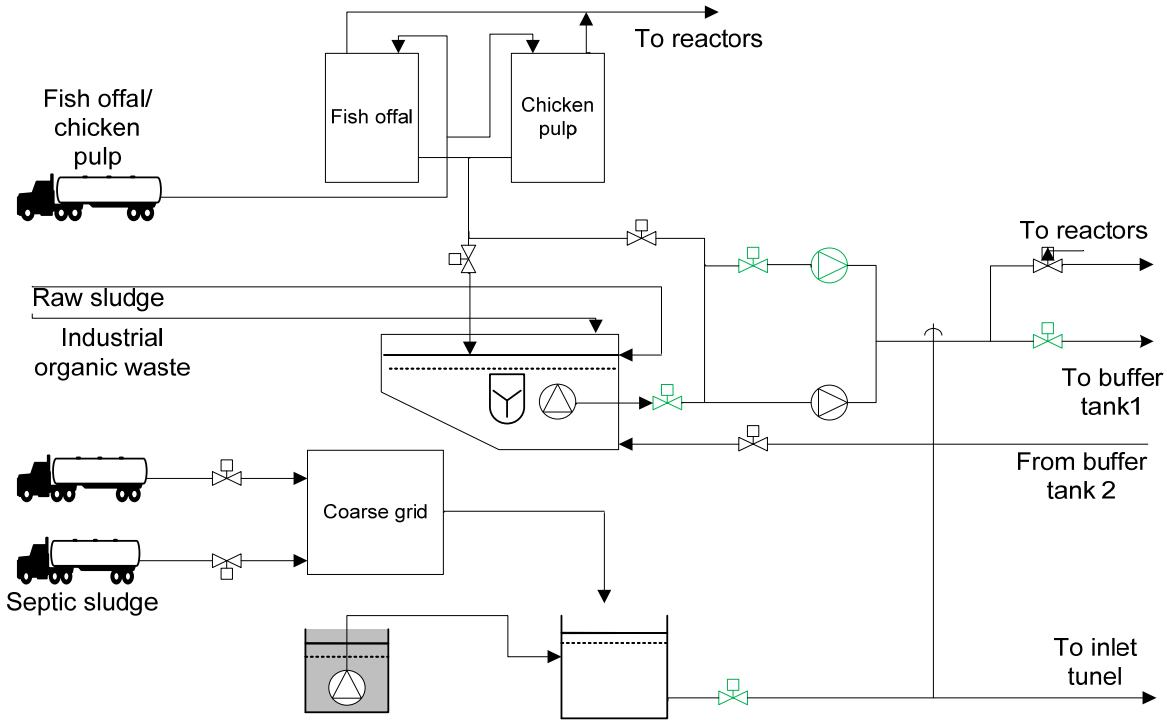

Figure 1.11 Flow diagram of facilities where sludge is received at SNJ plant

2. Materials and Methods

2.1 Model Formulation AQUASIM

In the program AQUASIM, a model consists of a system ordinary and/or partial differential equations and algebraic equations, which deterministically describe the behaviour of a given set of important state variables of an aquatic system. The differential equations for water flow and substance transport can be selected by the choice of environmental or technical compartments, which can be connected by links (Reichert, 1998). Figure 2.1 visualizes the mutual dependencies between four subsystems of variables, processes, compartments and links.

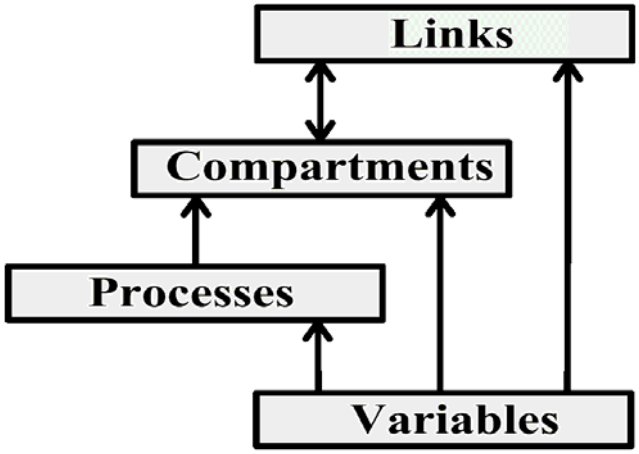

Figure 2.1 Main elements of model structure (Reichert, 1998)

The basic system of the AQUASIM model structure is the system of variables. Variables are objects which are characterized by the property of taking numerical value. This value may depend on the values of other variables. Seven types of variables are distinguished: State, program, constant, real list variables, variable list variables, formula and probe variables. The system of variables serves as a pool of variables for the formulation of the other subsystems (Reichert, 1998).

The next system of AQUASIM model structure is the system of processes. Two types of processes are distinguished: Dynamic and equilibrium processes. The next subsystem of the AQASIM model structure is the system of compartments. This subsystem is design to spatially divide the system under investigation. The last subsystem of the AQUASIM model structure is the system of links. The objects of this subsystem are used to connect the compartments to the desired spatial configuration. To connect the compartments two types of links are distinguished: advective and diffusive links (Reichert, 1998).

2.2 Nomenclature, State Variables and Expressions

The IWA Anaerobic Digestion Model No. 1 (ADM1) introduces generic nomenclature, units and definitions. IWA Task Group uses the empirical formula of $C_5H_7O_2N$ to represent biomass as in Activated Sludge Model (ASM) series.

2.2.1 Units

(Batstone et al., 2002) had chosen COD (kgCOD m^{-3} = gCOD m^{-1}) as the chemical component base unit because of its use as a wastewater characterisation measure in concentrated stream, its use in upstream and gas utilisation industries, the implicit balancing of carbon oxidation state and to enable partial compatibility with the IWA Activated Sludge Models. Molar basis (kmole m^{-3} = M) is used for components with no COD such as inorganic carbon (CO_2 and HCO_3^-) and inorganic nitrogen (NH_4^+ and NH_3). A molar (M) and kgCOD m^{-3} basis was chosen to facilitate $\log_{10}$ conversion (e.g. pH and pK_a) for physic-chemical equation (Batstone et al., 2002).

Table 2.1 Units (Batstone et al., 2002)

Measure	Units
Concentration	kgCOD m^{-3}
Concentration (non-COD)	kmoleC m^{-3}
Concentration (nitrogen non-COD)	kmoleN m^{-3}
Pressure	bar
Temperature	K
Distance	m
Volume	m^3
Energy	J (kJ)
Time	d (day)

2.2.2 Nomenclature and Description of Parameters and Variables

There are four main parameters and variables: stoichiometric coefficients, equilibrium coefficients, kinetic parameters, and dynamic state and algebraic variables.

Table 2.2 Stoichiometric coefficients (Batstone et al., 2002)

Symbol	Description	Units
C_i	Carbon content of component I	kmoleC $kgCOD^{-1}$
N_i	Nitrogen content of component i	kmoleN $kgCOD^{-1}$
$V_{i,j}$	Rate coefficient for component I on process j	nominally kgCOD m^{-3}
$F_{product,substrate}$	Yield (catabolism only) of product on substrate	kgCOD $kgCOD^{-1}$

Table 2.3 Equilibrium coefficients and constants (Batstone et al., 2002)

Symbol	Description	Units
H_{gas}	Gas law constant (equal K_H^{-1})	bar M^{-1} (bar m^{-3} $kmole^{-1}$)
$K_{a,acid}$	Acid-base equilibrium coefficient	M (kmole m^{-3})
K_H	Henry's law coefficient	M bar^{-1} (kmole $m^{-3}bar^{-1}$)
pK_a	$-\log_{10}[K_a]$	
R	Gas law constant ($8.314x10^{-2}$)	bar $M^{-1}K^{-1}$(bar m^3 $kmole^{-1}$ K^{-1})
ΔG	Free energy	J. $mole^{-1}$

Table 2.4 Kinetic parameters and rates (Batstone et al., 2002)

Symbol	Description	Units
$K_{A/Bi}$	Acid base kinetic parameter	$M^{-1}d^{-1}$
k_{dec}	First order decay rate	d^{-1}
$I_{inhibitor,process}$	Inhibition function (see K_I)	
$K_{process}$	First order parameter(for hydrolysis)	d^{-1}
k_La	Gas-liquid transfer coefficient	d^{-1}
$K_{I,inhibit,\ substrate}$	50% inhibitory concentration	kgCOD m^{-3}
$K_{m,process}$	Monod maximum specific uptake rate (μ_{max}/Y)	kgCOD_S $kgCOD\_X^{-1}$ d^{-1}
$K_{S,process}$	Half saturation value	kgCOD_S m^{-3}
ρ_j	Kinetic rate of process j	kgCOD_S $m^{-3}d^{-1}$
$Y_{substrate}$	Yield on biomass on substrate	kgCOD_X $kgCOD\_S^{-1}$
μ_{max}	Monod maximum specific growth rate	d^{-1}

Table 2.5 Dynamic state and algebraic variables (and derived variables) (Batstone et al., 2002)

Symbol	Description	Units
pH	$-\log_{10}[H^+]$	
$p_{gas,i}$	Pressure of gas i	bar
P_{gas}	Total gas pressure	bar
S_i	Soluble component i	kgCOD m^{-3}
$t_{res,X}$	Extended retention of solids	d
T	Temperature	K
V	Volume	m^3
X_i	Particulate component	kgCOD m^{-3}

2.2.3 Dynamic State Variables

Dynamic state variables are those calculated at a specific time (t) as solutions of the set of differential equations (defined by the ADM1 process rates), the process configuration modelled, inputs, and the initial conditions. As such, when a differential algebraic equation

(DAE) implementation is used, the state of a system at time = t is fully defined by the value of these 26 variables in each vessel (Batstone et al., 2002).

Table 2.6 Dynamic state variable characteristic (DAE) system (Batstone et al., 2002)

Name	I	Description	Units	MW	gCOD·mole^{-1}	Carbon content (C_i)	Nitrogen content (N_i)
X_c	13	Composite		varies	Varies	varies	Varies
X_{ch}	14	carbohydrates		varies	varies	0.0313	varies
X_{pr}	15	proteins		varies	varies	varies	varies
X_{li}	16	lipids		806	2320	0.0220	0
X_I	24	particulate inerts		varies	varies	varies	varies
S_I	12	soluble inerts		varies	varies	varies	varies
S_{su}	1	monosaccharide's		180	192	0.0313	0
S_{aa}	2	amino acids		varies	varies	varies	Varies
S_{fa}	3	total LCFA		256	736	0.0217	0
S_{va}	4	total valerate		102	208	0.0240	0
S_{bu}	5	total butyrate		88	160	0.0250	0
S_{pro}	6	total propionate		74	112	0.0268	0
S_{ac}	7	total acetate		60	64	0.0313	0
S_{h2}	8	hydrogen		2	16	0	0
S_{ch4}	9	methane		16	64	0.0156	0
S_{IC}	10	inorganic carbon	M	44	0	1	0
S_{IN}	11	inorganic nitrogen	M	17	0	0	1
X_{su-h2}	17-23	biomass		113	160	0.0313	0.00625
S_{cat}		cations	M	varies	0	0	0
S_{an}		anions	M	varies	0	0	0

2.3 Biochemical Processes

2.3.1 Structure of Biochemical Reactions in the ADM1

The model includes the three overall biochemical (cellular) steps (acidogenesis [fermentation], acetogenesis [anaerobic oxidation of organic acid] and methanogenesis) as well as an extracellular (partly non-biological) disintegration step and an extracellular hydrolysis step (figure 2.2). Three of the processes (hydrolysis, acidogenesis and acetogenesis) have a number of parallel reactions. Complex composite particulate waste is assumed to be homogeneous, which disintegrates to carbohydrate, protein and lipid particulate substrate (Batstone et al., 2002).

The IWA Task Group agreed upon, because this was mainly included to facilitate modelling of waste activated sludge digestion, a disintegration step is thought to precede more complex hydrolytic steps, but is also generally used when the primary substrate can be represented with lumped kinetic and biodegradability parameters (e.g. primary sludge and other substrates). The complex particulate pool is also used as a pre-lysis repository of dead biomass. Therefore the disintegration step is intended to include an array of steps such as lysis, non-enzymatic decay, phase separation and physical breakdown (e.g. shearing) (Batstone et al., 2002).

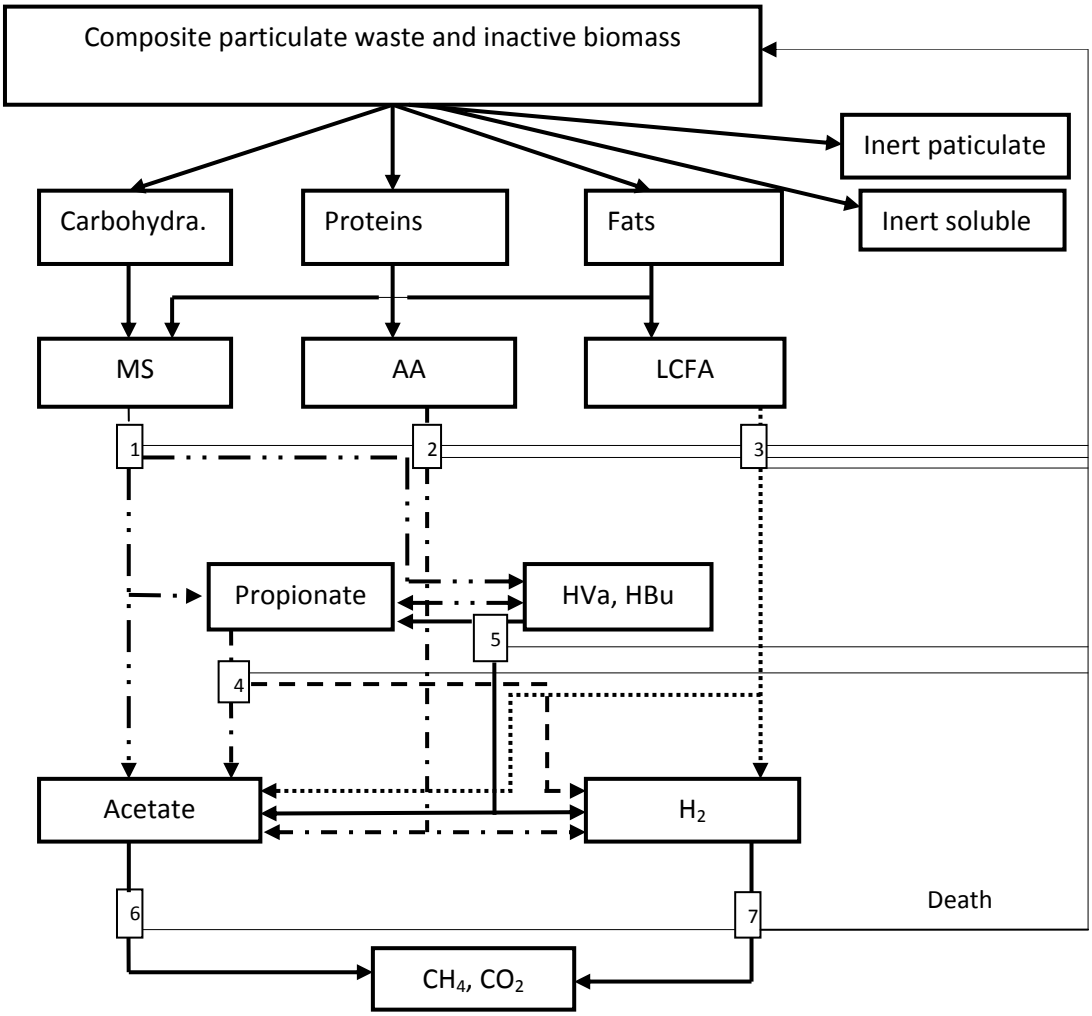

Figure 2.2: The anaerobic model as implemented including biochemical processes (1) acidogenesis from sugars; (2) acidogenesis from amino acids; (3) acetogenesis from LCFA; (4) acetogenesis from propionate; (5) acetogenesis from butyrate and valerate; (6) aceticlastic methanogenesis; and (7) hydrogenotrophic methanogenesis (Batstone et al., 2002).

All extracellular steps were assumed to be first order, which is an empirical function reflecting the cumulative effect of a multi-step process. Cellular kinetics is described by three expressions (uptake, growth, decay; see table 1.1 and 1.2 in Appendix A).

The key rate equation is substrate uptake, which is based on substrate level Monod-type kinetics. (Batstone et al., 2002) chose substrate uptake related kinetics (rather than growth related kinetics) to decouple growth from uptake, and allow variable yield.

2.4 Model Presentation in Matrix Format

The process rate and stoichiometry matrix for ADM1 biochemical reactions are given in Table 1.1 (soluble components) and Table 1.2 (particulate components) in Appendix A. For each component, the mass balance within the system boundary can be expressed as follows:

Accumulation = Input – Output + Reaction

The input and output terms describes flow across the system boundaries, and depend on physical characteristics of the system modelled. Within the reaction term, there are a number of specific processes (such as growth, hydrolysis, decay, etc.) that also influence other components. The matrix method represents the reaction terms for each component, subdivided by processes. Moving vertically through the matrix the process index (j) changes; while moving horizontally, the component index (i) changes (Batstone et al., 2002). The process index and description is given in the left hand column, while the component index and nomenclature is given in the topmost row. In the right hand column the process rate (ρ_j) for each process is given, while the remainder of each row is filled with stoichiometric coefficient ($V_{i,j}$) that describe the influence of that row's process on individual components. The overall volume-specific reaction term (r_i) for each component i can be formulated by summing the products of the stoichiometric coefficients in column i and their process rates (Batstone et al., 2002):

$$r_i = \sum_j V_{i,j}\rho_j \qquad \text{Eq. 3.1}$$

For example, the overall rate of reaction for monosaccharide's (r_1) is:

$$r_1 \sum_j V_{i,j}\rho_j = \underbrace{k_{hyd,ch}X_{ch}}_{\text{Hydrolysis of Carbohydrates}} + \underbrace{(1 - f_{fa,li})k_{hyd,li}X_{li}}_{\text{Hydrolysis of lipids}} - \underbrace{k_{m,su}\frac{S_{su}}{K_S+S}X_{su}I_1}_{\text{Uptake of sugars}} \qquad \text{Eq.3.2}$$

Matrix presentation method has the advantage, that conversion of COD, nitrogen, and carbon (continuity) can be easily checked. The stoichiometric coefficients (after adjustment to consistent units) for each row should add up to zero, as COD, carbon or nitrogen lost from reactants must flow to products. The matrix format allows easy comparison of different model and facilitates transforming the model into a computer program (Batstone et al., 2002).

2.5 Laboratory Experiments

All experimental data were generated in the laboratory at SNJ. In this study several analyses were done. Parameters which were investigated are pH, chemical oxygen demand (COD), measurement and determination of total solids (TS) and volatile solids (VS), and volatile fatty acids (VFAs). In this section are explained how the experiments were conducted including the names of the instruments and equipments used for these analyses. Methods for wastewater analysis were adapted from standard methods (APHA et al., 2006) according to (Ydstebø, 2008). Grab samples were taken from the reactor 1 and 2, buffer tank, raw sludge, external sludge and food waste using tap points in the process loop into 1000 ml poly ethylene bottles.

pH was measured 2-3 times per day in all compartments. Before measuring pH instrument was calibrated with two different solution pH: 4.01 and pH: 7.00. The instrument type is ORION960 Autochemistry system.

Closed reflux method (APHA et al., 2006) was used for COD analyses. The samples were prepared in the following order:

1. Solution was prepared with 1.1 g of sludge weighted at an analytical balance (two decimals) and then diluted into 250 ml distilled water. This was done because COD is in particulate form.
2. Digestion solution was prepared by dilution of 10.216 g $K_2Cr_2O_7$, previously dried at 150°C for 2 hours into 500 ml distilled water, 167 ml concentrated H_2SO_4 and 33.3 g H_2SO_4. These ingredients were dissolved, cooled to room temperature and diluted to 1000 ml.
3. Sulphuric acid solution was prepared by adding 5.5 g Ag_2SO_4 per kg concentrated H_2SO_4 (ρ=1.84 kg/l), mixed and left to dissolve for 1-2 days.

2.5 ml diluted sludge sample was transferred to a digestion vessel along with 1.5 ml digestion solution and 3.5 ml sulphuric acid solution. Samples were digested for 2 hours at 150°C in HACH heating oven. The samples were colorimetric determined using HACH DR-2000 spectrophotometer wavelength set at 600 nm. Before reading the samples, the instrument was calibrated by the preparation of five calibration standards of known concentration. A zero sample was also prepared containing distilled water for calibration of

zero. Calibration samples were prepared from a standard TOC solution (potassium phthalate) at 1000 mg/l.

For determination of total solids, a clean aluminium plate was weighted on an analytical balance (four decimals). Sample sludge is added to about 3 grams and weighed. The sample was dried at 105°C for around 20 min in a Sartorius/thermo control oven to constant weight. After this the plate and solids weight was determined, and TS found as the difference. To determine volatile solids the plate and sample is combusted at 550°C for 2 hours in Carbolite Furnaces oven. After combusting in the oven, samples were cooled down to room temperature and weight on balance. The volatile solids have combusted and the remaining solids are inorganic (fixed) solids.

Volatile fatty acids (VFAs) were analysed with Ion Chromatograph (IC) type Dionex ICS-3000 at the University of Stavanger. The procedure for preparation of samples for VFAs analysis is following:

1. Equal amounts (approximately 19 g) of sludge were transferred to conical centrifuge tubes and weighted (two decimals). All the analysed samples had the same weight (±0.1 g).
2. Samples were centrifuged at 4400 rpm for 10 min in Eppendorf Centrifuge model 5702. 2 ml supernatant was transferred to a 100 ml beaker and diluted with 18 ml of distilled water. From the diluted sample, 2 ml was filtered into sampler vials for IC analysis using pre-rinsed 0.2 µm syringe filters (PALL Acrodisc with Luer Lock).

During the period of analyses at SNJ plant, several process variables were measured online as part of the operational control system and logged for this project. The loading rates from buffer tanks to reactor 1 and 2, loading rates of sludge collected from sedimentation basins to the buffer tank, external sludge to buffer tank, out of reactor 1 and 2, food waste to buffer tank, gas produced in reactor 1 and 2, and methane content in the gas (Table 3.12) were all logged by the process control room (Osli, 2010).

3 RESULTS

3.1 Monitoring of Operational Parameters at SNJ Plant

In the first experimental campaign of this study (15-25 March), batch biodegradability assays were carried out with five different proportions of solid waste at mesophilic conditions (37°C) for period of two weeks. A description of the experimental set-up is found in (Ydstebø, 2008). Codigestion of raw waste involves the mixing of various substrates in various proportions. Reduction of organic matter can be measured through the fraction of volatile solids in the waste that are reduced in anaerobic codigestion process. Following the behaviour of organic fraction and inert fraction in the reactors, buffer tank, raw sludge, septic sludge and food waste, the most suitable mix ratios can be determined, in order to maximize the biogas production and solids reduction. Sludge in reactors, buffer tank, raw sludge, external sludge and food waste were characterised regarding their total and volatile solids concentrations (TS and VS respectively), pH, chemical oxygen demand (COD) and volatile fatty acids (VFA's). Experimental data conducted in reactor 1 is represented in Table 3.1.

Table 3.1 Characteristics of sludge in Reactor 1

Data	Time	pH	TS [g/l]	VS [g/l]	COD[kg/m^3]	COD/VSS
16.03	08:00	7.47	49.08	26.60		
17.03	09:00	7.46				
18.03	09:00	7.29	51.11	29.20		
19.03	08:30	7.5	49.47	27.64	45.31	1.64
20.03	12:30	7.39	49.30	27.38	40.09	1.46
22.03	12:00	7.43	48.70	26.85	37.90	1.41
23.03	10:30	7.31	49.59	27.51	32.46	1.18
24.03	08:30	7.3	48.92	27.48	34.09	1.2
24.03	12:00	7.26			36.53	
25.03	08:30	7.29	49.50	27.82		
25.03	12:00	7.25	50.21	28.60		
25.03	15:00	7.34			39.53	1.4

In Graph 3.1 represents the pH in Reactor 1. The pH range is rather constant and is in the range of 7.25 to maximum value of 7.5.

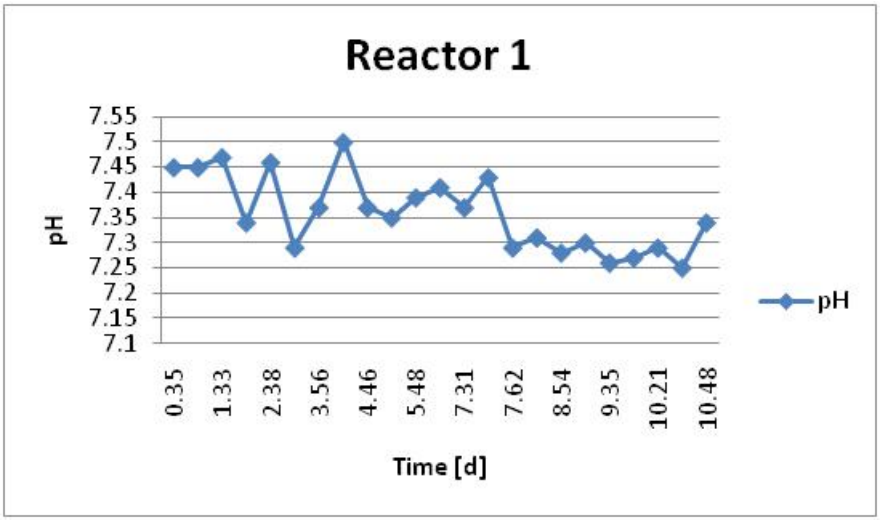

Graph 3.1 Behaviour of pH in the Reactor 1 during the first experimental test (15-25 March)

Data obtained from COD test (Table 3.1) are represented as plot in Graph 3.2. The COD ranges are between 32 and 45 [g/l].

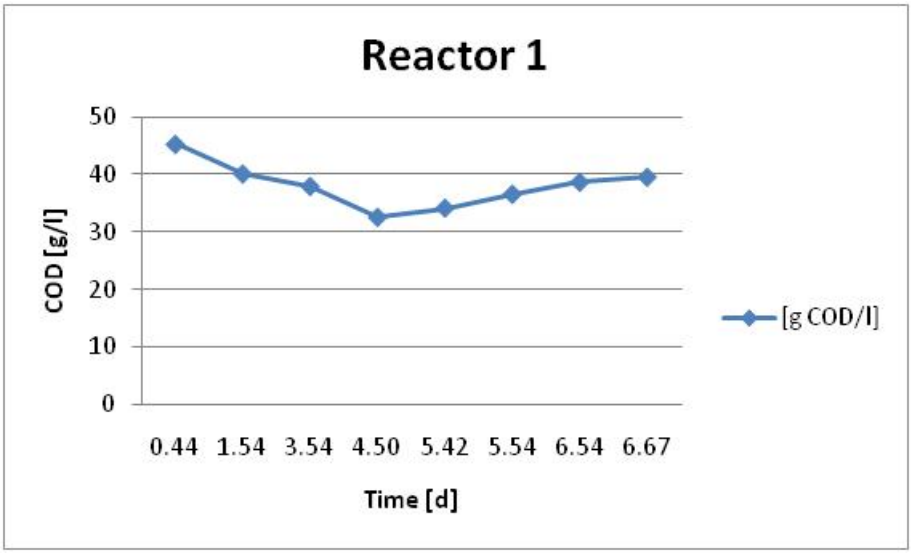

Graph 3.2 COD data obtained in Reactor 1 (15-25 March)

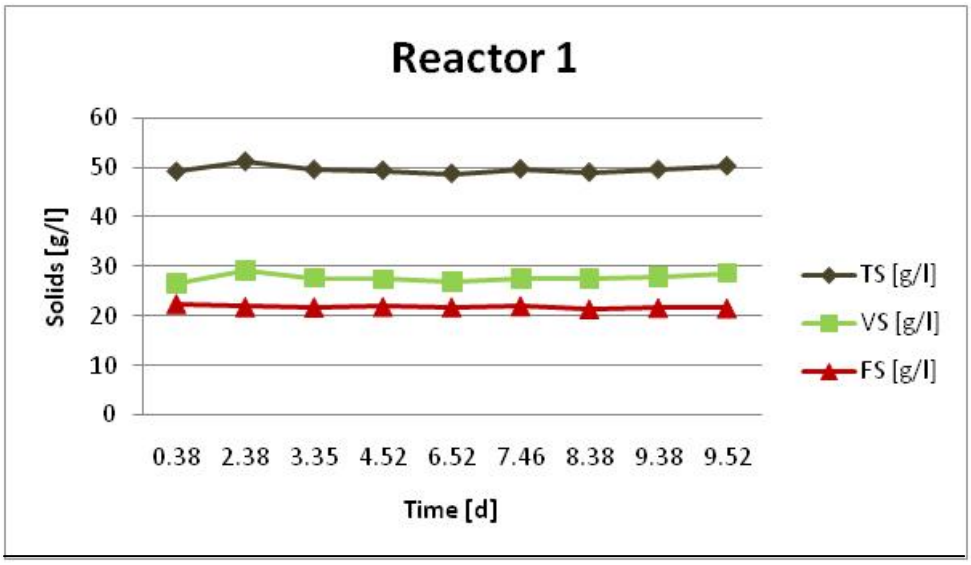

Graph 3.3 Solids content in the Reactor 1

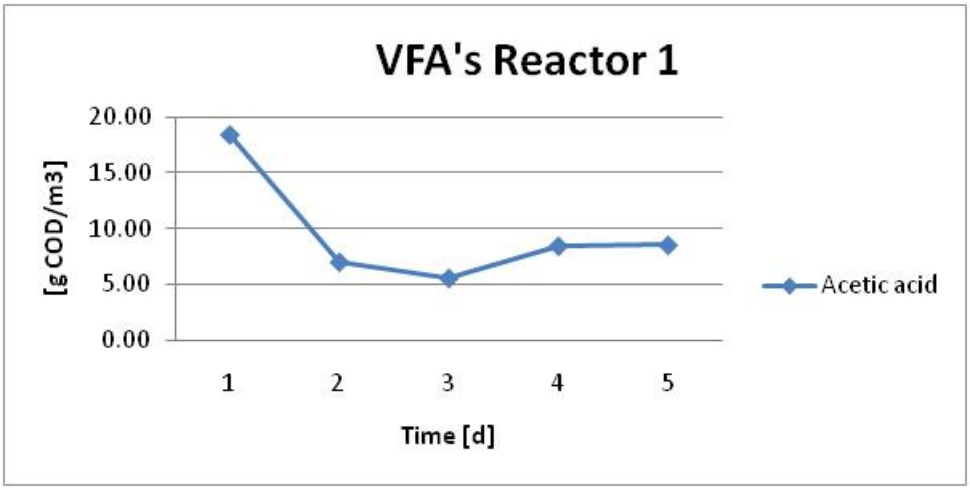

Graph 3.4 Concentration of Acetic acid in reactor 1

Table 3.2 Characteristics of sludge in the Reactor 2

Data	Time	Time[d]	pH	TS [g/l]	VS [g/l]	COD[kg/m3]	COD/VSS
16.03	09:20	0.39	7.39	50.76	28.83		
18.03	09:00	2.39	7.5	50.70	28.55		
19.03	09:30	3.38	7.67	49.73	27.86	36.28	1.30
20.03	12:30	4.40	7.53	50.13	28.19	37.88	1.34
22.03	12:00	6.52	7.32	49.40	27.55	44.38	1.61
23.03	10:30	7.50	7.3	49.89	43.37	37.09	
24.03	08:30	8.44	7.24	49.30	27.73	40.44	1.46
25.03	08:30	9.35	7.23	50.33	28.72		
25.03	12:00	9.35	7.34	48.99	27.55	41.38	1.44
25.03	15:00	9.50				40.63	1.47

Behaviour of the pH in the reactor 2 is shown in Graph 3.5. The pH range is between 7.23 up to 7.67.

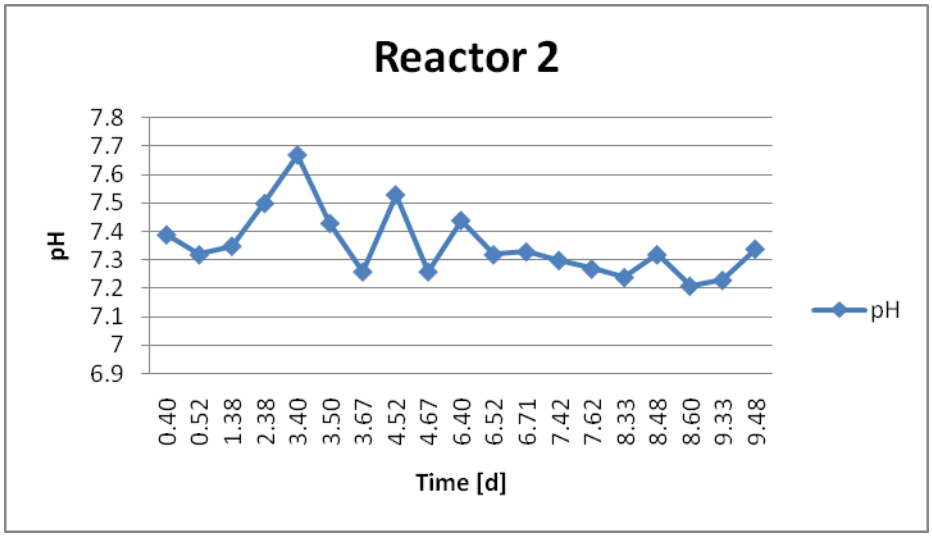

Graph 3.5 Behaviour of pH in Reactor 2

Following Graph 3.6 shows the COD values measured over a period of two weeks.

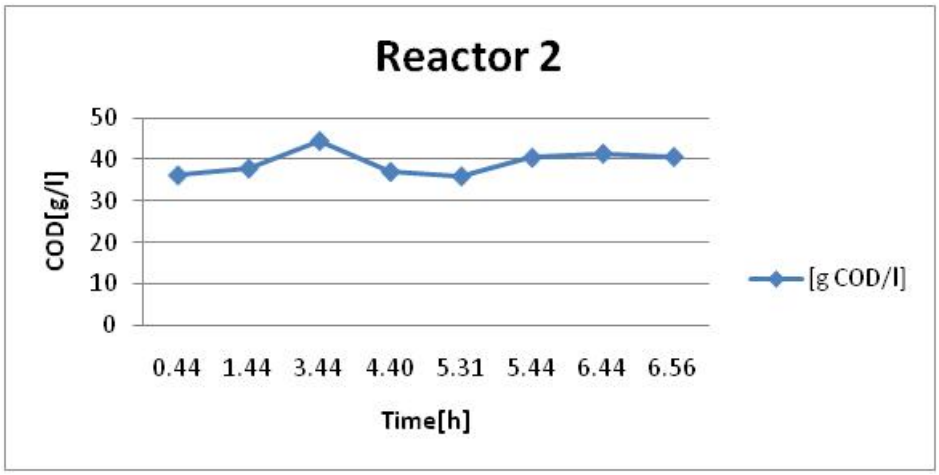

Graph 3.6 COD data obtained in Reactor 2

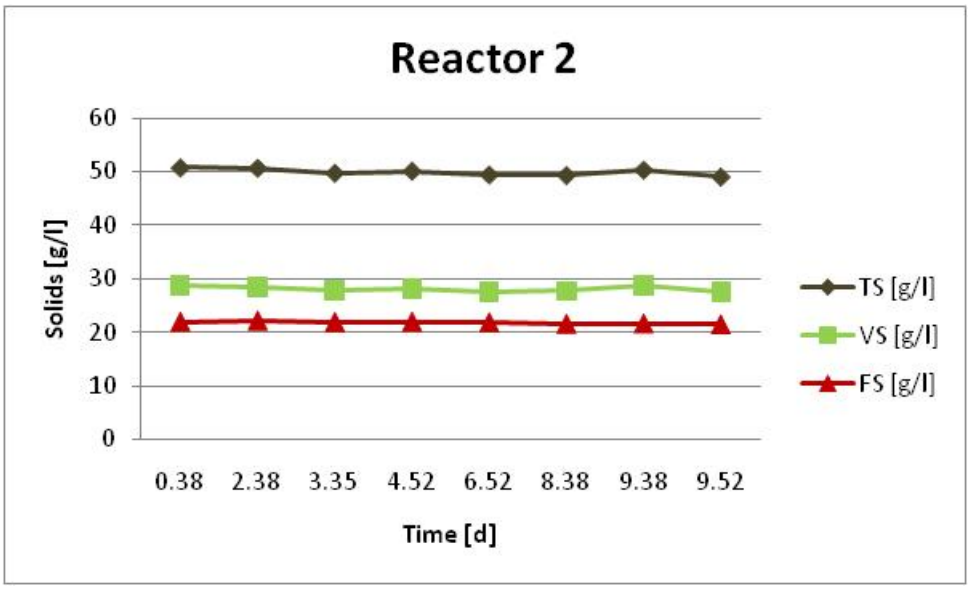

Graph 3.7 Solids content in Reactor 2

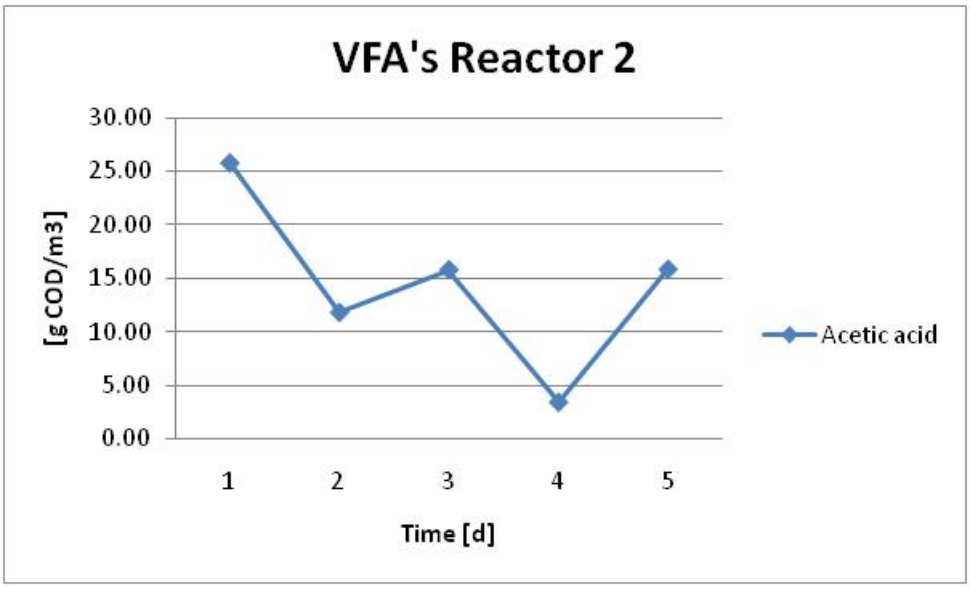

Graph 3.8 Concentration of acetic acid in reactor 2

Following table represents the characteristics of buffer tank. Data is represented in Table 3.3.

Table 3.3 Characteristics of slurry in buffer tank

Data	Time	pH	TS [g/l]	VS [g/l]	COD[kg/m3]	COD/VSS
16.03	09:00	6.37	75.96	53.88		
16.03	12:00	6.46	82.78	58.98		
18.03	09:00	6.44	74.44	54.13		
19.03	08:30	6.49	69.54	48.37	73.78	1.53
19.03	16:00	6.46	73.66	52.61	74.28	1.41
20.03	12:30	6.44	72.82	50.92	69.50	1.36
22.03	12:00	6.48	72.14	51.88	77.84	1.50
23.03	10:30	6.68	74.79	52.25	77.91	1.49
24.03	08:30	6.47	66.11	46.71	81.66	1.75
25.03	08:30	6.53	76.76	52.51	70.63	1.35
25.03	12:00	6.61	72.53	52.07	69.25	1.33

The pH behaviour in buffer tank is shown in Graph 3.9.

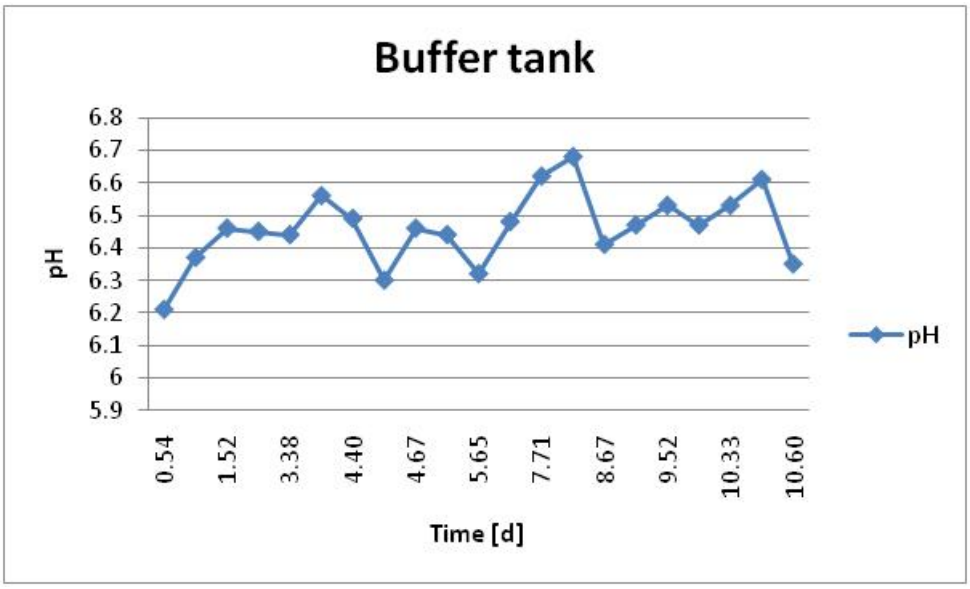

Graph 3.9 Behaviour of pH in Buffer Tank

Graph 3.10 shows COD values measured in Buffer Tank.

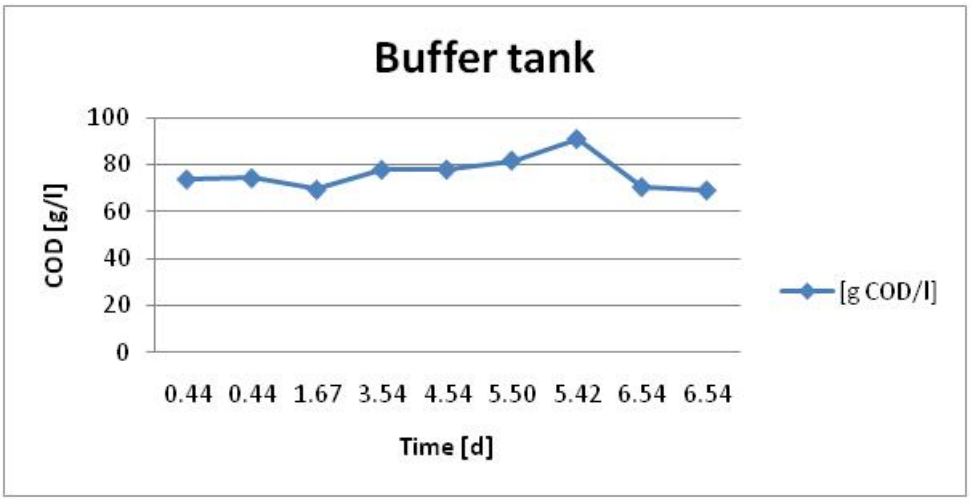

Graph 3.10 COD data obtained in Buffer Tank

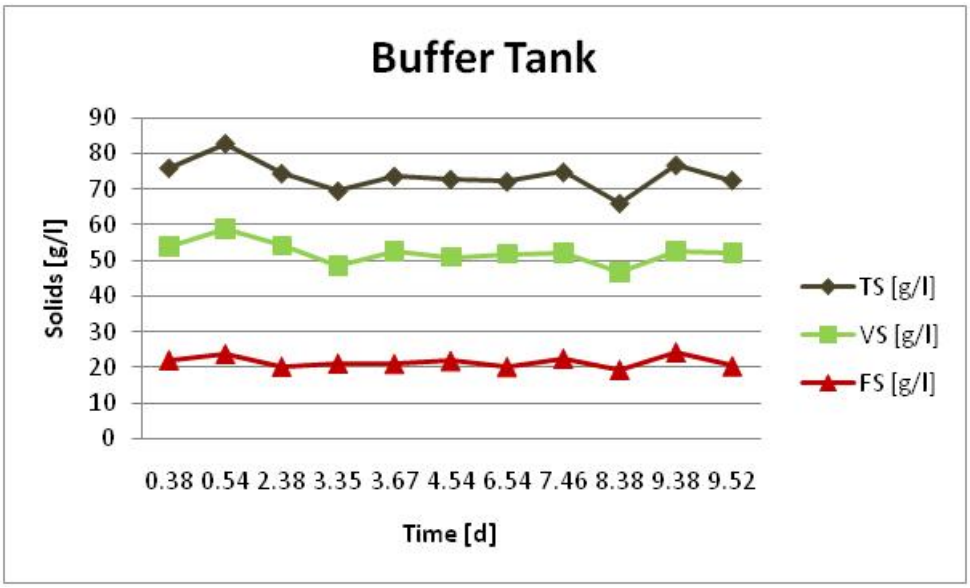

Graph 3.11 Solids content in Buffer Tank

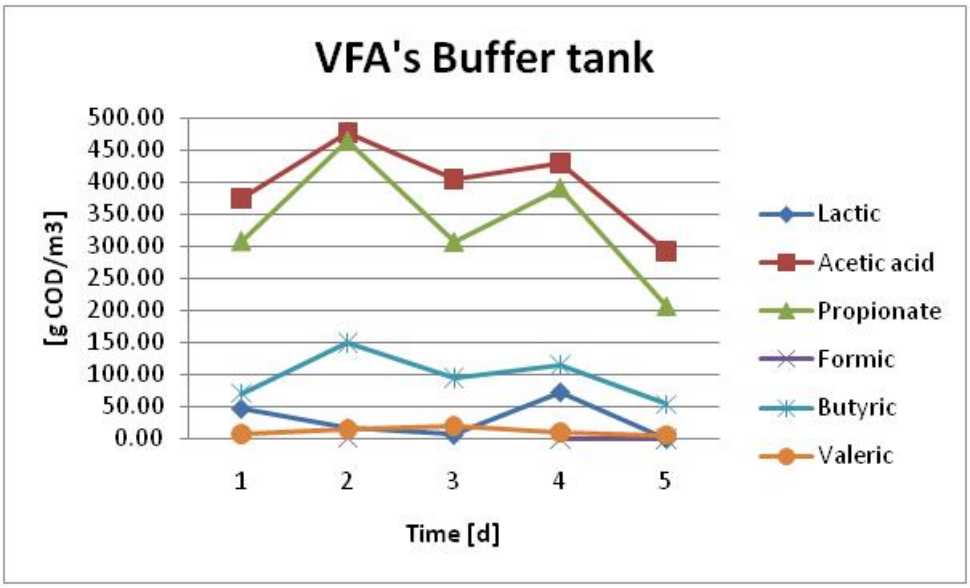

Graph 3.12 Concentrations of volatile fatty acids in buffer tank

Characterization of raw sludge is shown in Table 3.4

Table 3.4 Characterization of raw sludge

Data	Time	pH	TS [g/l]	VS [g/l]	COD[kg/m3]	COD/VSS
16.03	08:30	6.51	70.75	47.68		
18.03	09:00	6.71	71.87	50.33		
19.03	08:30	6.53	100.30	68.92	98.66	1.43
20.03	12:30	6.78	80.19	54.02	79.63	1.47
22.03	12:00	6.68	60.67	41.07	59.50	1.45
23.03	10:30	6.67	60.03	41.80	56.84	1.36
24.03	08:30	6.68	71.03	48.74	68.28	1.40
25.03	08:30	6.65	73.63	52.12		
25.03	12:00	6.69	53.79	39.01	74.72	1.43

Measured pH in raw sludge is represented in Graph 3.13.

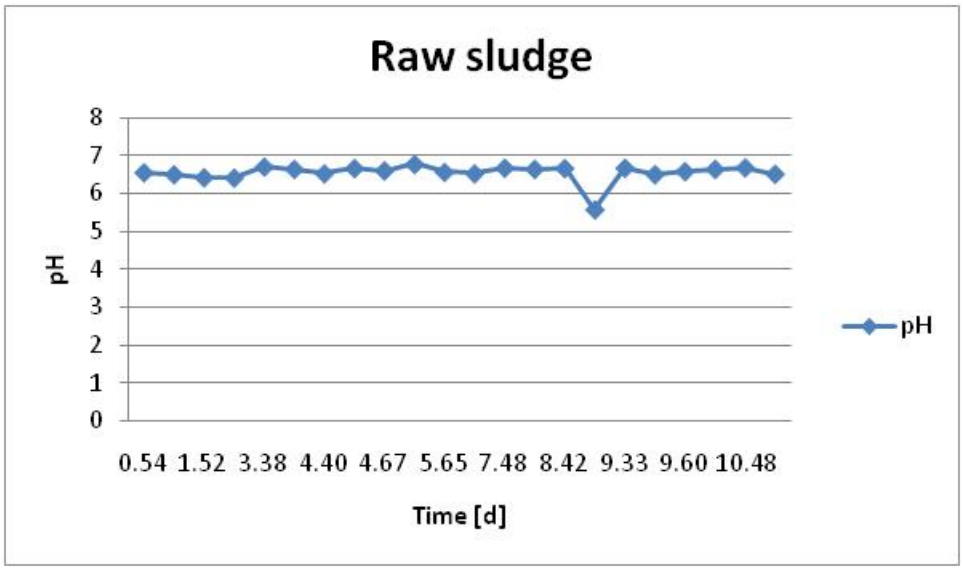

Graph 3.13 Monitoring of pH in raw sludge over time

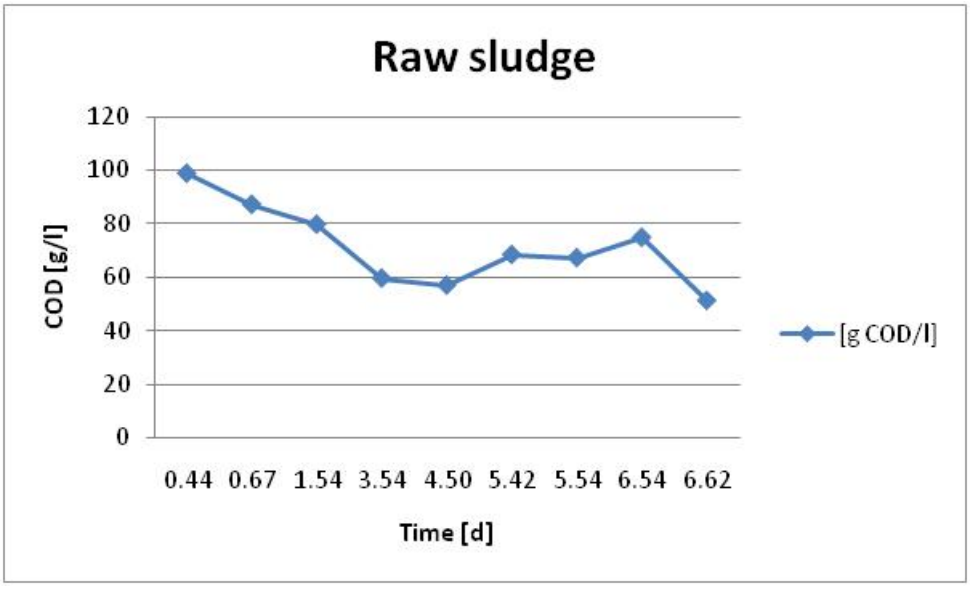

Graph 3.14 COD data obtained in raw sludge

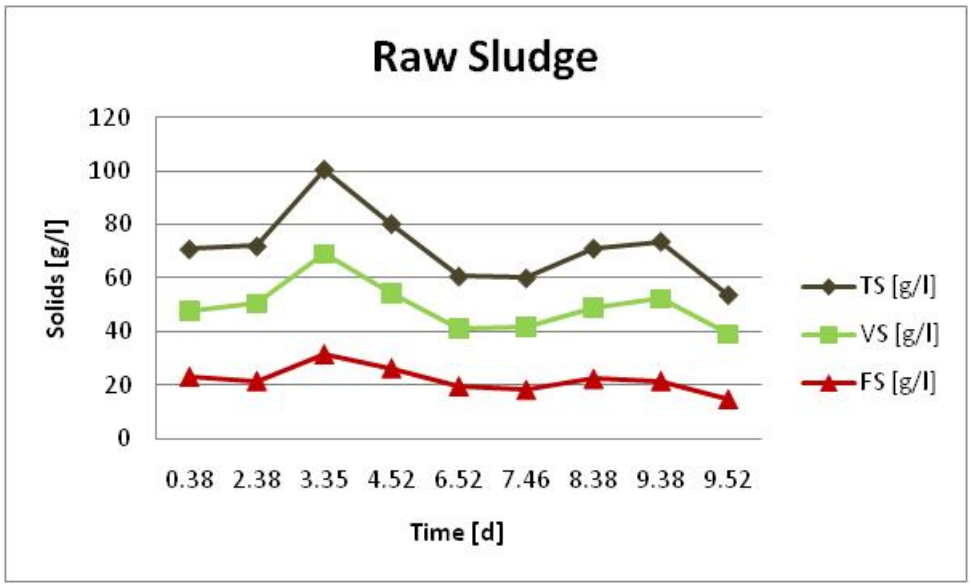

Graph 3.15 Solids content in raw sludge

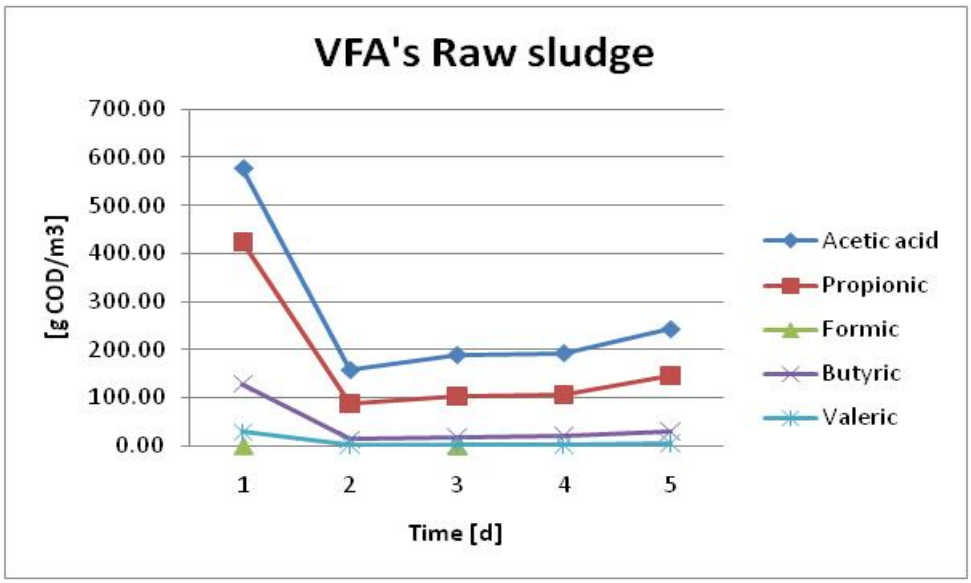

Graph 3.16 Concentration of VFA's in raw sludge

Characteristics of external sludge used in the experiments shown in Table 3.5.

Table 3.5 Characterization of external sludge

Data	Time	pH	TS [g/l]	VS [g/l]	COD[kg/m3]	COD/VSS
16.03	09:00	5.71	91.13	77.37		
16.03	12:30	5.69	92.40	78.31		
18.03	13:30	6.12				
19.03	12:00	5.94				
19.03	16:00	5.83	97.86	84.07	129.00	1.53
22.03	12:00	6.24	86.43	72.41	124.50	1.72
23.03	16:30	6.09				

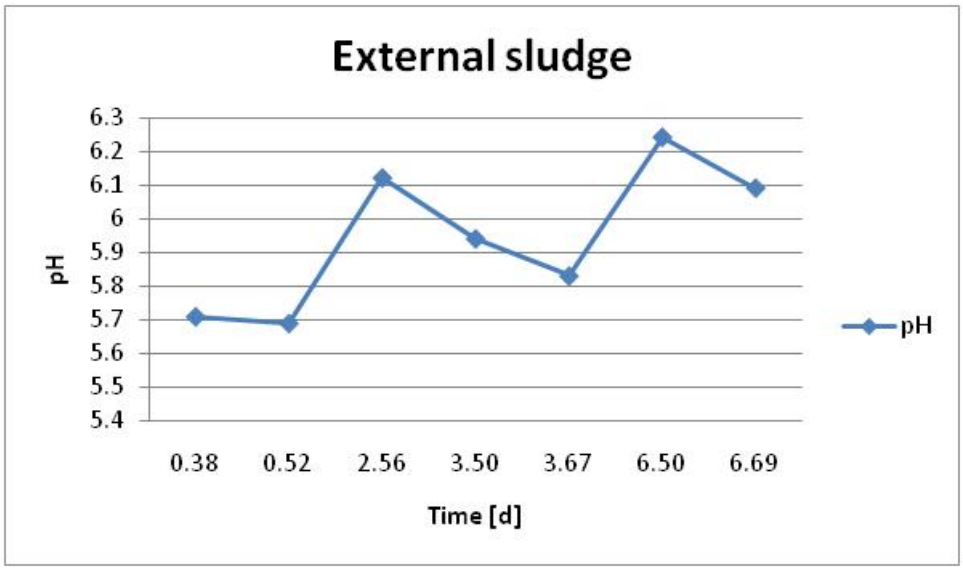

Graph 3.17 Monitoring the pH in external sludge over time

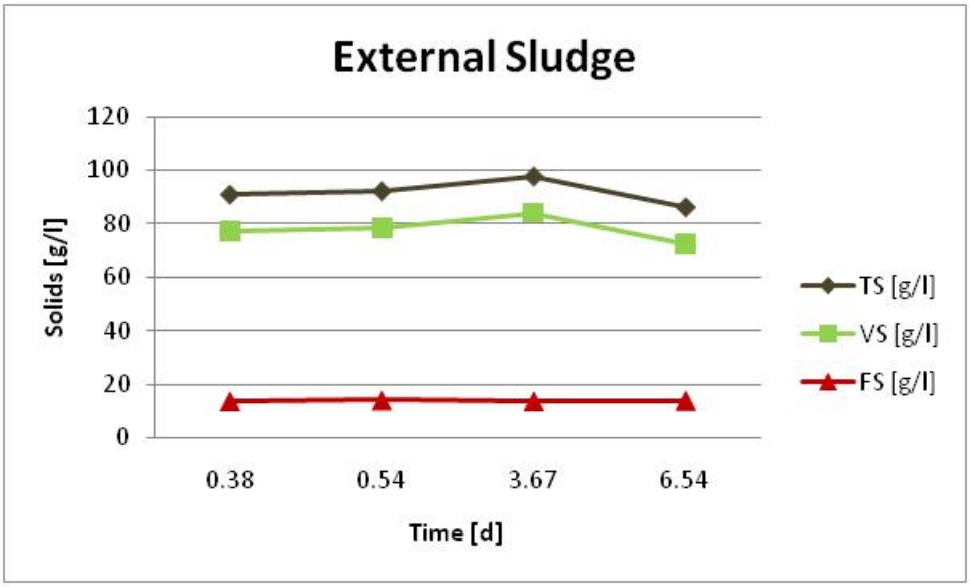

Graph 3.18 Solids content in external sludge

Characterization of food waste is shown in Table 3.6.

Table 3.6 Characterization of food waste

Data	Time	pH	TS [g/l]	VS [g/l]	COD[kg/m3]	COD/VSS
24.03	15:00	4.95	304.49	269.43	293.25	1.09

3.2 Calculating Mass Balance Based on the Measured Data

Two reactors at SNJ plant operate with processes of wastewater stream flow of 428.4 [m^3/d] to reactor 1 and 2. COD concentration in buffer tank and reactors is 76167 and 38074 [g/m^3] respectively. These are average values taken from the data analysed at SNJ plant during the first campaign (15-25 March).

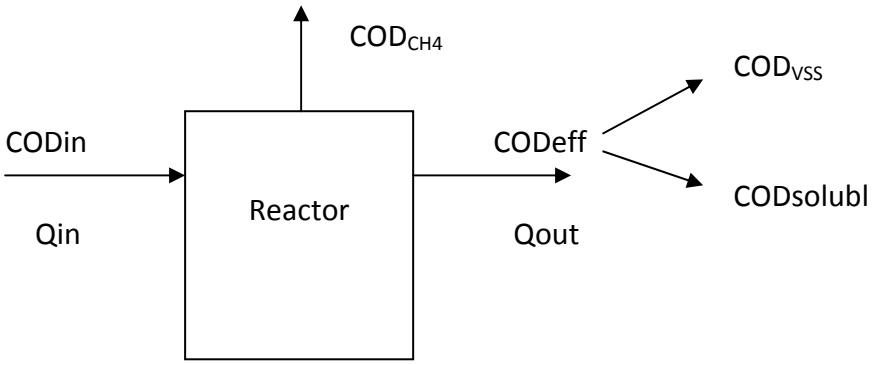

$$0 = \text{Influent COD} - \text{portion of influent COD in effluent} - \text{influent COD converted to methane}$$

$$COD_{in} = COD_{eff} + COD_{methane}$$

During the period of one week, mass balances were set up every day.

Table 3.7 Extended mass balance over one week

Date	CODin [kg/d]	CODout [kg/d]	CODch4 [kg/d]	CODvss [kg/d]	COD Soluble [kg/d]	COD Removed [kg/d]	Biogas production [m^3/d]
19.03	32050.6	17722.2	20207.6	502.3	17219.8	14328.4	8804
20.03	32192.4	18057.6	21845	544.7	17512.9	14134.8	8862
22.03	35309.9	18661.4	18130.9	522.3	18139.1	16648.5	10090
23.03	27485.3	12270.8	20846.6	401.7	11869.1	15214.5	9363
24.03	34491.6	14810.4	17891.3	494.1	14316.3	19681.2	12019
25.03	28137.0	15942.2	21006.3	466.0	15476.2	12194.8	7598

To express the biogas production measured at SNJ plant in terms of COD unit we had to calculate the oxygen demand for content in 1 m^3 biogas. The purpose of this calculation is to

check whether COD entering the reactor equals to COD converted into biogas plus COD leaving the reactor (Kommedal, 2010).

$$1\ \mathrm{m^3 biogas} = \frac{\mathrm{n \cdot R \cdot T}}{\mathrm{P_{atm}}}$$

$$\frac{\mathrm{n_{CH4}}}{\mathrm{m^3}} = \frac{\mathrm{P_{atm}}}{\mathrm{R \cdot T}} = \frac{0.67 \cdot 101 \cdot 10^3\,\mathrm{Pa}}{8.314\,\frac{\mathrm{atm \cdot m^3}}{\mathrm{mole \cdot K}} \cdot 313\mathrm{K}} = 26\,\frac{\mathrm{mole\ CH4}}{\mathrm{m^3 biogas}} \cdot 2\,\frac{\mathrm{mole O_2}}{\mathrm{mole\ CH_4}}$$

$$= 52\,\frac{\mathrm{mole\ O_2}}{\mathrm{m^3 biogas}} \cdot 32\,\frac{\mathrm{g\ O_2}}{\mathrm{mole\ O_2}} = 1664\ \frac{\mathrm{g\ COD}}{\mathrm{m^3 biogas}}$$

Where, 0.67 is partial pressure of CH_4

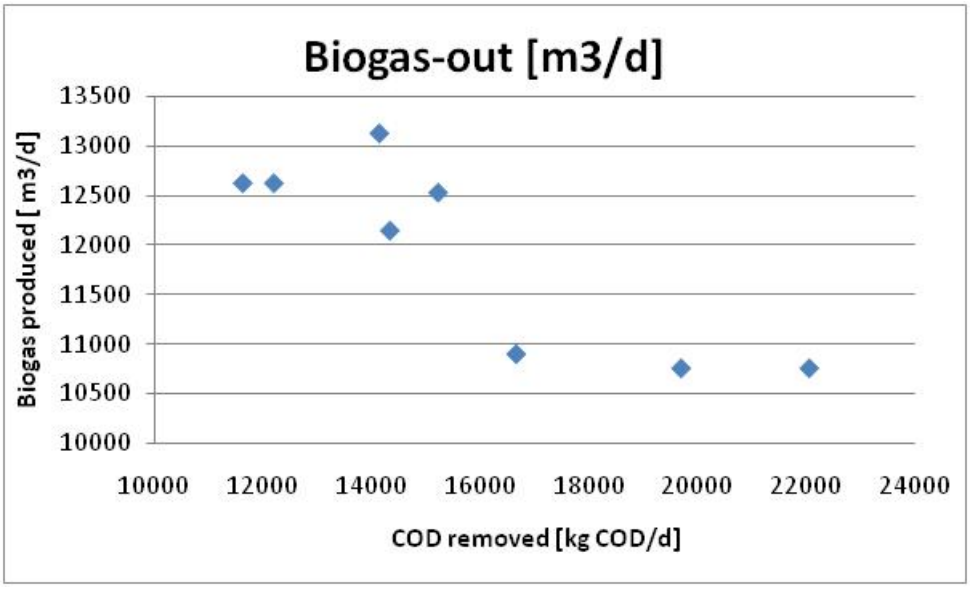

Graph 3.19 Plotted biogas measured at SNJ plant over COD removed

In the Graph 3.19 is plotted the measured biogas produced at SNJ plant over the calculated COD removed.

3.3 Determination of Volatile Solids Reduction

From the following analysis of untreated and digested biosolids, the total volatile solids reduction is determined during digestion. It is assumed that (1) the weight of the fixed solids in the digested biosolids equals the weight of fixed solids in the untreated sludge and (2) the volatile solids are the only constituents of the untreated sludge lost during digestion. The method to determine volatile solids reduction is extracted from the book (Tchobanoglous et al., 2003)

	Volatile solids, %	Fixed solids, %
Untreated sludge	70.76	29.23
Digested sludge	44.21	55.78

Fixed solids in undigested sludge,

$$29.223\% = \frac{0.2923\ \text{kg} \cdot 100}{0.2923\ \text{kg} + 0.7076}$$

X equals the weight of volatile solids after digestion. Then,

Fixed solids in untreated sludge,

$$55.78\% = \frac{0.2923\ \text{kg} \cdot 100}{0.2923\ \text{kg} + \text{X kg}}$$

$$\text{X} = \frac{0.2923 \cdot 100}{55.78} - 0.2923 = 0.232\ \text{kg to VS}$$

Weight of digested solids = 0.2923 + X = 0.5243 kg

Percent reduction in total suspended solids:

$$\text{R}_{\text{TSS}} = \frac{(1 - 0.5243)\text{kg}}{1\ \text{kg}} \cdot 100 = 47.57\%$$

Percent reduction in volatile suspended solids:

$$\text{R}_{\text{VSS}} = \frac{(0.7076 - 0.2923)\text{kg}}{0.7076\ \text{kg}} \cdot 100 = 58.69\%$$

Quantity of fixed solids remains the same, the weight of the digested solids based on 1 kg of dry untreated sludge, as computed above, is 0.5243 kg.

3.4 Estimation of SRT, Volumetric Loading and Percentage Stabilization at SNJ Plant

From the data analysed in SNJ laboratory, it has been found that the quantity of dry volatile solids and biodegradable COD removed is 22.9 kg/m^3 and 37.5 kg/m^3, respectively. As mentioned above the sludge contains about 95 percent moisture and has specific gravity of 1.02. Efficiency of waste utilization *E*= 0.49. Y= 0.08 kg VSS/kg COD utilized and k_d= 0.03 d^{-1}. The way of computing these characteristics is extracted from the book (Tchobanoglous et al., 2003)

Daily volume of sludge is computed with following expression:

$$\text{Sludge volume} = \frac{22.92933\text{kg/m}^3 \cdot 428.4\text{m}^3/\text{d}}{1.02 \cdot 10^3\text{kg/m}^3 \cdot 0.05} = 192.6\ \text{m}^3/\text{d}$$

Determination of bCOD loading:

bCOD = 37.4987 kg/m^3 · 428.8 m^3/d = 16064.44 kg/d

Solids retention time SRT

$$\text{SRT} = \frac{\text{V}}{\text{Q}} = \frac{3500\text{m}^3}{192.6\ \text{m}^3/\text{d}} = 18.17\ \text{d}$$

Volumetric removal rate is computed as follow:

$$\text{kg}\frac{\text{bCOD}}{\text{m}^3} \cdot \text{d} = \frac{16064.44\ \text{kg/d}}{3500\ \text{m}^3} = 4.59\ \text{kg/m}^3 \cdot \text{d}$$

Volumetric loading is calculated:

$$\frac{\text{CODin} \cdot \text{Flow}}{\text{Volume}} = \frac{75.85\text{kg COD/m}^3 \cdot 420.8\text{m}^3/\text{d}}{3500\text{m}^3} = 9.11\text{kg/m}^3 \cdot \text{d}$$

The quantity of volatile solids produced per day by using equation:

$$\text{P}_\text{x} = \frac{\text{YQ}(\text{S}_\text{o} - \text{S})(10^3\text{g/kg})}{1 + (\text{k}_\text{d})\text{SRT}}$$

Where, Y = yield coefficient, g VSS/g COD
K_d = endogenous coefficient, d^{-1} (0.02 – 0.04)

SRT = solids retention time, d
Q = flow rate, m^3/d
S_o = bCOD in influent, kg/m^3
S = bCOD in effluent, kg/m^3
P_X = net mass of cell tissue produced per day, kg/d

S_o = 16064.44 kg/d
S = (1 – 0.49) ·16064.44 = 8192.9 kg/d
S_o – S = 16064.44 – 8192.9 = 7871.6 kg/d

$$P_x = \frac{0.08 \cdot [(16064.44 - 8192.9)\text{kg/d}]}{1 + (0.03\text{d}^{-1}) \cdot 18.17} = 407.6\ \text{kg/d}$$

Percent stabilization is computed as following:

$$\text{Stabilization}, \% = \frac{8674.84\ \text{kg/d} - 1.42 \cdot 407.6\text{kg/d}}{16064.44\ \text{kg/d}} \cdot 100 = 50.4\ \%$$

The same calculations were carried out with the daily measured data during the 7 days period of analysis (Table 3.8)

Table 3.8 Parameters analysed at SNJ plant during one week

Date	Sludge Volume [m3/d]	bCOD loading [kg/d]	SRT [d]	COD Loading rate [$kg/m^3 \cdot d$]	COD removal rate [$kg/m^3 \cdot d$]	Effic.	VS prod [kg/d]	Stabil. [%]
19.03	175.60	14328.41	19.93	9.16	4.09	0.45	396.65	51.36
20.03	210.11	14134.84	16.66	9.20	4.04	0.44	422.93	51.84
22.03	219.49	16648.54	15.95	10.09	4.76	0.47	476.13	48.79
23.03	171.09	15214.50	20.46	7.85	4.35	0.55	336.74	41.50
24.03	158.27	19681.20	22.11	10.40	5.96	0.57	406.44	40.01
25.03	187.44	12194.78	18.67	7.96	3.40	0.43	354.29	52.53

3.5 Steady State Simulations

The implemented ADM1 model adapted to SNJ was simulated into steady state using the inlet conditions as measured over the steady state experimental campaign (15-25 March 2010). The model matrix configuration is shown in Appendix A. Table 3.9 and Table 3.10 represents the hydraulic and COD loadings, respectively. Inlet data was extended to a 14 days period, and then used for subsequent inlet conditions by repeated loadings. Loadings were all linked to the inlet buffer tank compartment (model) (Kommedal, 2010).

Table 3.9 Represents several operational parameters measured at SNJ plant

Date	Simulation Time	Q_{SNJ}	$Q_{Septic\ Sludge}$	$Q_{Organic\ Waste}$	Gas prod. R1	Gas prod. R2	Gas production (total)	Methane content
(data obtained)	[d]	[m3/d]			[st. m^3/d]			[%], (vol/vol)
15.03.2010	0	476.6	0	0	5928	6744	12672	66.7
16.03.2010	1	517.0	38.4	24.3	5808	7488	13296	66.5
17.03.2010	2	529.9	8.64	26.4	6336	6552	12888	66.4
18.03.2010	3	453.6	26.4	24.2	6552	7176	13728	64.9
19.03.2010	4	538.6	52.8	0	5808	6336	12144	65.1
20.03.2010	5	522.7	0	0	6048	7080	13128	63.8
21.03.2010	6	488.2	0	0	5088	5808	10896	66
22.03.2010	7	492.5	16.8	15	6120	6408	12528	65
23.03.2010	8	413.3	19.2	0	5088	5664	10752	65.5
24.03.2010	9	424.8	14.4	15	5904	6720	12624	64.2
25.03.2010	10	453.6	26.4	24.2	5928	6744	12672	66.7
26.03.2010	11	538.6	52.8	0	5808	7488	13296	66.5
27.03.2010	12	522.7	0	0	6336	6552	12888	66.4
28.03.2010	13	488.2	0	0	6552	7176	13728	64.9

Table 3.10 Represents COD loading rates from different wastes

	Simulation Time	COD_{SNJ}	$COD_{Sewage\ Sludge}$	$COD_{Organic\ Waste}$
Date Time	[d]	[kg/m^3]		
14.03.10 19:32	0	67.1		
15.03.10 06:06	0.44	60		
16.03.10 11:37	1.67	67.9		
18.03.10 08:30	3.54	71.6		
19.03.10 08:30	4.54	91.2		
20.03.10 05:37	5.42	80		
20.03.10 07:32	5.5	72		
21.03.10 08:15	6.53	56.8	125.6	293
21.03.10 19:32	7	67.1		
22.03.10 06:06	7.44	59.5	(constant value)	(constant value)
23.03.10 11:37	8.67	56.9		
24.03.10 08:30	9.54	68.3		
25.03.10 08:30	10.54	74.2		
27.03.10 05:37	12.42	80		
27.03.10 17:08	12.9	59.5		
28.03.10 08:15	13.53	56.8		

The inlet speciation of the COD in raw sludge (denoted SNJ in the above tables) and imported sewage sludge was calculated based on analytical results from previous analysis during waste and sludge characterization. COD fractions used are shown in table 3.11.

Table 3.11 COD fractions in three different waste types

State variable inlet	Wastewater sludge (SNJ)	Sewage Sludge (imported/external)	Organic waste
	[1]		
S_{aa}	0.048	0.048	0
S_{fa}	0.071	0.071	0
S_I	0.126	0.126	0
S_{su}	0.035	0.035	0
X_C	0.55	0.55	0
X_I	0.17	0.17	0.14
X_{Ch}	0	0	0.46
X_{Li}	0	0	0.18
X_{Pr}	0	0	0.22
Total	1	1	1

Specific inlet concentrations for each state variable was calculated as the product of the inlet COD (total) and the COD fraction in Table 3.11. As seen, codigestion substrates (organic waste) are implemented as polymer loadings, not as particulate organic carbon. This is a simplification made due to the ADM1 use of fixed COD composition of the organic sludge (as percentages of the inlet COD) assuming fixed polymeric decomposition products.
All inlet data was implemented in AQUASIM using real list variables, and variations was smoothened using the Spline function (Reichert, 1998). The simulation was run for 112 days, and measured steady state data was adopted into plots starting day 100 (equivalent to the 15. march 2010 (start of steady state measurements).

Figure 3.1 show the hydraulic loading of raw sludge from SNJ wastewater treatment plant, imported sewage sludge and organic waste at pseudo steady state conditions (representative of the steady state sampling period 15-25 march). The total loading rate is smoothed due to splince curve fitting of the total input hydraulic load.

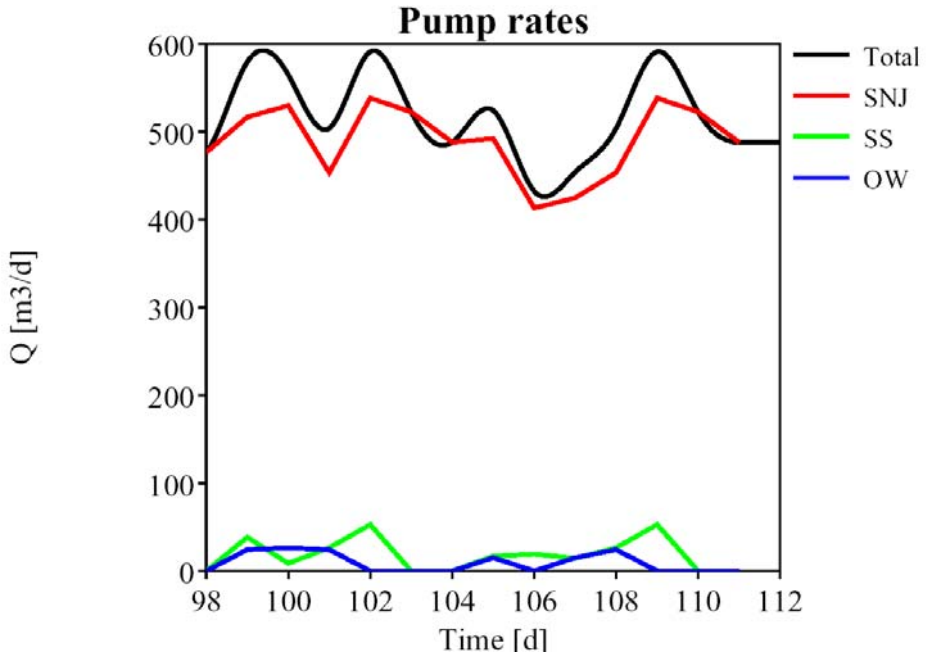

Figure 3.1 Hydraulic loading during steady state conditions as measured during 15 – 25 March. SNJ is raw wastewater sludge from the chemical precipitation process at SNJ, SS is imported sewage sludge and OW is imported organic waste.

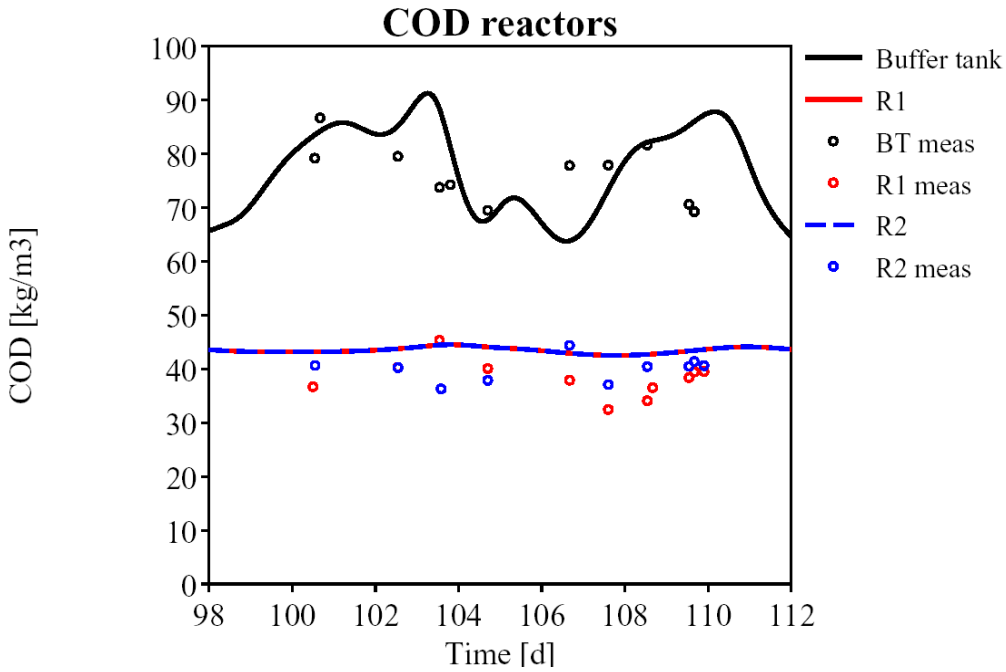

Figure 3.2 COD concentrations during simulated steady state (representative of the steady state sampling period, 15 – 25 March) in the Buffer Tank (which is the inlet to both

digesters), and anaerobic digesters 1 and 2. Measured data during the steady state sampling period is shown.

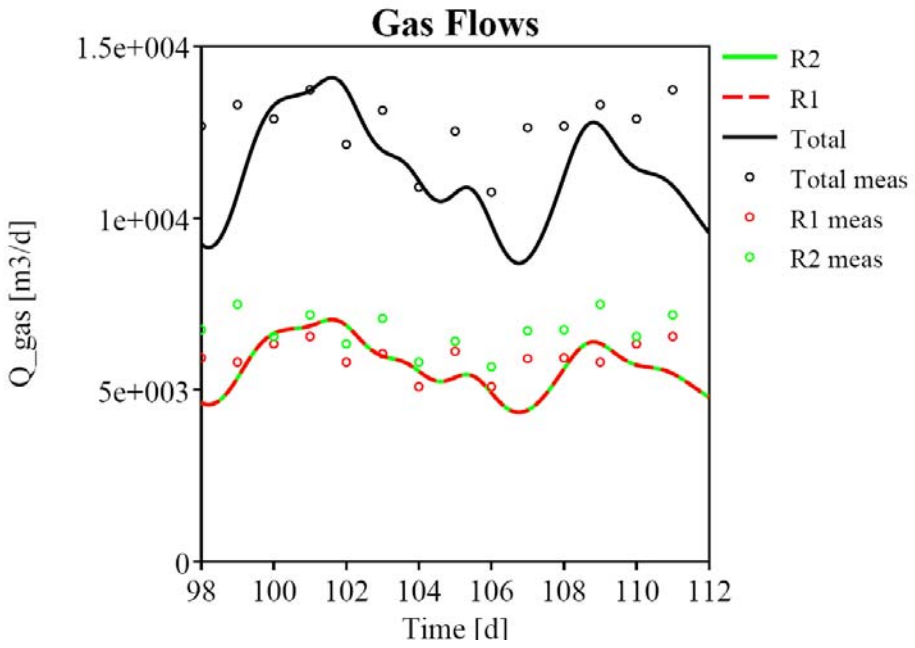

Figure 3.3 Simulated (lines) and measured biogas flow rates during the steady state period.

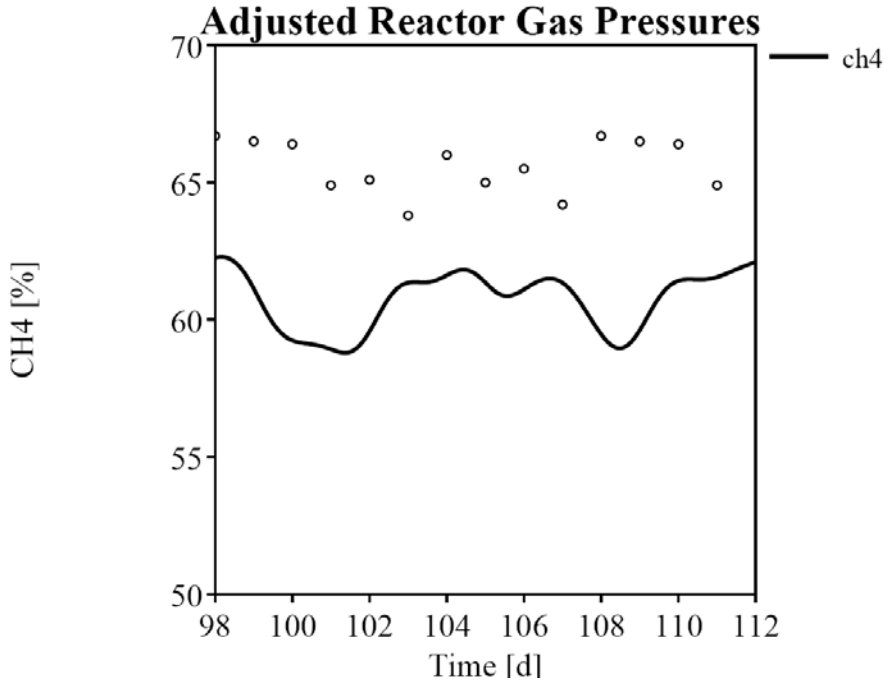

Figure 3.4 Methane biogas volumetric ratio simulated (line) and as measured (circle) during the steady state sampling period (15 – 25 March).

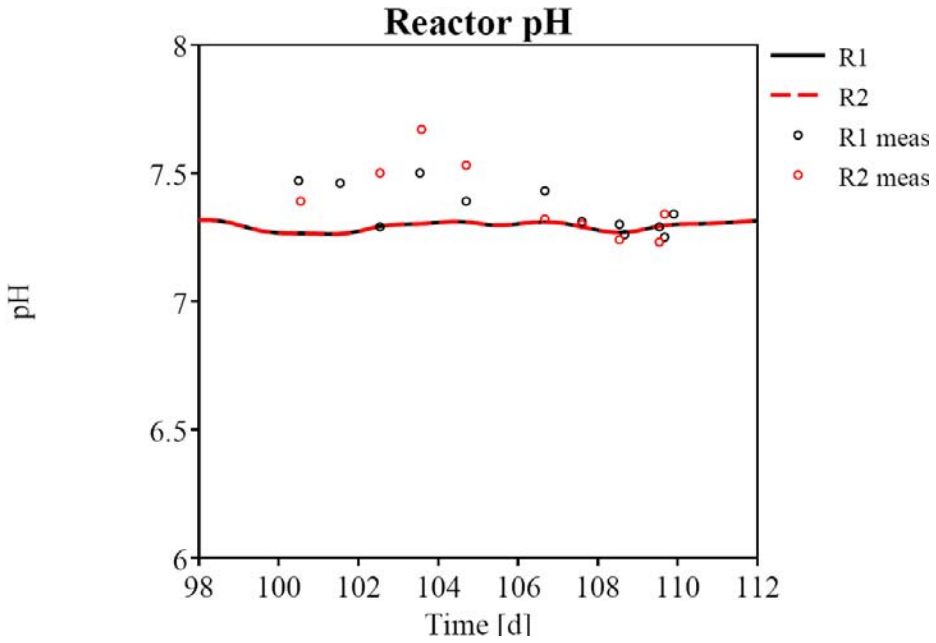

Figure 3.5 Reactor pH during the test period. Simulated values (lines) and measured pH (circle) in the digesters 1 and 2.

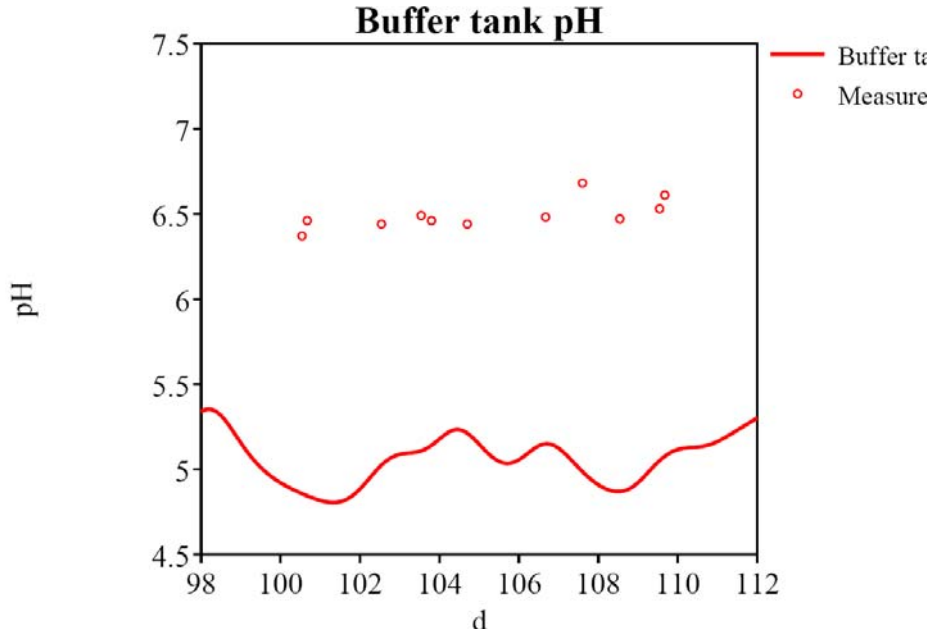

Figure 3.6 Buffer tank pH as measured (circles) and simulated (line) during the steady state test period.

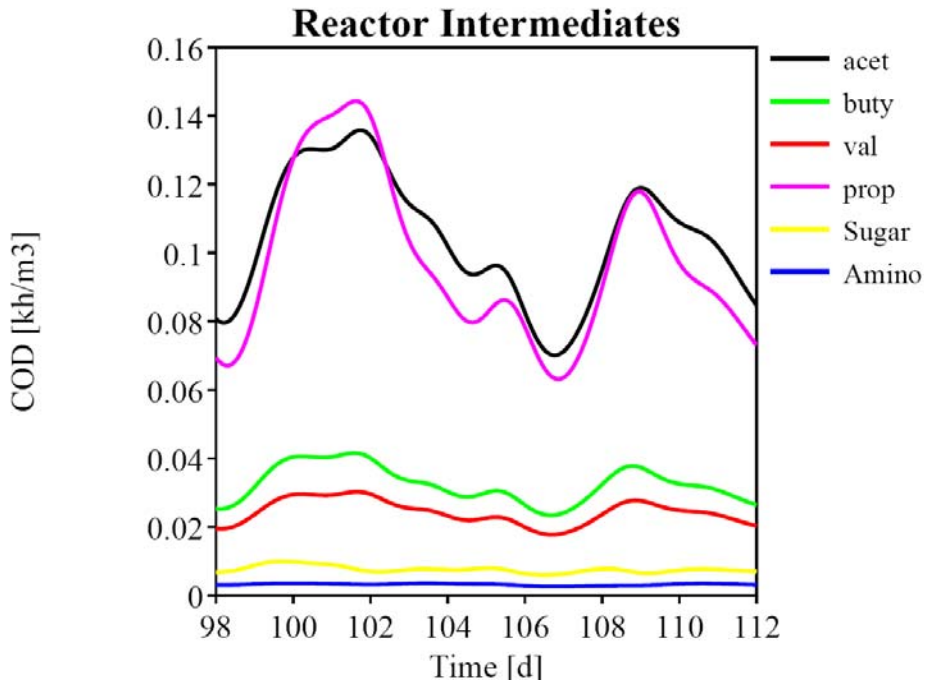

Figure 3.7 Simulated VFA (fermentation products) in the digester 1 (during steady state reference period).

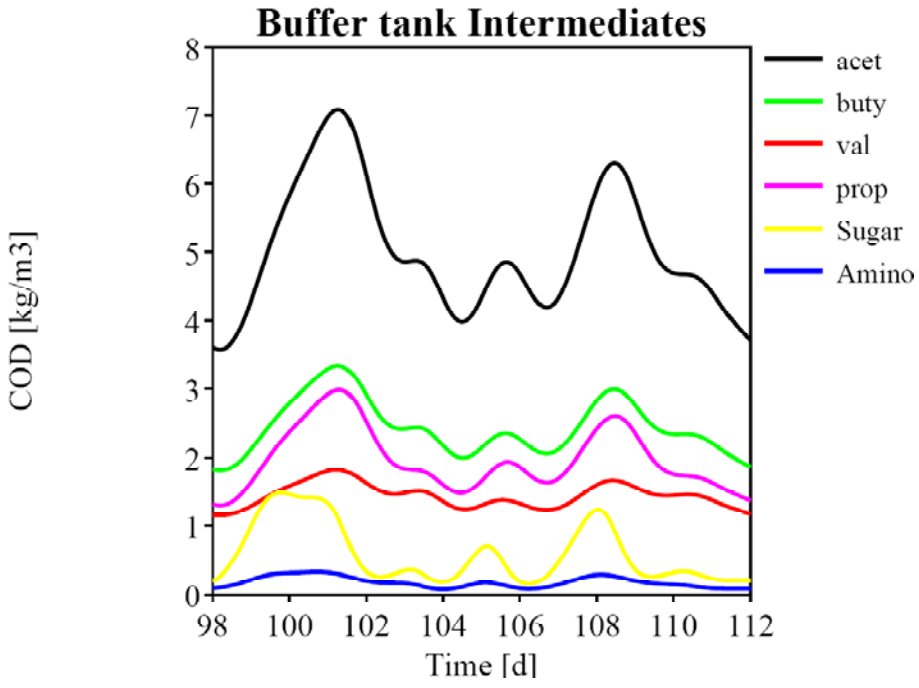

Figure 3.8 Simulated VFA and monomers in the buffer tank during the steady state reference period.

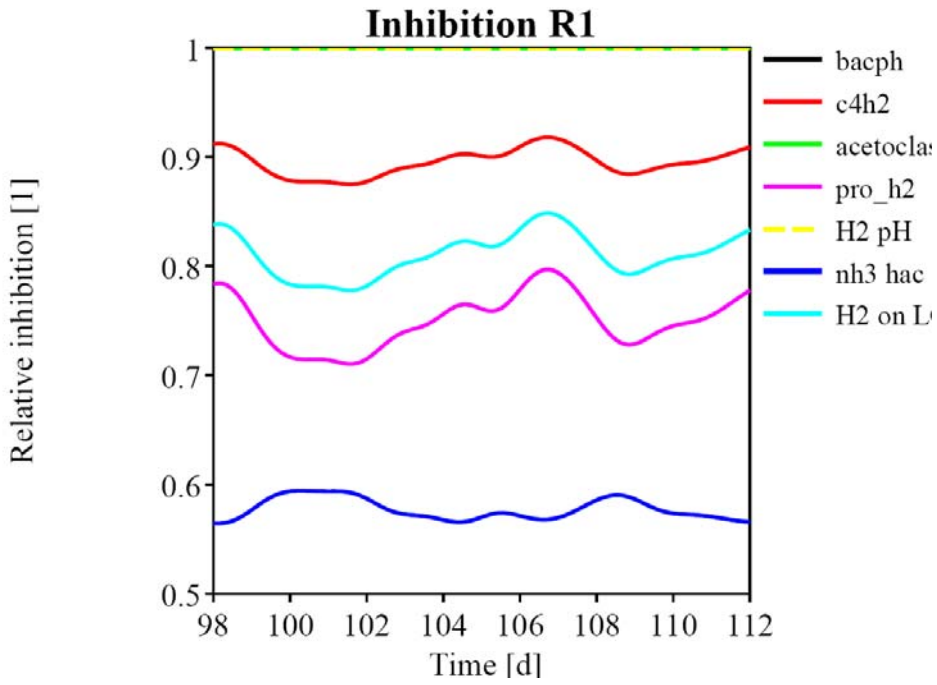

Figure 3.9 Simulated inhibitions (relative) in anaerobic digesters. Non-inhibited processes equal unity.

Figure 3.9 show simulated relative inhibition due to pH on bacterial growth kinetics (black), hydrogen inhibition of acidogenesis from C4+ VFA's (red) pH effects on acetoclastic (green), inhibition of acetogenesis of propionate due to H_2 (magenta), pH inhibition of syntrophic, ammonia inhibition of acetoclastic bacteria (blue) and H_2 inhibition of LCFA fermentation (cyan).

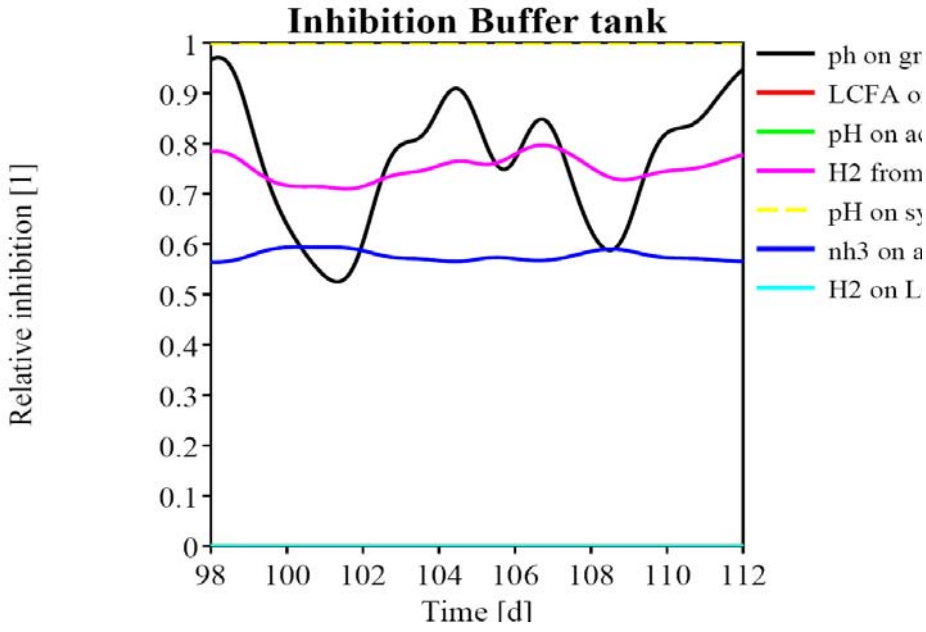

Figure 4.10 Simulated relative inhibition (kinetic) in the buffer tank during the steady state reference period.

3.6 Non Steady State Analysis

In order to evaluate the biogas stimulating effect of co-digestion, and calibrate and validate the non steady state functionality of the AQUASIM simulation tool, a non steady state experiment was been performed by step loading of a defined organic waste to steady state digester 1, keeping digester 2 at normal operation (at steady state). Every day from 2 June to 9 June, pH, chemical oxygen demand (COD), solids and volatile fatty acids (VFA's) were analysed in buffer tank, reactor 1 and 2, raw sludge and the loaded organic food waste. Ways of executing the experiments are described in section materials and methods. The purpose of the analysis is to examine the potential of food waste in the codigestion process, specifically assess how it effects the process biogas output when food waste is injected directly into the bioreactor. Graph 3.19 shows the flow characteristics during the survey In the Graph 3.19 is shown the flow characteristics during the survey period.

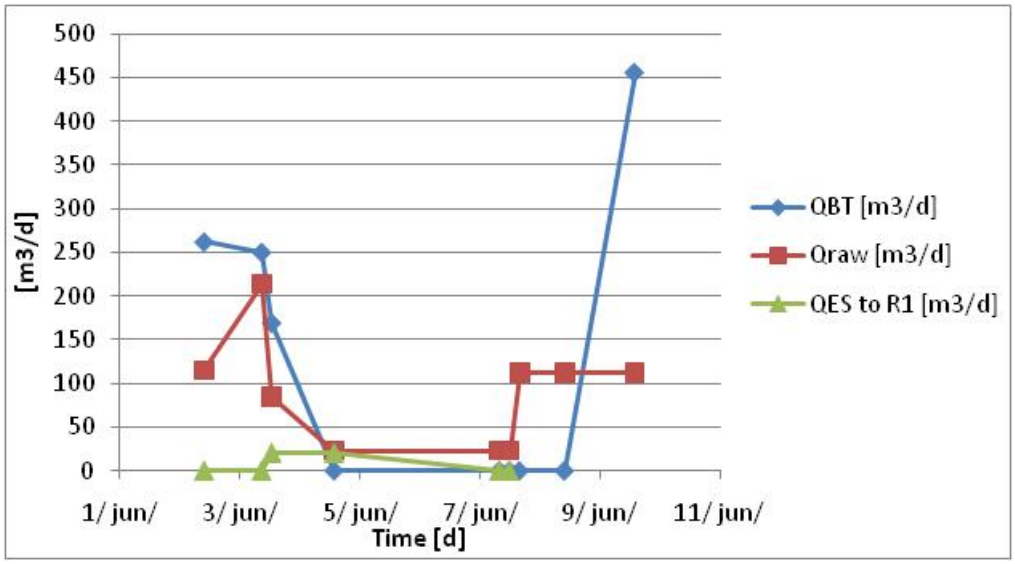

Graph 3.20 Flow characteristics during the survey period. In this figure is shown the flow from the buffer tank, flow from raw sludge to buffer tank and septic sludge to the reactor 1.

Measurements conducted in reactor 1 are represented graphically. The Graph 3.21 represents the pH behaviour in reactor 1.

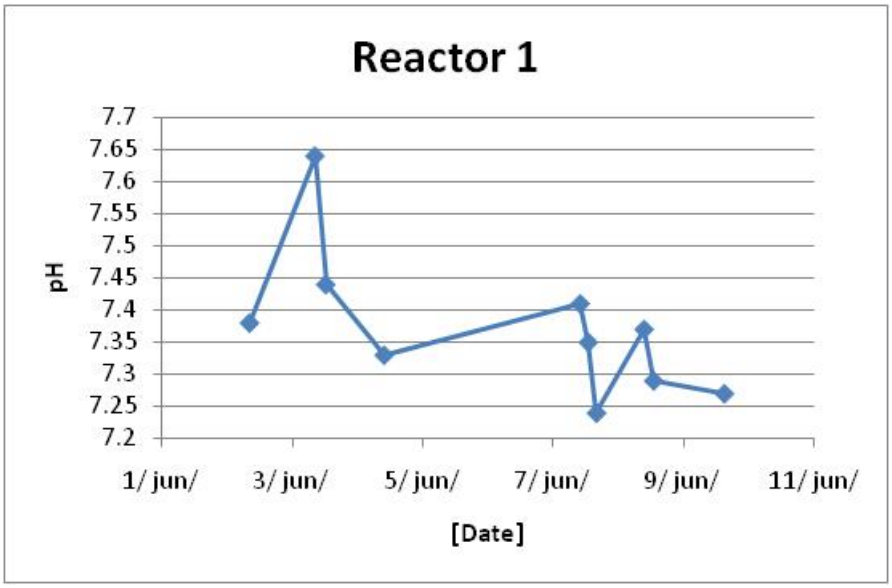

Graph 3.21 Monitoring the pH behaviour in reactor 1

COD changes during the survey period are shown in Graph 3.22.

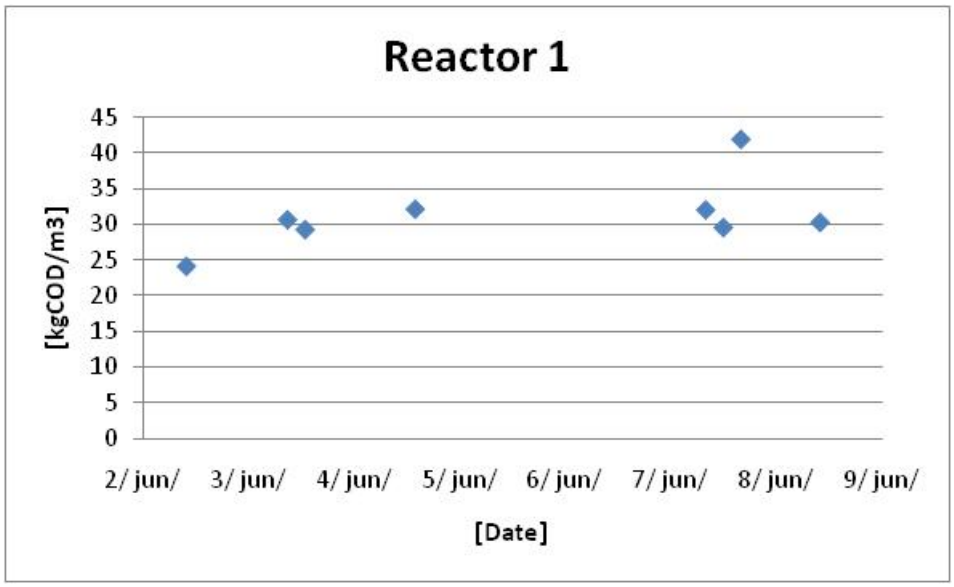

Graph 3.22 COD changes in the reactor 1

Distribution of solids in reactor 1 is represented in Graph 3.23.

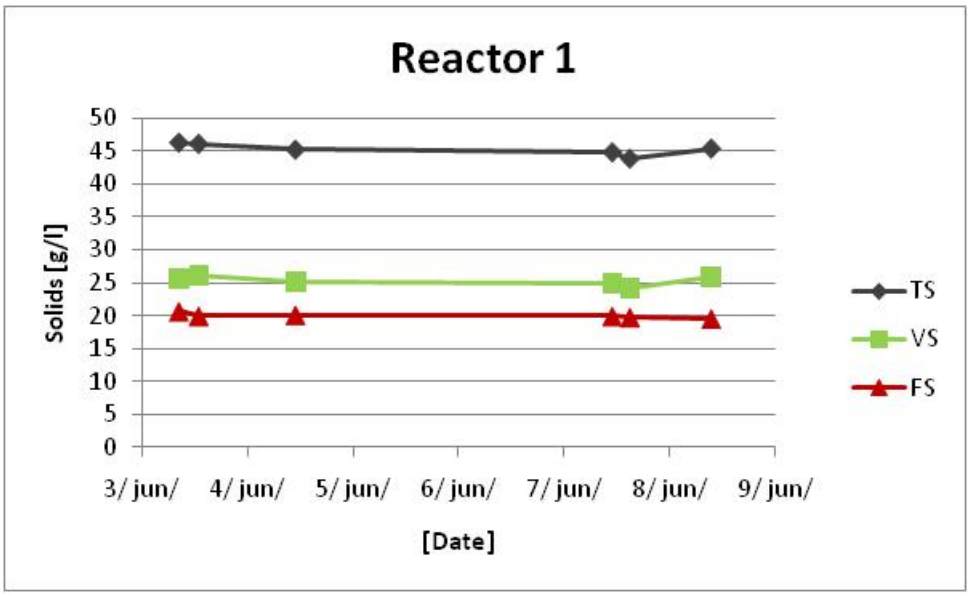

Graph 3.23 Solids analyses conducted in reactor 1

Volatile fatty acids in reactor 1 are shown in Graph 3.24.

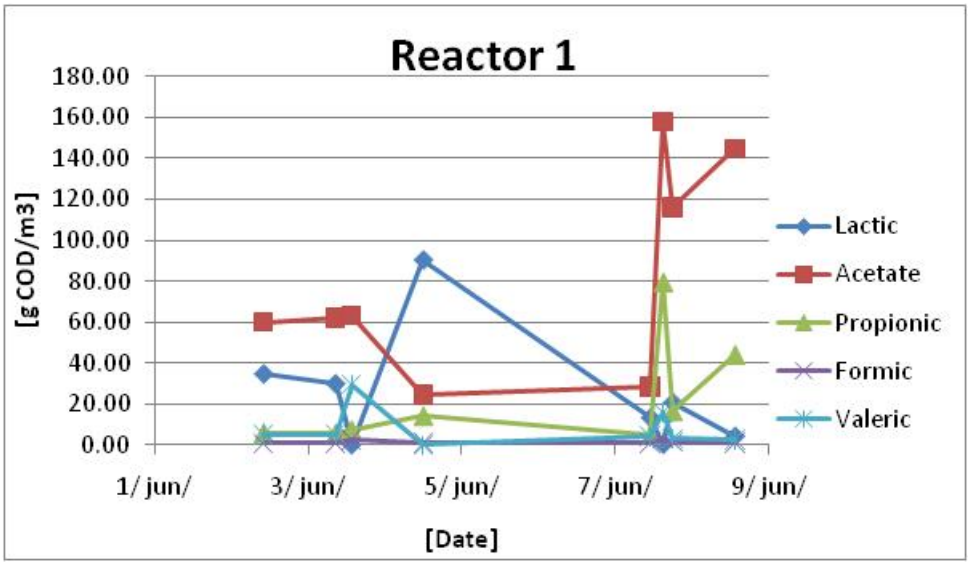

Graph 3.24 Concentrations of volatile fatty acids in reactor 1

Following figures represent the analyses done in reactor 2.

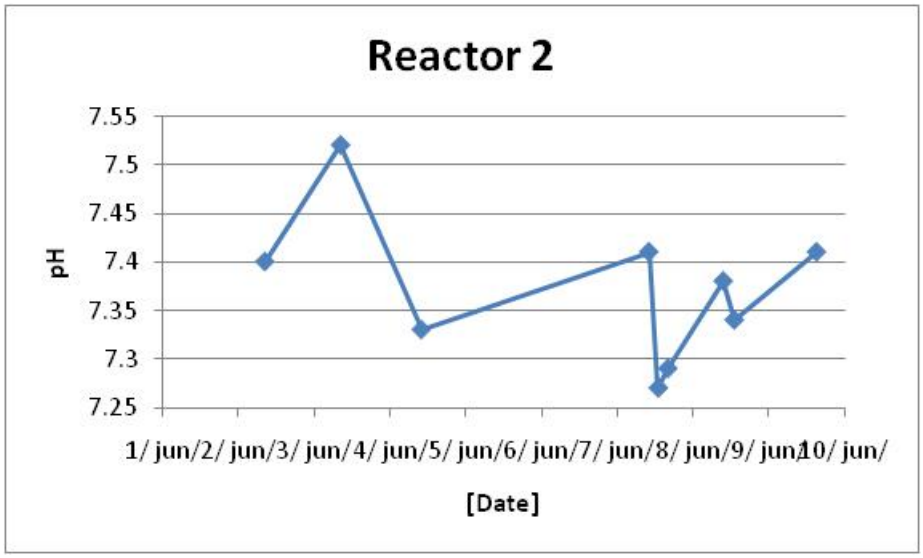

Graph 3.25 Monitoring the pH behaviour in reactor 2

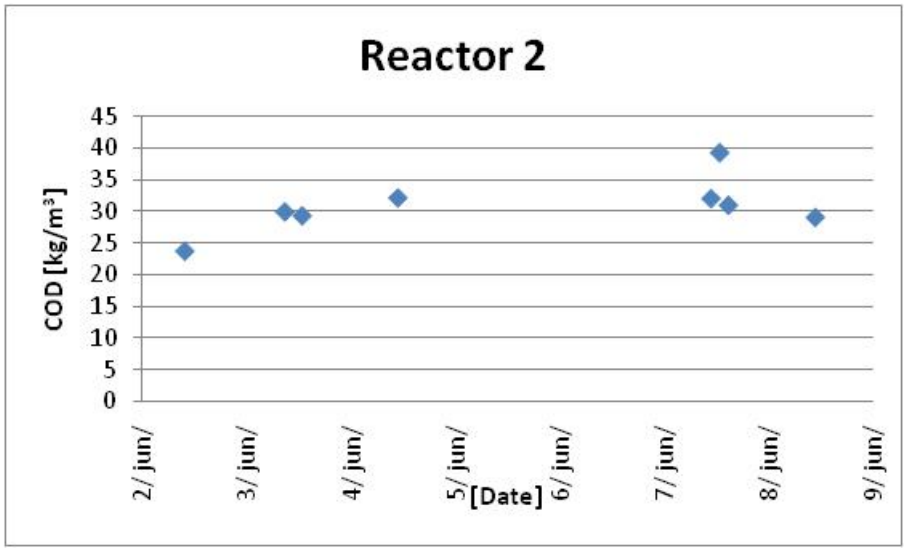

Graph 3.26 COD concentration in reactor 2

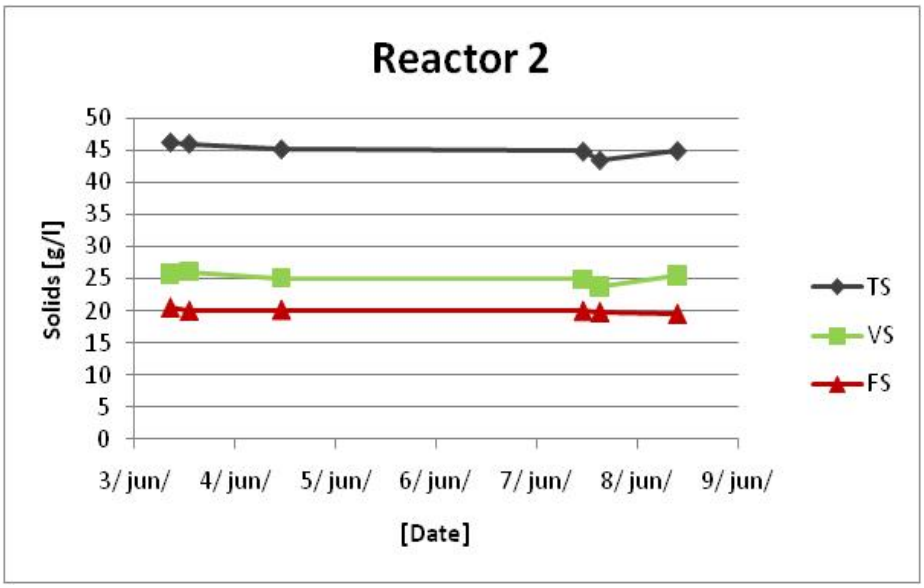

Graph 3.27 Solids analyses conducted in reactor 2

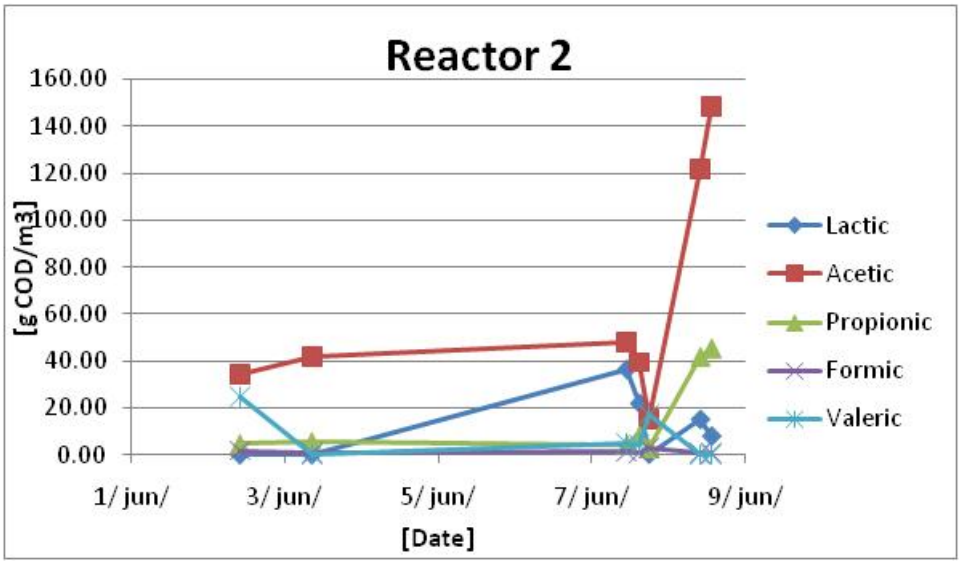

Graph 3.28 Concentration of volatile fatty acids in reactor 2

Characteristics of sludge in buffer tank are represented in the following figures.

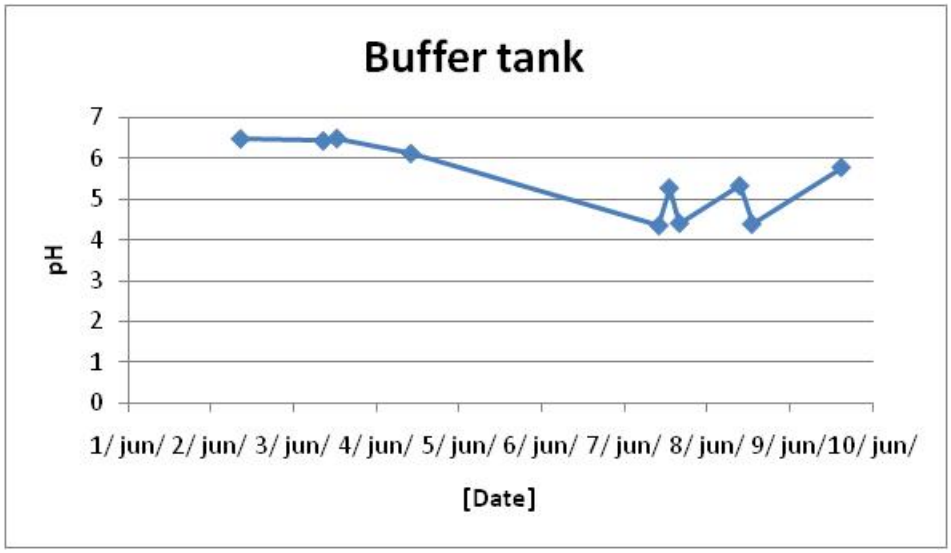

Graph 3.29 Measured pH values in buffer tank over time

COD measurements in buffer tank are shown in Graph 3.30

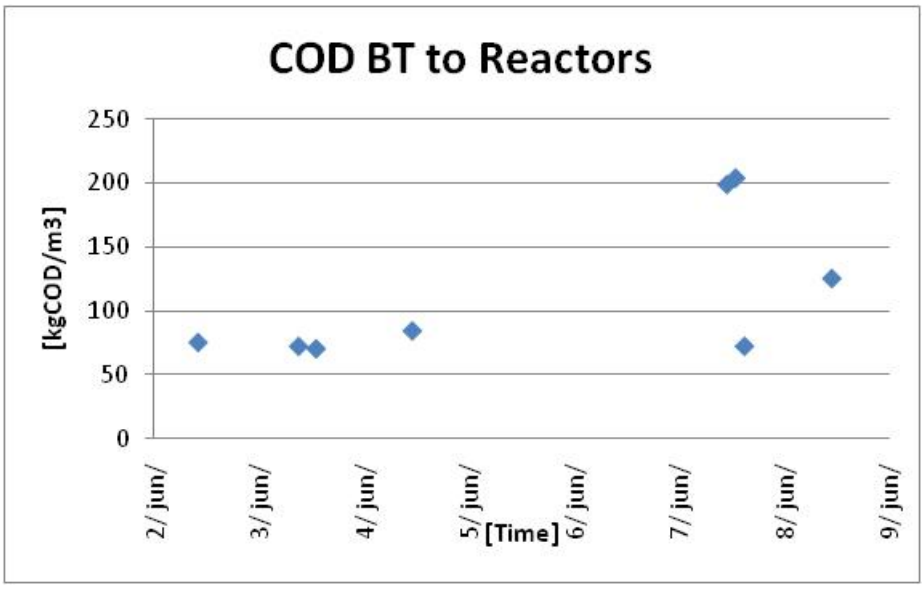

Graph 3.30 COD concentration in buffer tank

Solids content in buffer tank is shown in Graph 3.31.

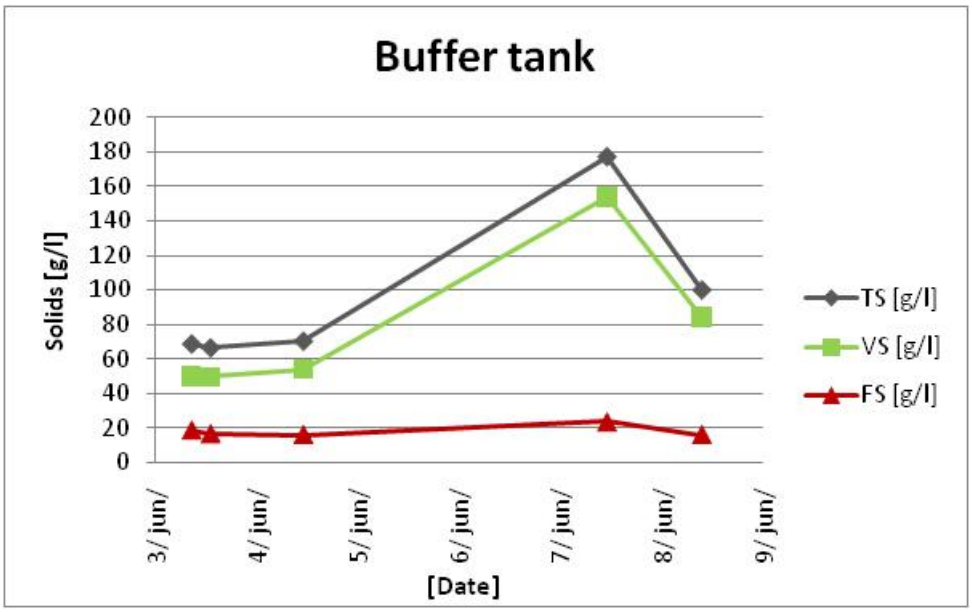

Graph 3.31 Solids content in buffer tank

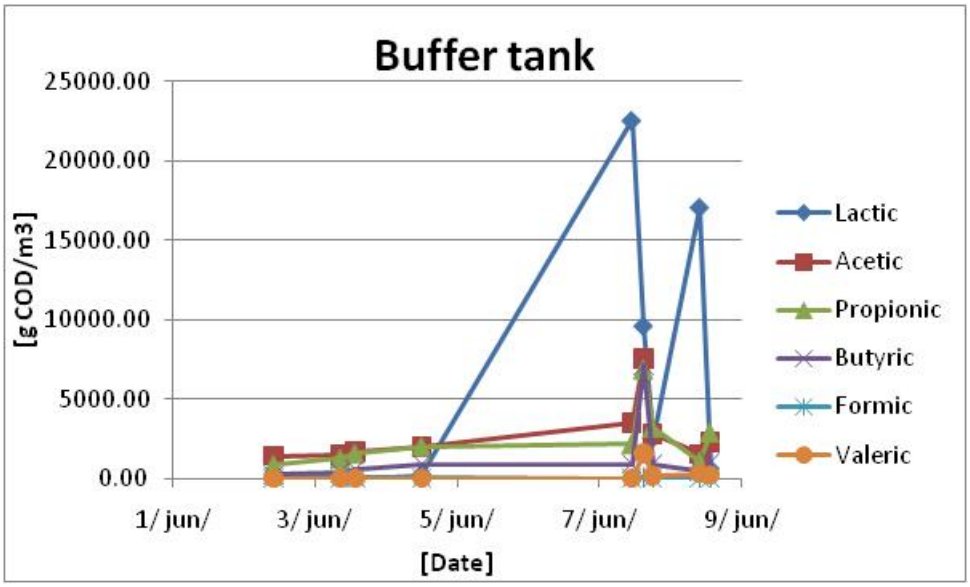

Graph 3.32 Concentrations of volatile fatty acids in buffer tank

Following figures represent the characteristics of raw sludge. Graph 3.33 shows pH behaviour in raw sludge.

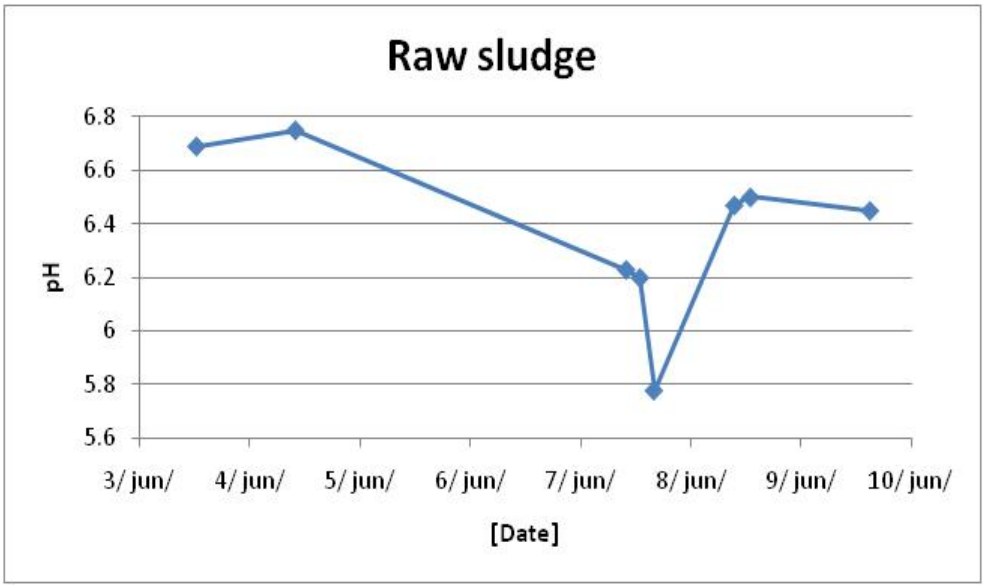

Graph 3.33 Monitoring the pH behaviour in raw sludge

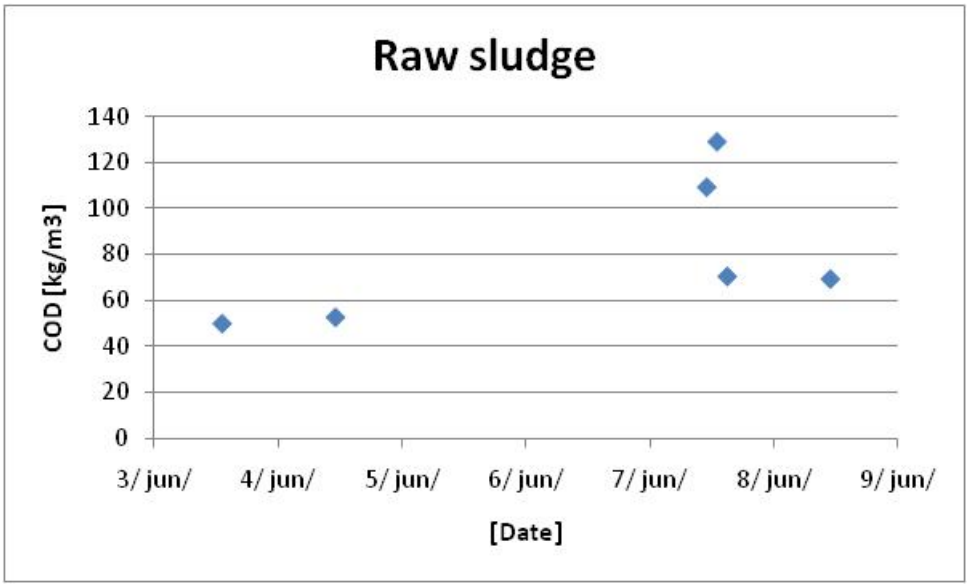

Graph 3.34 COD concentration in raw sludge

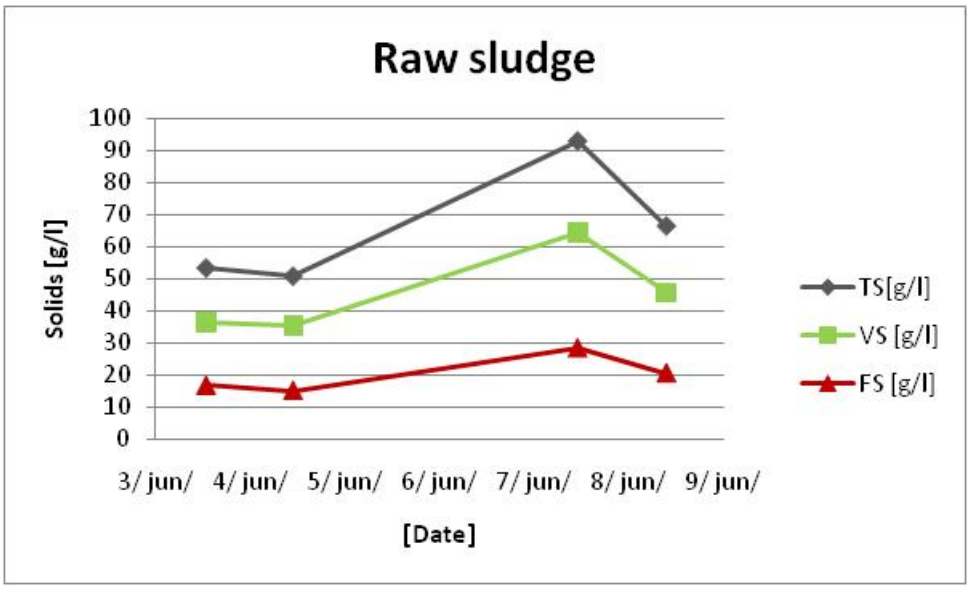

Graph 3.35 Solids content in raw sludge

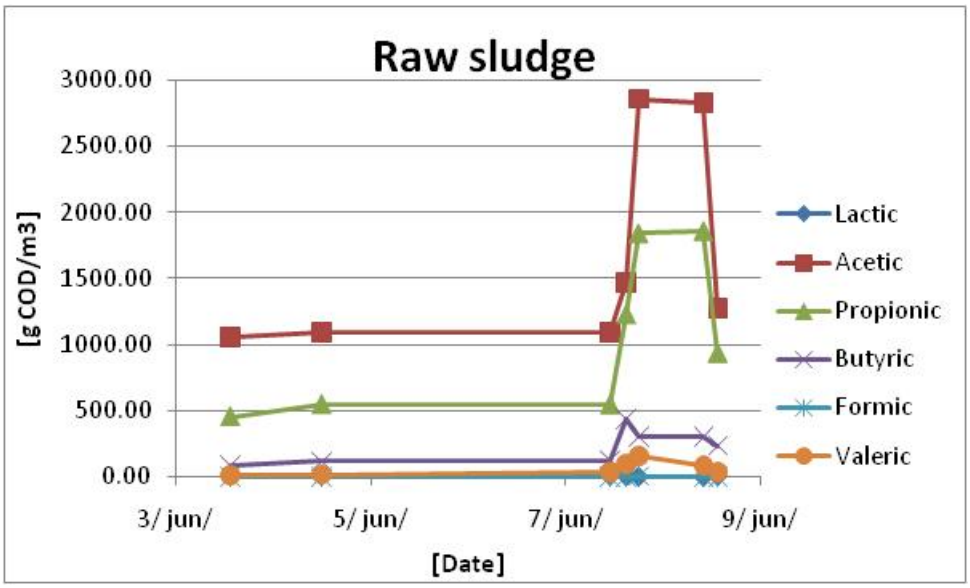

Graph 3.36 Concentration of volatile fatty acids in raw sludge

Characteristics of food waste are represented in Table 3.12

Table 3.12 Characteristics of food waste obtained during non steady state analyses

Data	Time	pH	TS [g/l]	VS [g/l]	COD [kg/m^3]	COD/VSS
03.06.10	12:30	4.62	288.27	265.08	304.13	1.15
07.06.10	13:00	4.6	264.66	247.09	360.81	1.46

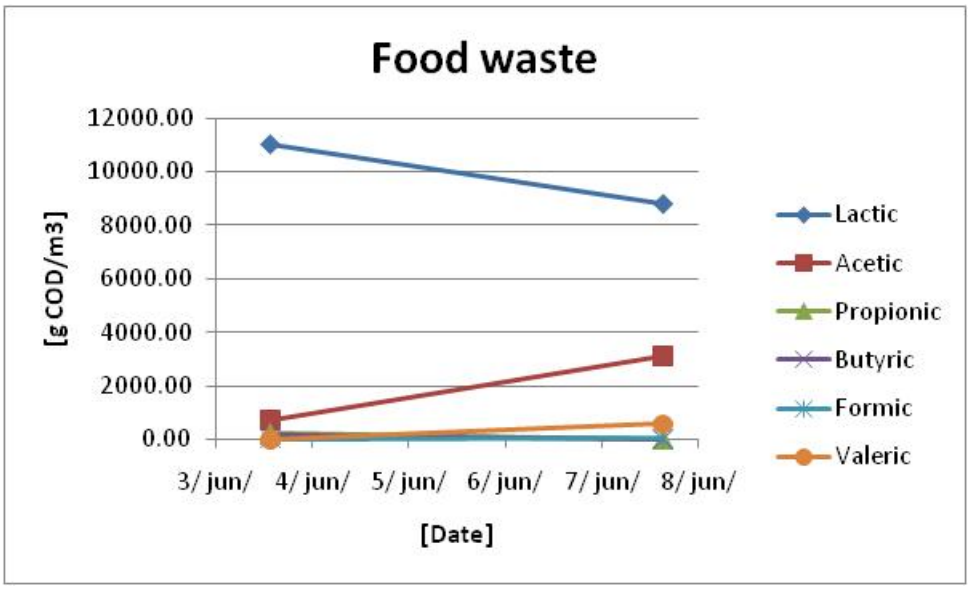

Graph 3.37 Concentration of volatile fatty acids in food waste

Biogas output was measured on 7 June when food waste was pumped into reactor 1, while reactor 2 was fed from buffer tank. The effect of food waste on biogas production is shown in Graph 3.38.

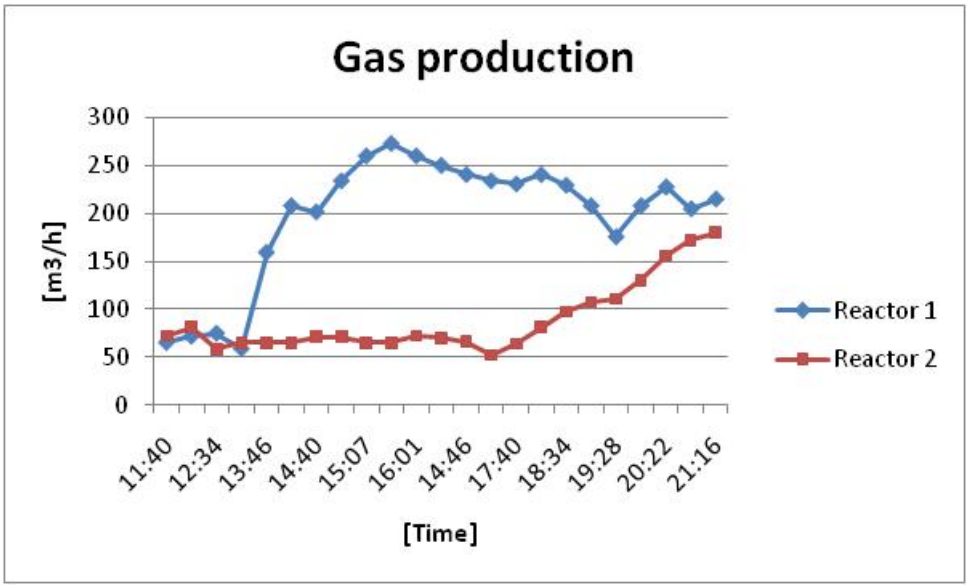

Graph 3.38 Biogas productions from reactor 1 and reactor 2

Methane fluctuation in biogas is represented in the following Graph 3.39.

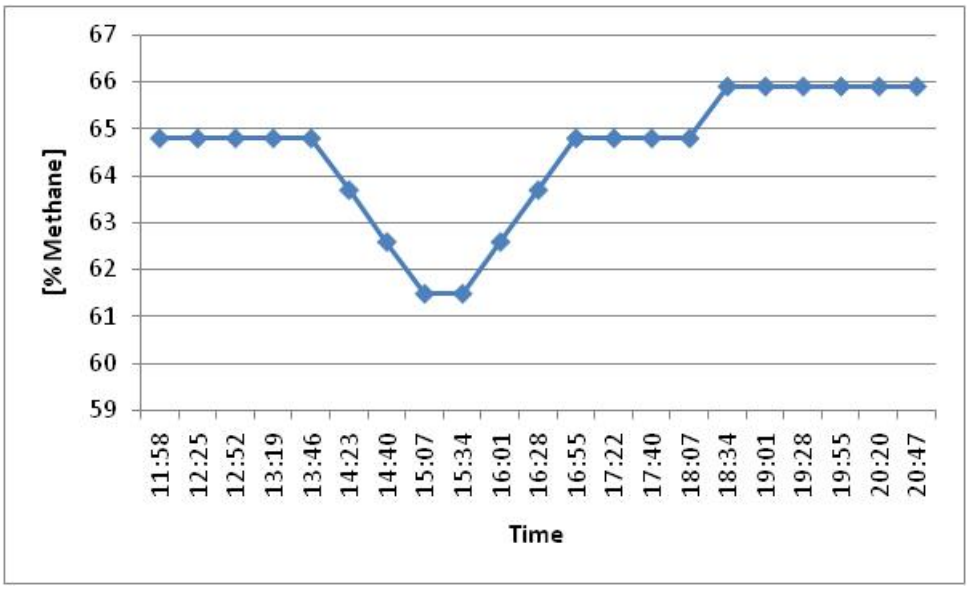

Graph 3.39 Methane concentrations in biogas vary over time

4. Discussion

General SNJ Plant Operation

During the steady state survey period at SNJ plant there were no reactor failures due to sharp drops in pH which is usually associated with generating enormous amount of volatile fatty acids and thus resulting in an imbalance between acetogens and methanogens. The pH in reactor 1 remained between 7.25 and 7.5 and the pH range in reactor 2 was between 7.23 and 7.67 hence we can conclude that the reactors operated at fairly constant pH range.

There are two possible reasons I found relevant for explaining the fairly constant pH in both reactors. One is related to the buffering capacity of dissolved carbon-dioxide (and bicarbonate through the bicarbonate buffering system) and the other is simply the concentration of volatile fatty acids in the reactor.

The portion of CO_2 in the gases produced at SNJ plant was 35 percent which indicates that the system contained adequate buffering capacity to compensate the pH drop caused by production of volatile acids.

The analysis of VFA's in reactors showed the presence of only one type of acid, acetic acid, there was only minor residuals of other VFA's in the reactors (Graph 3.4 and 3.8). The concentration of acetic acid in reactor 1 is in the range 5.58 to 18.43 g COD/m^3 and concentration in reactor 2 is between 3.44 and 25.71 g COD/m^3. These data indicate, as expected, that the final two steps of anaerobic degradation process; acetogenesis and methanogenesis take place in the reactors. Fermentation is ongoing process because there are fermentative bacteria present already in the raw sludge, and the buffer tank concentration of VFA's strongly indicates active depolymerisation and fermentation upstream the anaerobic digesters. This was also seen in raw sludge VFA data, especially after weekends when sludge was retained in the sedimentation basin thickeners. Pre-fermentation is also indicated by the fact that the concentration of VFA's in raw sludge was somewhat lower compared to values measured in the buffer tank at SNJ. The residual concentration of acetic acid in the outlet of the reactor showed that 5.58 and 18.43 g COD/m^3 was not converted into methane.

The buffer tank, which serves as supplier of sludge to reactors, had shown pH values between 6.21 and 6.68. The concentrations of VFA's in buffer tank were very high and the analysis had shown presence of lactic, acetic, propionic, butyric, and valeric acid. The concentration of acetic acid in buffer tank varies from 291.18 to 476 g COD/m^3. The concentration of formic acid generated in buffer tank is negligible. Based on this it can be noted that much of the fermentation (acidogenesis) process took place in the buffer tank.

The data obtained for VFA's showed rapid generation of volatile acids (including acetic acid) in buffer tank. Up to the certain extend acetogenesis also takes place in buffer tank.

The analyses conducted in raw sludge have also confirmed that fermentation takes place in the buffer tank as It was found that the raw sludge entering the buffer tank has 3 to 5 times lower values of VFA compared to the sludge leaving the buffer tank. The pH in raw sludge remained between 5.58 and 6.78 throughout the studies.

As it is mentioned above, SNJ receives food waste which is rich in COD, especially carbohydrates and sugars (reference to your own results (figure or table) needed). Findings in this work indicate that whenever the plant receives food waste, the output of biogas increases, depending on the loading, dramatically. The sample of food waste was analysed and showed very high concentration of acetic acid, up to 2363g COD/m^3 and an organic strength of 293 [kg COD/m^3]. The calculated COD/VSS ratio of food waste is 1.09, which is very close to glucose COD/VSS ratio of 1.067. This indicates that the sugar content of food waste dominates the biodegradable COD, and is known to be an easily consumable substrate for bacteria. It also suggests that food waste has a very high potential of increasing the biogas production through codigestion.

Septic sludge has low pH and high concentration of acetic, propionic and butyric acid. These characteristics are typical for stored sludge under anaerobic conditions. The low pH indicates that acid formers have an optimal pH under acidic conditions. Their metabolic rates at this pH are still favourable compared to the methane formers responsible for the final conversion of organics into methane (Droste, 1997).

COD Removal

COD percentage removed varied between 42–57%. Highest COD removal was observed at the highest COD loading rate. From the Table 3.11 can be seen that the highest COD removal rate 5.96 [kg/m^3·d] was observed with highest COD loading rate with 10.40 [kg/m^3·d]. The results from Table 3.8 are shown in Graph 4.1.

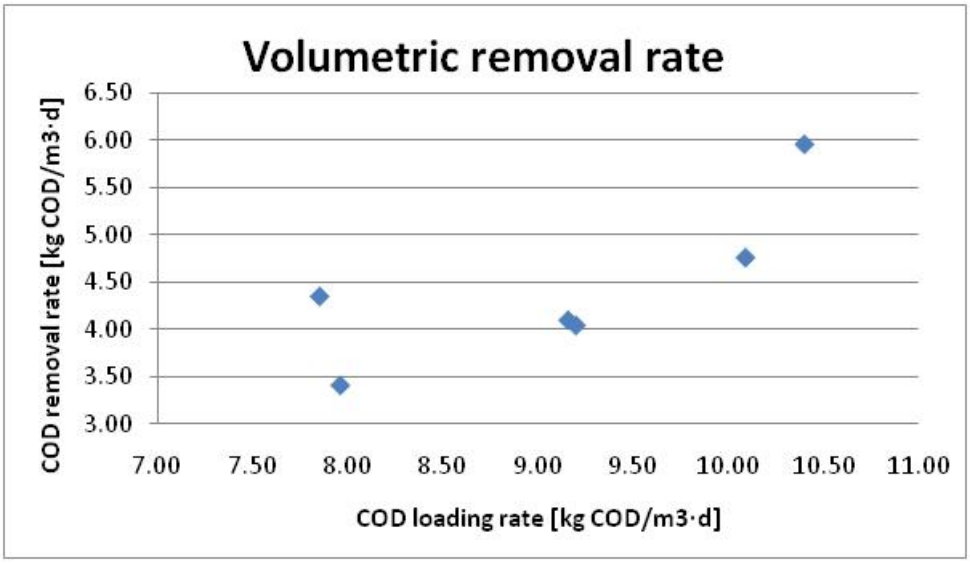

Graph 4.1 Interdependency between COD loading rates and COD removal rates

From the Graph 4.1 shows the variation of COD removal rate as COD loading rates increase. The COD removal rate increases with increasing COD loading rate. COD loading rates are increasing in a non-linear fashion. However, data shows slightly high COD removal rate of 4.35 [kg/m^3·d] when the COD loading rate was 7.85 [kg/m^3·d]. This can be explained by an increasing the ratio COV/VSS increases the COD removal rates. From Table 3.2 it can be seen that on 23 March the ratio COD/VSS had value of 1.61. On the same date, COD loading rate had high value of 10.09 [kg/m^3·d] and thus high COD removal rate of 4.76 [kg/m^3·d]. Similarly, following the date on 23 March the ratio COD/VSS had low value of 1.18 (Table 3.1) and COD loading rate is 7.85 [kg/m^3·d] and COD removal is 4.35 [kg/m^3·d].The highest observable COD removal rate 5.96 [kg/m^3·d] is on 24 March with the highest COD loading rate of 10.40 [kg/m^3·d]. At high F/M the biomass is overloaded and cannot process the incoming COD as efficiently as at low F/M (Cassidy D. et al., 2008).
This can be explained that not always by increasing the COD loading rate can be achieved high COD removal rate. The art of anaerobic digestion process is to determine the most appropriate COD loading rate.

COD mass balance calculated on measured data showed portion of COD which is missing in the system. The results did not show that COD which enters the reactors ended up as COD converted into methane plus COD leaving the reactors. The COD which is missing in reactors

is with an average deviation of 14.5%. The results showed that sum of COD converted into biogas plus COD leaving the reactor is more than COD entered the reactors. This situation is nonsense and there are no real possibilities to occur in high-rate digesters. As mentioned earlier, this may be due to too high measurements of biogas productions (as seen when comparing simulated biogas produced and measured).

The discrepancy is also seen when comparing the result between the theoretical methane production calculated on COD data and the actual methane production measured at SNJ (during the steady state reference period). The results showed an average deviation of 29.7%.
In the following Graph 4.2 the theoretically estimated biogas production is plotted over the measured COD removal. This plot makes more sense and is more reasonable than the Graph 3.18. This plot clearly shows that as COD removed increases, biogas produced is theoretically expected to increase in a linear fashion, with a slope of 0.6142 [m^3] methane produced per kg COD removed.

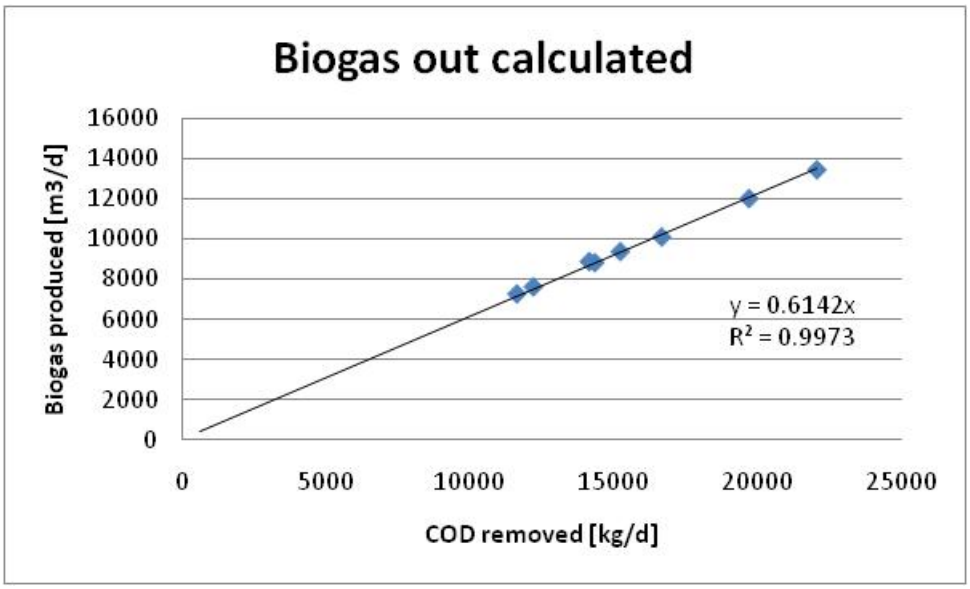

Graph 4.2 Theoretically biogas produced over COD removed

However when plotting measured biogas production over measured COD removal, no such relationship can be found (Graph 3.18). The figure shows that significantly more biogas is produced when COD removed is lower. Similarly, less biogas is produced when the COD removed was at higher values. This situation is an unrealistic and practically there is no possibility to occur in any high-rate anaerobic treatment plant. Again, this could be explained by possible errors occurring during laboratory measurements at SNJ, or the online measurements of volumetric biogas rate. In fact, SNJ has had a problem with the instrument measuring the biogas production, and according to the process personnel, this problem was present during both experimental campaigns at SNJ in this work (Osli, 2010). Recently a

new instrument has been installed, but after measurements was performed as part of this project.

Calculations were done to compute percent reduction of total suspended solids and volatile suspended solids. In a high-rate digester such as the one at SNJ the total solids are expected to be reduced approximately by 45 to 50 percent (Tchobanoglous et al., 2003). Based on data in this project, the reduction of total suspended solids at SNJ is 47.6 %, in accordance with values found in literature.
The degree of stabilization obtained is often measured by the percent reduction in volatile solids. Volatile suspended solids are reduced by 58.7% at SNJ and solids retention time in reactors had an average value of 19 days. Estimated volatile solids destruction in high-rate mesophilic anaerobic digestion is shown Table 4.1 Adapted from WEF (1998).

Table 4.1 Estimated volatile solids destruction in high-rate complete-mix mesophilic anaerobic digestion Adapted from WEF (1998) (Tchobanoglous et al., 2003)

Digestion time, d	Volatile solids destruction, %
30	65.5
20	60.0
15	56.0

The calculated result for volatile solids reduction is very close to values in Table 4.1. Anaerobic digestion over 20 days is predicted to give 60% volatile solids reduction.

Steady State Simulation

The biopolymeric composition of co-digestion wastes is the main difference compared to standard wastewater sludge composition. In order to allow for various polysaccharides to lipid to protein composition of the wastes, these inputs are defined directly as polymeric substances. This may lead to a slightly over-estimated overall biogas conversion rate, however the difference should be limited, especially considering (Henze, 2002) conclusion that depolymerisation (or hydrolysis) is the overall rate limiting step in the biogas process.

Due to acid – base equilibrium processes implemented in the AQUASIM ADM1 model, simulations were run from given initial conditions (consistent set given in Batstone et al., 2002). A minor (numerical) deviation from a consistent set of equilibrium initialization values would immediately lead to initialisation error in AQUASIM, hence, the given set of consistent values was used and long term simulation used to establish the true steady state conditions (based on the steady state input values described in the result section).

Figure 3.2 shows the COD concentrations into and out of the anaerobic digesters during the steady state sampling period. Both digesters are loaded and operated identically in the model, COD curves are exactly overlaid. Measured buffer tank concentration (equal to the digester inlet) shows the same average concentration as the simulated inlet, while the simulated digester outlet is slightly higher than the measured total COD. A somewhat reduced COD reduction by the model is also indicated by the biogas production rate shown in Figure 3.3. As seen, the simulated biogas production rate is slightly lower than the measured. This could be due to too low COD conversion rate (to biogas), or too high values measured. The latter is especially interesting looking at the difference between measured production rates from R1 and R2. There should be no significant difference as these reactors are loaded similarly; however, as seen in Figure 3.3, the biogas measured out of R2 is on the average higher than R1 rates. As this is transferred to the simulated and measured total production rate discrepancy could be due to inaccurate gas flow meters.

Another deviation between measured and simulated performance is the methane ratio in the biogas. Figure 3.4 show this and there is an obvious difference.

Reactor pH is another standard process parameter usually used for process control. The simulated and measured digester pH (both reactors) is shown in Figure 3.5. Again, the measured value is slightly higher compared to the simulated value. Measured values show higher variability, indicative of not optimal measurements (process pH is known to be quite stable in anaerobic digesters due to high reactor alkalinity).

One hypothesis identified during the project was significant fermentation (acidogenesis) in the 1 day retention time buffer tank. Simulated and measured pH values during the steady state reference period are shown in Figure 3.6. Simulation results show significant acidogenesis by the dramatic pH reduction; however, this is not supported by the measurements. However, significant elevated concentrations of VFA's in the buffer tank (Graph 3.12) has been measured, so further investigations are needed for conclusions regarding possible pre-fermentation during buffer tank storage. This can also be seen in Figure 3.7 and 3.8. High levels (about 50 times) of VFA and hydrolysis products (fermentation substrates) are seen in the simulated buffer tank compared to the methanogenic (VFA consuming) digesters. A third observation of pre-fermentation by the model is the elevated hydrogen partial pressure in the buffer tank compared to the digester (Figure 3.9). The high H_2 gas levels in the buffer tank is many orders of magnitude outside the syntrophic hydrogen window (Angelidaki et al.), and clearly show the lack of consistent hydrogen window inhibition implemented in ADM1 (the H_2 window is implemented as kinetic expressions, not bioenergetics on/off switching). Nevertheless, it also indicates the high fermentative activity in the buffer tank.

Similarly, Figure 3.10 shows the same inhibitions in the simulated buffer tank. While the digester is only partially inhibited, the complete biogas production process is totally inhibited in the buffer tank. Inhibition in digesters are mainly due to ammonia inhibition (and no pH inhibition whatsoever), while the complete buffer tank inhibition is cause by elevated hydrogen gas partial pressure. This indicate the two step anaerobic digestion self regulation mechanism whereby fermentation only occurs in the first reactor, and methanogenesis dominates the second (CFSTR dilution of H_2 gas into the methanogenic reactor avoids syntrophic substrate inhibition). Also, this effect is exploited in the novel processes of bio-hydrogen digesters (Kommedal, 2010).

Non Steady State Analysis

Purpose of non steady analysis was to investigate the effect of food waste in a codigestion process. As mentioned in the description of non steady state analysis, the reactor 1 was directly fed with food waste and small quantity of septic sludge, while reactor 2 was used as reference reactor. The reactor 2 was loaded with standard composition waste sludge from the buffer tank (at the time of study containing a mixture of raw sludge (from SNJ), food waste and slaughterhouse waste. On 7 June at 13:00 o'clock inn pumping started in reactor 1. The feed flows are represented in Graph 3.19. 15 m^3 of food waste and 5.5 m^3 were injected directly to digester 1.
Table 4.12, but had a small impact in reactor 1 upon loading, indicating high buffering capacity in digesters. The COD value in reactor 1 increased from average value of 29.6 [kg COD/m^3] before loading to 41.9 [kg COD/m^3] after the loading with food waste. The solids content in reactor 1 remained unchanged at constant levels. VFA's in reactor 1 after feeding with food waste increased, especially acetic and propionic acids with 116 and 79.9 [g COD/m^3] respectively.
In the buffer tank on 7 June high concentration of COD, maximum value of 203.6 [kg COD/m^3], was observed. The pH value dropped from approximately 6.4 to 4.7. This was probably due to the high organic acids content of the waste. On 7 June solids content in buffer tank increased. Volatile solids increased from average value of 51.13 [g/l] to 153.9 [g/l]. VFA's in buffer tank had shown two high picks of lactic acid. From 7 to 8 June the concentration of lactic acid was going from 22580 to 17087 [g COD/m^3]. This is probably due to high presence of milk products that originates from the food waste. VFA's analyses in food waste had shown high concentration of lactic acid. The concentration of lactic acid in food waste has average value of 9917 [g COD/m3].

Analyses conducted in reactor 2 did not show any big changes. Small pH fluctuation was observed between 7.27 and 7.52. On 7 June a bit high COD value of 39.3 [kg COD/m3] was observed in reactor 2. This is probably caused by storage of waste with high organic content (raw sludge, food waste, and slaughterhouse waste) on June 7 in the buffer tank. Thus, increase in the biogas production in reactor 2 would be expected. Solids content in reactor 2 remained within the constant steady state values. Several VFA's were observed in reactor 2 such as lactic, acetic and propionic acid, while formic and valeric acids were present in very

small concentrations. On 8 June after feeding the reactor 2 with rich organic waste on 7 June, increase in concentration of acetic acid 148.65 [g COD/m3] and probably also lactic acid was observed. This is probably due to the increased loading of reactor 2.

In the raw sludge analyzed on 7 June a sudden drop in pH was seen, down to 5.78. This is most likely due to no pumping of raw sludge into buffer tank during weekends. Thus, raw sludge was not removed from sedimentation basins and started to putrescent. As pumping commenced, this resulted in an increased COD values of 129 [kg COD/m3] and total solids content of 92.88 [g/l]. VFA's in the raw sludge also increased on 7 June.

After 45 min. following step loading of organic waste to reactor 1, an increasing the biogas production rate was observed. Before inn pumping started the approximately biogas production was 65 [m3/h], however this increased to 129 [m3/h] after 45 min. After 3 hours digestion in reactor 1, the biogas reached a maximum value of 273 [m3/h] (Graph 3.38). Likewise, when the biogas production was at the highest rates the percentage of methane in biogas were reduced. From approximately 64.9% methane, the portion of methane in biogas dropped down to 61.5% (Graph 3.39). The result of non-steady state analysis showed that the biogas production had increased by 62 % in reactor 1 in comparison with reactor 2 (Osli, 2010).

5. CONCLUSIONS

As far as plant condition is concerned, results shows that the plant is working at the efficiency of 49% average based on COD measured data. There was no deviation observed in the SNJ plant operational parameters during steady state.

Theoretically estimated biogas production based on the measured data was found to be 0.56 m^3 methane produced per kg COD removed.

Comparing the results between calculated biogas productions based on measured data with actual biogas situation obtained from the monitoring centre at SNJ plant. It was found that there is big discrepancy in comparison between the theoretical methane production calculated on measured data through me and the actual methane production measured by SNJ plant. The results showed 29.7% average deviation.

The VSS reduction during the digestion of raw sludge along with septic sludge and food waste was 58.69%. Likewise, I calculated percent reduction in TSS of 47.57%.

ADM1 was successfully implemented and applied to the SNJ plant. The model simulation confirmed that biogas measured at SNJ is higher than simulated and the reason was located due to inaccurate gas flow meter. Simulation also showed low content of methane in the biogas than measured at SNJ. Results gained by simulation indicate significant acidogenesis in buffer tank.

The result of non-steady state analysis (the codigestion step test) showed that the biogas production increased by 62 % in reactor 1 in comparison with reactor 2 (reference). The biogas production obtained here, by the addition of food waste, could be attributed to the higher biodegradability of food waste. On the other hand, the high carbohydrates and polysaccharides content of food waste – it has been recognized as a main reason for the increased biogas production. Although food waste was introduced at a very low pH value, biodegradation proceeded normally without the need for pH correction, due to high buffer capacity in the reactor. Therefore codigestion of food waste with raw sludge stimulates biogas production and represents an environmentally attractive method to treat and simultaneously convert such a waste mixture to a useful energy source.

Appendix A

Table A.1: Biochemical rate coefficient ($V_{i,j}$) and kinetic rate equations (ρ_j) for soluble components (i=1-12; j=1-19) (Batstone et al., 2002)

Component → i		1	2	3	4	5	6	7	8	9	10	11	12	Rate (ρ_j, kg COD.m^{-3}.d^{-1})
j	Process ↓	S_{su}	S_{aa}	S_{fa}	S_{va}	S_{bu}	S_{pro}	S_{ac}	S_{h2}	S_{ch4}	S_{IC}	S_{IN}	S_I	
1	Disintegration												$f_{cl,xc}$	$k_{dis}X_c$
2	Hydrolysis Carbon	1												$K_{hyd,ch}X_{ch}$
3	Hydrolysis of Prot		1											$K_{hyd,pr}X_{pr}$
4	Hydrolysis of Lipid	1-$f_{fa,li}$		$f_{fa,li}$										$K_{hyd,li}X_{li}$
5	Uptake of Sugars	-1				(1-Y_{su}) $f_{bu,su}$	(1-Y_{su}) $f_{pro,su}$	(1-Y_{su}) $f_{ac,su}$	(1-Y_{su}) $f_{h2,su}$		$-\sum_{i=1-9,11-24} C_i v_{i,}$	-(Y_{su}) N_{bac}		$k_{m,su}\frac{S_{su}}{K_S+S}X_{su}I_1$
6	Uptake of Amino Acids		-1		(1-Y_{aa}) $f_{va,aa}$	(1-Y_{aa}) $f_{bu,aa}$	(1-Y_{aa}) $f_{pro,aa}$	(1-Y_{aa}) $f_{ac,aa}$	(1-Y_{aa}) $f_{h2,aa}$		$-\sum_{i=1-9,11-24} C_i v_{i,}$	N_{aa}-(Y_{aa})N_{bac}		$k_{m,aa}\frac{S_{aa}}{K_S+S_{aa}}X_{aa}I_1$
7	Uptake of LCFA			-1				(1-Y_{fa}) 0.7	(1-Y_{fa}) 0.3			-(Y_{fa}) N_{bac}		$k_{m,fa}\frac{S_{fa}}{K_S+S_{fa}}X_{fa}I_2$
8	Uptake of Valerate				-1		(1-Y_{c4}) 0.54	(1-Y_{c4}) 0.31	(1-Y_{c4}) 0.15			-(Y_{c4}) N_{bac}		$k_{m,c4}\frac{S_{va}}{K_S+S_{va}}X_{c4}\frac{1}{1+S_{bu}/S_{va}}I_2$
9	Uptake of Butyrate					-1		(1-Y_{c4}) 0.8	(1-Y_{c4}) 0.2			-(Y_{c4}) N_{bac}		$k_{m,c4}\frac{S_{bu}}{K_S+S_{bu}}X_{c4}\frac{1}{1+S_{va}/S_{bu}}I_2$
10	Uptake of Propionate						-1	(1-Y_{pr}) 0.57	(1-Y_{pr}) 0.43		$-\sum_{i=1-9,11-24} C_i v_{i,}$	-(Y_{pro}) N_{bac}		$k_{m,pr}\frac{S_{pro}}{K_S+S_{pro}}X_{pro}I_2$
11	Uptake of Acetate							-1		(1-Y_{ac})	$-\sum_{i=1-9,11-24} C_i v_{i,}$	-(Y_{ac}) N_{bac}		$k_{m,ac}\frac{S_{ac}}{K_S+S_{ac}}X_{ac}I_3$
12	Uptake of Hydrogen								-1	(1-Y_{h2})	$-\sum_{i=1-9,11-24} C_i v_{i,}$	-(Y_{h2}) N_{bac}		$k_{m,h2}\frac{S_{h2}}{K_S+S_{h2}}X_{h2}I_1$
13	Decay of X_{su}													$k_{dec,Xsu}X_{su}$
14	Decay of X_{aa}													$k_{dec,Xaa}X_{aa}$
15	Decay of X_{fa}													$k_{dec,Xfa}X_{fa}$
16	Decay of X_{C4}													$k_{dec,Xc4}X_{c4}$
17	Decay of X_{pro}													$k_{dec,Xpro}X_{pro}$
18	Decay of X_{ac}													$k_{dec,Xac}X_{ac}$
19	Decay of X_{h2}													$k_{dec,Xh2}X_{h2}$
		Monosaccharides (kgCOD m^{-3})	Amino Acids (kgCOD m^{-3})	Long chain fatty acids (kgCOD m^{-3})	Total Valerate (kgCOD m^{-3})	Total Butyrate (kgCOD m^{-3})	Total Propionate (kgCOD m^{-3})	Total Acetate (kgCOD m^{-3})	Hydrogen gas (kgCOD m^{-3})	Methane gas (kgCOD m^{-3})	Inorganic Carbon (kmoleC m^{-3})	Inorganic Nitrogen (kmoleN m^{-3})	Soluble inerts (kgCOD m^{-3})	Inhibition factors: $I_1 = I_{pH}I_{IN,lim}$ $I_2 = I_{pH}I_{IN,lim}I_{h2}$ $I_3 = I_{pH}I_{IN,lim}I_{NH3,Xac}$

Table A.2: Biochemical rate coefficients ($V_{i,j}$) and kinetic rate equations (ρ_j) for particulate components (i=1-12; j=1-19) (Batstone et al., 2002)

Component → i		13	14	15	16	17	18	19	20	21	22	23	24	Rate
j	Process ↓	X_c	X_{ch}	X_{pr}	X_{li}	X_{su}	X_{aa}	X_{fa}	X_{c4}	X_{pro}	X_{ac}	X_{h2}	X_I	(ρ_j, kg COD.m^{-3}.d^{-1})
1	Disintegration	-1	$f_{ch,xc}$	$F_{pr,xc}$	$F_{li,xc}$								$f_{xI,xc}$	$k_{dis}X_c$
2	Hydrolysis Carbon		-1											$K_{hyd,ch}X_{ch}$
3	Hydrolysis of Prot			-1										$K_{hyd,pr}X_{pr}$
4	Hydrolysis of Lipid				-1									$K_{hyd,li}X_{li}$
5	Uptake of Sugars					Y_{su}								$k_{m,su}\frac{S_{su}}{K_S+S}X_{su}I_1$
6	Uptake of Amino Acids						Y_{aa}							$k_{m,aa}\frac{S_{aa}}{K_S+S_{aa}}X_{aa}I_1$
7	Uptake of LCFA							Y_{fa}						$k_{m,fa}\frac{S_{fa}}{K_S+S_{fa}}X_{fa}I_2$
8	Uptake of Valerate								Y_{c4}					$k_{m,c4}\frac{S_{va}}{K_S+S_{va}}X_{c4}\frac{1}{1+S_{bu}/S_{va}}I_2$
9	Uptake of Butyrate								Y_{c4}					$k_{m,c4}\frac{S_{bu}}{K_S+S_{bu}}X_{c4}\frac{1}{1+S_{va}/S_{bu}}I_2$
10	Uptake of Propionate									Y_{pro}				$k_{m,pr}\frac{S_{pro}}{K_S+S_{pro}}X_{pro}I_2$
11	Uptake of Acetate										Y_{ac}			$k_{m,ac}\frac{S_{ac}}{K_S+S_{ac}}X_{ac}I_3$
12	Uptake of Hydrogen											Y_{h2}		$k_{m,h2}\frac{S_{h2}}{K_S+S_{h2}}X_{h2}I_1$
13	Decay of X_{su}	1				-1								$k_{dec,Xsu}X_{su}$
14	Decay of X_{aa}	1					-1							$k_{dec,Xaa}X_{aa}$
15	Decay of X_{fa}	1						-1						$k_{dec,Xfa}X_{fa}$
16	Decay of X_{c4}	1							-1					$k_{dec,Xc4}X_{c4}$
17	Decay of X_{pro}	1								-1				$k_{dec,Xpro}X_{pro}$
18	Decay of X_{ac}	1									-1			$k_{dec,Xac}X_{ac}$
19	Decay of X_{h2}											-1		$k_{dec,Xh2}X_{h2}$
		Composites (kgCOD m^{-3})	Carbohydrates (kgCOD m^{-3})	Proteins (kgCOD m^{-3})	Lipids (kgCOD m^{-3})	Sugar degraders (kgCOD m^{-3})	Amino acids degraders (kgCOD m^{-3})	LCFA degraders (kgCOD m^{-3})	Valerate and Butyrate degraders (kgCOD m^{-3})	Propionate degraders (kgCOD m^{-3})	Acetate degraders (kgCOD m^{-3})	Hydrogen degraders (kgCOD m^{-3})	Particulate inerts (kgCOD m^{-3})	Inhibition factors: $I_1 = I_{pH}I_{IN,lim}$ $I_2 = I_{pH}I_{IN,lim}I_{h2}$ $I_3 = I_{pH}I_{IN,lim}I_{NH3,Xac}$

References

ABBASSI, E., B. (2003) Improvement of Anaerobic Sludge Digestion by Disintegration of Activated Sludge using Vacuum Process. Water Qual. Res. J. Canada, 38**,** 515-526.

ALATRISTE-MONDRAGON, F., SAMAR, P., HUUB, H., J., COX, AHRING, K., BIRGITTE & IRANPOUR, R. (2006) Anaerobic Codigestion of Municipal Farm and Industrial Ogranic Wastes: A Survey of Recent Literature. Water Environment Research, 78**,** 29.

ANGELIDAKI, I., MATHRANI M., I., SCHMIDT, E., J. & AHRING, K., B. The Biogas Process. 52 s.

APHA, AWWA and WPCF, Standard Methods for the Examination of Water and Wastewater (20 th edition), American Public Health Association, American WaterWorks Association and Water Pollution Control Federation, Washington DC, 2006

BATSTONE, D., J., , KELLER, J., ANGELIDAKI, I., KALYUZHNYI, V., S., , PAVLOSTATHIS, G., S., , ROZZI, A., SANDERS, W., T., M., SIEGRIST, H. & VAVILIN, A., V. (2002) Anaerobic Digestion Model No.1. Scientific and Technical Report, 13**,** 1-77.

BOUALLAGUI, H., LAHDHEB, H., BEN ROMDAN, E., RACHDI, B. & HAMDI, M. (2009) Improvement of fruit vegetable waste anaerobic digestion performance and stability with co-substrate addition. Journal of Environmental Management, 90**,** 1844-1849.

CAPELA, I., RODRIGUES, A., SILVA, F., NADAIS, H. & ARROJA, L. (2008) Impact of industrial sludge and cattle manure on anaerobic digestion of the OFMSW under mesophilic conditions. Biomass and Energy, 32**,** 245-251.

CASSIDY D., P., HIRL J., P. & BELIA E. (2008) Methane production from ethanol co-products in anaerobic SBRs. Water Science&Technology-WST**,** 789-793.

CECCHI, F., PAVAN, P. & MATA-ALVAREZ, J. (1996) Anaerobic co-digestion of sewage sludge: application to the macroalgae from Resources, Conservation and Recycling 17**,** 57-66.

DINSDALE, M., R., PREMIER, C., G., HAWKES, R., F. & HAWKES, L., D. (2000) Two-stage anaerobic co-digestion of waste activated sludge and fruit/vegetable waste using inclined tubular digesters. Bioresource Technology 72**,** 159-168.

DROSTE, R. L. (1997) Theory and practice of water and wastewater treatment, New York, Wiley.

EDELMANN, W., ENGELI, H. & GRADENECKER, M. (2000) Co-digestion of organic solid waste and sludge from sewage treatment. Water Science and Technology, 41**,** 213-221.

ENGINEERING, W. E. F. A. A. S. O. C. (1998) Design of municipal wastewater treatment plants, Alexandria, Va., WEF.

FENG, Y., BEHRENDT, J., WENDLAND, C. & OTTERPOHL, R. Parameters Analysis and Discussion of the IWA Anarobic Digestion Model No.1 (ADM1) for the Anaerobic Digestion of Blackwater puls Kitchen Refuse. 8 s.

FENG, Y., BEHRENDT, J., WENDLAND, C. & OTTERPOHL, R. Implementation of the IWA Anaerobic Digestion Model No.1 (ADM1) for Simulating Digestion of Blackwater from Vacuum Toilets. 8 s.

FYLKESKOMMUNE, R. (June 2010) <http://www.rogfk.no/>

GELEGNENIS, J., GEORGAKAKIS, D., ANGELIDAKI, I. & MAVRIS, V. (2007) Optimization of biogas production by co-digesting whey with diluted poultry manure. Renewable Energy, 32**,** 2147-2160.

GERBER, M. & SPAN, R. (2008) An Analysis of Available of Mathematical Models for Anaerobic Digestion of Organic Substances for Production of Biogas. International Gas Union Research Conference**,** 30 s.

HARTMANN, H., ANGELIDAKI, I. & AHRING, K., BIRGITTE (2002) Co-digestion of the organic fraction of municipal waste with other waste types. Biomethanization of the organic fraction of municipal solid wastes**,** 41-56.

HARTMANN, H., MØLLER, H., B. & AHRING, K. B. (2004) Efficiency of the anaerobic treatment of the organic fraction of municipal solid waste: Collection and pretreatment. waste Menagment & Research, 22**,** 35-41.

HARTMANN, H. & AHRING, K. B. (2005) Anaerobic digestion of the organic fraction of municipal solid waste: Influence of co-digestion with manure. Water Research, 39**,** 1543-1552.

HENZE, M. (1995) Activated sludge model no. 2, London, IWA Publishing.

HENZE, M. (2002) Wastewater treatment: biological and chemical processes, Berlin, Springer.

HENZE, M. (2008) Biological wastewater treatment: principles, modelling and design, London, IWA Publ.

KIELY, G., TAYFUR, G., DOLAN, C. & TANJI, K. (1997) Physical and mathematical modelling of anaerobic digestion of organic wastes. Wat. Res., 31**,** 534-540.

KOMMEDAL, R. (2008) Anaerobic Digestion - Lecture notes. Stavanger, University of Stavanger.

KOMMEDAL, R. (2010) Steady State Simulation, Personal communication and data acquisition, University of Stavanger (roald.kommedal@uis.no)

MADIGAN, M. T., MARTINKO, J. M. & BROCK, T. D. (2006) Brock biology of microorganisms, Upper Saddle River, N.J., Pearson Prentice Hall.

MISI, S., N. & FORSTER, C., F. (2001) Batch Codigestion of Multi-Component Agro-Wastes. Bioresource Technol. , 80**,** 19-28.

OSLI K.P. (2010) Personal communication, SNJ (kjetil.osli.pedersen@ivar.no)

REICHERT, P. (1998) AQUASIM 2.0 - User Manual. Computer Program for the Identification and Simulation of Aquatic Systems. Dubendorf.

RITTMANN, B. E. & MCCARTHY, P. L. (2001) Environmental biotechnology: principles and applications, Boston, Mass., McGraw-Hill.

SWITZENBAUM, M., S., GIRALDO-GOMEZ, E. & HICKEY, R., F. (1990) Monitoring of Anaerobic Methane Fermentation Process. Enz. Mic. Technol., 12**,** 722-730.

TCHOBANOGLOUS, G., BURTON, F. L. & STENSEL, H. D. (2003) Wastewater engineering: treatment and reuse, Boston, McGraw-Hill.

WANG, G., GAVALA, N. H., SKIADAS, V. I. & AHRING, K. B. (2009) Wet explosion of wheat straw and codigestion with swine manure: Effect on the methane productivity. Waste Menagment, 29**,** 2830-2835.

YDSTEBØ, L. (2008) Analytical methods in the wastewater laboratory. University of Stavanger**,** 9 s.

YDSTEBØ, L. (2010) Personal communication, University of Stavanger(leif.ydsteboe@uis.no)

HTTP://EN.WIKIPEDIA.ORG/WIKI/SLUDGE (June 2010) Sludge.

http://www.ivar.no/getfile.php/IVAR%20Dokumenter/IVAR%20Engelsk.pdf